Chapter II

Evolution of the Expanding Hot Universe

Humitaka SATO, Takuya MATSUDA* and Hidenori TAKEDA

Department of Physics, Kyoto University, Kyoto

**Department of Aeronautical Engineering, Kyoto University, Kyoto*

(Received April 14, 1971)

In this review article, evolution of the expanding hot universe is discussed from the point of view of astrophysical cosmology. Main effort is devoted to the theory of galaxy formation in connection with the physical state of matter and radiation in the early stage of the hot universe.

Contents

§1. Historical survey and introduction

§2. The very early stage
- (i) Quantum fluctuation
- (ii) Cold universe or hot universe
- (iii) Particle annihilation and relic particles
- (iv) Matter and antimatter
- (v) Neutrino sea

§3. Formation of nuclear elements
- (i) Proton-neutron ratio
- (ii) Formation of helium element
- (iii) Formation of elements heavier than helium
- (iv) Formation of elements in other universe models

§4. Thermal radiation in the expanding medium
- (i) Establishment of thermal equilibrium
- (ii) Recombination of plasma
- (iii) Formation of hydrogen molecules
- (iv) Origin of the microwave background radiation

§5. Inhomogeneous motions of the cosmic fluid and formation of galaxies
- (i) Dissipative process in the radiative gas
- (ii) Dissipative decay of acoustic and vortical motions
- (iii) A possible origin of magnetic field
- (iv) Size spectrum of inhomogeneities
- (v) Heating rates by dissipation
- (vi) Formation of condensed objects and their masses

§6. Thermal history of the hot universe
(i) Heating of matter before the decoupling
(ii) Evolution of heating rate
(iii) Thermal history after the decoupling
(iv) Heating by galactic activity and thermal instability
(v) Heating of matter and background radiation
§7. Evolutions of the whole universe and of a galaxy
(i) Importance of the middle era for the galactic era
(ii) Evolution of galaxies
Acknowledgements
Appendices
A. Microwave background radiation
B. Observational data of helium abundance
C. Cosmic expansion and red-shift parameter
D. Interaction of radiation with matter in the hot universe
E. Recombination of hydrogen in the hot universe
F. Atomic psocesses of hydrogen
G. Hydrodynamic equation of radiative fluid
H. A size spectrum of turbulence
References

§1. Historical survey and introduction

Until the World War II, the studies of cosmology had been concerned mainly with a framework of the universe based on the theory of general relativity.[1] After the war, some authors studied astronomical processes in relation to the expanding universe. For example, Lemaitre[2] and Gamow[3),4),5] advocated the evolutionary cosmology, whereas Bondi, Gold[6] and Hoyle[7] proposed the steady state consmology.[8] Gamow, Alpher and Herman put foward an interesting hypothesis that elements were synthesized in a stage earlier than the formation of galaxies.[4),5] According to their hypothesis, the sequence of evolution is controlled by the cosmic expansion from a hot and dense state of matter to a cold and diffuse state. On the other hand, Bondi, Gold and Hoyle proposed a continual creation of matter in order to maintain the constant density of the universe, despite of the cosmic expansion.[7),8] The steady state hypothesis denied the sequential evolution of the whole universe. It has been one of the most controversial problems in the study of cosmology whether the universe is evolutionary or steady. However, the observational data were insufficient at that time to decide the superiority between these rival theories.

The non-equilibrium theory on the origin of elements was a prologue to the evolutionary cosmology.[3] In the $\alpha\beta\gamma$ theory, associated with the names of Alpher, Bethe and Gamow,[4] elements were assumed to be synthesized from the matter which was initially composed of free neutrons.[9] However, Hayashi[10] correctly pointed out that the initial matter was composed of protons and neutrons intervened by electron pairs and neutrinos through weak interactions. Following the neutron-proton ratio calculated by him, Hayashi and Nishida[11] contrived to synthesize heavy elements through the 3α reaction, assuming a very high density at the time of nuclear reactions. Different from the hot model or the fire-ball model, there was a cold version of the origin of elements in the early stage of the universe. For example, Mayer et al.[12] and Peierls et al.[13] considered that the degenerate neutron gas broke up into polyneutron nuclei and they became heavy elements. Soon, however, these theories of the primordial origin of elements were replaced by the theory of the stellar origin of elements, according to which elements were synthesized in stellar interior during a long period of stellar evolution.[14] This view of stellar origin was incorporated with the evolutionary scheme of Galaxy by Taketani, Hatanaka and Obi.[15]

Then, studies on the evolutions of stars and galaxies have made much progress thereafter, whereas the progress in the study of cosmology has been rather slow. Classical tests of the model of the universe, such as the redshift-magnitude relation[16),17] and the luminosity-number relation[18] were attempted by several authors, but they were not too successful.[19a] Since 1960, new observational data on radio galaxies and quasars have been accumulated and made available for checking various models of the universe,[19),20] since these new objects have been the most remote ones observed until now. However, the result has been subject to our poor knowledge about their nature. As these methods of distinguishing models are based on the differences in the dynamics of the expansion, quantitative data are required to compare the evolutionary cosmology with the steady state cosmology. However, it may be better to distinguish them in some other critical characteristics which are qualitatively different from each other. One of these characteristic features is the cosmic black-body radiation.

In 1965, Penzias and Wilson discovered by accident the isotropic background radiation in the microwave band.[21),22] This discovery destroyed the coexistent state of the two rival theories, because this background radiation is inherent only to the evolutionary hot universe model. In fact, Gamow had predicted the existence of the isotropic radiation with the Planckian spectrum.[5] Thereafter, this isotropic radiation has been observed by many other authors, as summarized in Appendix A. The source of the isotropic radiation is considered to be the cosmic black-body radiation which uniformly fills up the metagalactic space. The determination of radiation temperature of the cosmic black-body radiation enables us to evaluate the abundances of elements produced at the initial stage of the universe.[23] In this way, the helium abundance is calculated to be $Y=0.27\sim0.3$ by a fraction in weight and the abundance of the other elements except D and Li^7 are found to be negligible.[24),25)] The calculated abundance of helium can well explain the observed value. Therefore, the theory of primordial origin of elements is revived as far as the helium abundance is concerned, about which the stellar origin had a very severe contradiction with observation.[26)]

Thus, the evolutionary cosmology enriched by the fire-ball hypothesis has acquired two observational bases, the cosmic black-body radiation and the helium abundance, and therefore got an advantage over the steady state cosmology. As described in Appendices A and B, however, these observational bases have not been completely confirmed, and several unfavorable evidences have been pointed out; the spectrum of the background radiation seems to have a departure from the Planckian spectrum in sub-mm wave length (see Appendix A), the helium deficient objects including the sun have been discovered (see Appendix B), the existence of super-high energy cosmic rays in the metagalactic space contradicts the cosmic black-body radiation,[27),28),28a)] and so on. However, we consider that these unfavorable events themselves are not so firmly founded to overthrow the evolutionary cosmology that we should look for other interpretations to explain these events. Therefore we adopt the hot universe model as the most reliable model at present.

Formation of galaxies in the expanding universe was studied by Gamow and others as early as in 1950.[5)] The turbulence hypothesis for galaxy formation was advocated by Gamow[30)] and Weizsäcker.[29)] Nariai studied the cosmic turbulence in the expanding universe.[31)] Since the discovery of the microwave background radiation this problem has been investigated extensively.[32),33)] The first problem is to explain a large density contrast in the early stage of the expanding universe. The evolution of weak inhomogeneity in density, velocity and metric was studied by Lifshitz[34)] and by many authors.[35)] However, the Jeans-Lifshitz instability, i.e., the instability due to the self-gravity, has been recognized to be very ineffective to form a strong density inhomogeneity. In their treatment, less attention has been paid to the physical state of the cosmic medium, and hydrodynamic motion has been regarded to be adiabatic. Following the investigations on the physical state of cosmic medium, e.g., the decoupling of radiation from matter (see §4) and the viscous effect of the medium (see §5), other mechanisms such as thermal instability[36),37),38)] and hydrodynamic instability[39),35)] have been proposed. Beside the mechanism to form a large density contrast, a mechanism to explain the mass of a galaxy has been discussed.[40),41)] As will be discussed in §5, we shall advocate two important effects, the dissipative decay of weak inhomogeneous motion and the appearance of supersonic motion by the sudden decoupling of radiation. Dissipation of the inhomogeneous motion also affects the thermal history of the expanding universe,[42),43)] about which we shall discuss in §6.

As the framework of the expanding universe has been studied thoroughly,[1)] the purpose of this paper is to study physical processes in the expanding medium. We describe the evolution in the expanding hot universe from a very early stage to a later stage of galaxy formation. Some parts of this paper are a review and the other parts an original work. Reviews of the recent development of cosmology have also been given in Refs. 44)~50). Original parts of this paper are mainly concerned with the problems of galaxy formation and thermal history in the universe in §§5 and 6.

§2. The very early stage

It has not been clarified what the physical state at the beginning of the universe is. According to the conventional model of the universe, the cosmic expansion starts from a singularity involving infinite density before a finite time in the past. This is not affected by an introduction of structual complexity different from the isotropic homogeneous metric.[51)] Although the true singularity may arise from an erroneous extrapolation of the theory of general relativity beyond its applicability,[52)] it is plausible that the density at the initial state is enormously larger than the nuclear density of the order of $3\cdot 10^{14}$ g/cm^3. As physical behaviour of matter at such a high density is completely unknown to us,[*)] we cannot give any decisive answer for these very early stages except for some speculative discussion. In this section, we summarize some discussions on the evolution of medium before the stage of nuclear synthesis.

(i) *Quantum fluctuations*

A characteristic length of the quantum effect of gravitational field is the Planck length defined by $L_* = (Gh/c^3)^{1/2} \simeq 10^{-33}$ cm, corresponding to which a characteristic mass is defined as $m_* = h/cL_* = 10^{-5}$ g. An energy density associated with the quantum fluctuation is given by

$$\rho_* = \frac{m_*}{L_*^3} = \frac{c^5}{G^2 h} \simeq 10^{94} \text{ g/cm}^3. \tag{2·1}$$

This represents a critical density, above which the quantum effect of gravitation becomes dominant. The expansion time at this density is about 10^{-43} sec.

Some authors contrived to relate the creation of elementary particles to this super-high density state, Wheeler regarded "worm hole", which arises from the disturbed space-time structure, as a source of elementary particles,[52)]

*) A fireball of super-high density state may be realized by the collision of cosmic rays. However, a time of maintenance of the cosmic-ray fireball is much shorter than that of the Big-Bang fireball: A state of $\rho = 10^{18}$ g/cm^3 is maintained for 10^{-24} sec in the former but for 10^{-5} sec in the latter.

and Markov considered a gravitational collapse of the fundamental particles named "maximon" with mass of m_* to form elementary particles.[53] Hokkyo[54] noticed that the radius of the univese at ρ_* is the order of the classical electron radius $L_c = e^2/m_e c^2$;

$$\rho_* L_c^3 = M_U\,, \tag{2·2}$$

$M_U = 10^{56}$ g being the mass of the universe. On the basis of this coincidence, he considered that the mass of the elementary particles is given, using the radius of the universe L_c, by a radiationless condition as

$$m_n = nh/(cL_c) \quad \text{and} \quad n = 1, 2, 3, \cdots, \tag{2·3}$$

which is Nambu's mass formula.

Beside ρ_*, there is another critical density ρ_{l_0} corresponding to the fundamental length l_0, which is much larger than L_*, ρ_{l_0} being the order of 10^{23} g/cm^3 assuming $l_0 = 10^{-15}$ cm. Tati[55] considered that the finite degrees of freedom of the space, which relates the existence of l_0, may introduce a finite size of the universe according to the Miln's cosmology.

(ii) *Cold universe or hot universe*

The total energy density ρ_t is given as a summation of the partial densities $\rho_{i,s}$ of all the species of particles. Representing ρ_t in terms of the energy density of photons ρ_γ as

$$\rho_t(T) = S(T)\rho_\gamma(T), \tag{2·4}$$

the multiplicative constant $S(T)$ may be an increasing function of temperature. If we assume a chemical equilibrium state of thermal creation of particles, $S(T)$ is roughly given by

$$S(T) \simeq \frac{(2\bar{s}+1)}{2}(N_B + N_F), \tag{2·5}$$

where N_B and N_F are the numbers of species of Bose particles and those of Fermi particles respectively, whose rest masses are smaller than the thermal energy, and $\bar{s}$ is the average value of spins. For example,

$$S(T) \simeq 300 \qquad \text{for } T = 10^{13.55}\,{}^\circ\text{K}$$

and

$$S(T) \simeq \frac{(11/4)^{4/3} + (7/4)}{(11/4)^{4/3}} = 1.45 \qquad \text{for } T < 10^{9.77}\,{}^\circ\text{K}.$$

A behaviour of $S(T)$ at extremely high temperature is dependent on a mass spectrum of massive particles beyond the known resonance-particles. If the species of particles increases with mass, the temperature decreases rather slowly at an earlier stage and then more rapidly at a later stage, as the universe expands. In an extreme case, the temperature reaches a constant value T_0 at the early stage, T_0 being taken about 160 MeV, if we take a mass spectrum which increases with mass as $\exp(mc^2/kT_0)/m^{5/2}$.[56] These considerations imply that the early state of the hot model does not necessarily hot, because the thermal energy may have been supplied from the rest mass energy of annihilated massive particles. However, it is impossible to obtain the hot model if we start from a cold state of nuclear density, since the heating in this case is due mainly to hyperonic decays.[57],[58]

(iii) *Particle annihilation and relic particles*

At high temperatures, the reaction rate is high enough to maintain thermodynamic equilibrium for particles whose masses are smaller than thermal energy: $mc^2 < kT$. As the temperature decreases, however, a time scale of particle creation exceeds the expansion time scale, τ_{ex} of Eq. (C·14a), and the thermal equilibrium ceases to hold for massive particles. Putting the annihilation rate as $\langle\sigma v\rangle$, a critical temperature T_c at which a creation time scale equals τ_{ex} is determined by

$$S(T_c)^{-1/2}\left(\frac{mc^2}{kT_c}\right)^2 \exp\left(-\frac{2mc^2}{kT_c}\right) = \frac{m}{m_*}\frac{1}{f}, \tag{2·6}$$

where $f \equiv \langle\sigma v\rangle/(h/mc)^2 c$ and m_* is the Planck mass. The number density at T_c is given as

$$n(T_c) \simeq \sqrt{\frac{m}{m_* f}}\left(\frac{mc}{h}\right)^3. \tag{2·7}$$

Below T_c, only the annihilation of particles proceeds until τ_{ex} exceeds the annihilation time scale. The particles which have survived up to this time remain to survive thereafter without annihilation as relic particles.[47] The ratio of the number of the relic particles to that of the thermal photons is given as

$$\frac{n_{rel}}{n_\gamma} \sim \frac{m}{m_*}\frac{mc^2}{kT_c}\frac{S(T_c)^{1/2}}{f}. \tag{2·8}$$

This relation shows that the ratio is larger for massive particles, if f is insensitive to mass. If the urbaryon is a stable particle, the number of the survived urbaryons is estimated as

$$n_U/n_\gamma \simeq 10^{-17.5}, \tag{2·9}$$

assuming $f=1$ and $m=10m_p$, where m_p is the nucleon mass.[59] If both the nucleon pairs and the electron pairs have existed symmetrically, the numbers of survived pairs are estimated as[60]

$$n_{N\bar{N}}/n_\gamma \sim 10^{-19.0} \text{ and } T_c = 10^{11.7}\,^\circ\text{K} \quad \text{for nucleon pairs}$$

and

$$n_{ee^+}/n_\gamma \sim 10^{-15.5} \text{ and } T_c = 10^{8.4}\,^\circ\text{K} \quad \text{for electron pairs,} \tag{2·10}$$

where we have used $f_{N\bar{N}}=10$ and $f_{ee^+}=10^{-5.6}$. On the other hand, the observed value of the nucleon number is

$$n_N/n_\gamma = n_e/n_\gamma \sim 10^{-8\sim-10}, \tag{2·11}$$

which is very large compared with Eq. (2·10). Thus, a symmetry between the particle and antiparticle leads to a contradiction of radiation catastroph.[60]

Combining Eqs. (2·9) and (2·11), we have

$$n_U/n_N \simeq 10^{-9.5\sim-7.5}. \tag{2·12}$$

This number of urbaryons is very large, comparing with the accumulated amount of urbaryons which have been produced in the earth's atmosphere by cosmic rays; $n_U/n_N = 10^{-17}$. Detection of these urbaryons by physicochemical effects has been discussed in Ref. 59). Recent experiment of quark hunting has apparently denied such a high abundance of fractionally charged particles as given in Eq. (2·12).[61]

(iv) *Matter and antimatter*

In order to avoid the radiation catastroph, we have to assume an asymmetrical population or a spatial separation of matter and antimatter. The symmetrical population advocated by Goldharber[62] and by Alfvén and Klein[63] is incompatible with the fire-ball model unless matter and antimatter are separated spatially.[64] As pointed out by Harrison,[65] the pair annihilation of matter and antimatter with a slight inhomogeneity of composition results in the spatial separation, and there remain eventually many separated regions of matter and antimatter. To complete this idea, we have to find a cause of the composition inhomogeneity of the order of $\Delta n_B/n_B \simeq 10^{-8\sim-10}$, n_B and Δn_B being a sum of baryon and antibaryon densities and a difference of them.

The simplest origin of the inhomogeneity is the thermal fluctuation of composition. In a state of equilibrium, the numbers of baryons and antibaryons are equal to each other but there arises necessarily a thermal fluctuation; an amount of it can be estimated as

$$\Delta n_B/n_B \sim 1/\sqrt{N_B}, \tag{2·13}$$

where $N_B = n_B \mathcal{V}_{th}$, $\Delta N_B = \Delta n_B \mathcal{V}_{th}$ and $\mathcal{V}_{th}$ is a proper volume within which a causal relationship is maintained thermodynamically. Taking $\mathcal{V}_{th} \simeq (c_S t)^3$, c_S being the sound velocity given by $c/\sqrt{3}$, Eq. (2·13) gives

$$\Delta N_B/N_B \sim [L_*/(hc/kT)]^{3/2}, \tag{2·14}$$

where L_* is the Planck length. The value required in Eq. (2·11) for the Harrison's mechanism is obtained for $T \simeq 10^{12}$ eV$\simeq 10^{16}$ °K. However, the inhomogeneity is as small as $\Delta N_B/N_B \sim 10^{-13}$ at the temperature of nucleon annihilation $T \simeq 10^9$ eV and we cannot avoid the radiation catastroph.

Taking into account interactions among baryons and antibaryons, Omnes[66] showed that a state of symmetric population is not necessarily a stable state of thermal equilibrium; the free energy is smaller for inhomogeneous composition than for homogeneous one at temperatures above 350 MeV, because the cores of the baryon and the antibaryon are repulsive to each other.

A slight composition inhomogeneity produced by some mechanism is amplified after the pair annihilation, and the difference between the local densities of two species remains to be as relic particles. As a result, the separate regions of matter and antimatter are distributed in a mosaic pattern. By the encounter of the regions of matter and antimatter, a strong repulsion due to the annihilation energy at the contact surface prevents a further annihilation of matter and antimatter. As noticed by Alfvén, such an effect is analogous to the calefaction effect of water drop on a hot plate.[63] On the other hand, the regions of the same species will coalesce by their encounter and these regions will grow larger and larger. By the repulsive force at the encounter of different species, the turbulent motions of cosmic medium may arise. Furthermore, a small trapped region of antimatter in a larger region of matter has been annihilating gradually and it might be observed as a strongly radiating object such as the quasars.[67]

(v) *Neutrino sea*

In the very early stage, neutrinos are coupled with matter.[10),68] The energy distribution of thermal neutrinos is represented by the Fermi-Dirac spectrum, which depends not only on temperature but also on the chemical potential of the neutrinos. If neutrinos are in chemical equilibrium with photons through reactions such as

$$\begin{aligned} &\nu_\mu + \bar{\nu}_\mu \rightleftarrows \mu^+ + \mu^- \rightleftarrows 2\gamma, \\ &\nu_e + \bar{\nu}_e \rightleftarrows e^+ + e^- \rightleftarrows 2\gamma, \end{aligned} \tag{2·15}$$

the chemical potential of the neutrino divided by kT_ν, ψ, and that of the antineutrino, $\bar{\psi}$, are related as

$$\psi_{e,\mu} + \bar{\psi}_{e,\mu} = 0, \tag{2·16}$$

where the subscripts e and μ denote the electron and the muon neutrinos, respectively. Therefore, the energy density of neutrinos ρ_ν is expressed in terms of ρ_γ as

$$\rho_\nu(T_\nu, \psi_{e,\mu}) = \rho_\gamma(T_r)\left(\frac{T_\nu}{T_r}\right)^4 N(\psi_e, \psi_\mu)$$

and

$$N(\psi_e, \psi_\mu) = \frac{15}{2\pi^3}\sum_{e,\mu}\int_0^\infty\left(\frac{1}{e^{x-\psi}+1}+\frac{1}{e^{x+\psi}+1}\right)x^3dx, \tag{2·17}$$

where the summation is taken over the electron and the muon neutrinos, and T_r and T_ν are temperatures of photons and neutrinos, respectively; ρ_ν takes the minimum for $\psi_{e,\mu}=0$. In the strongly degenerate case, ρ_ν is given, assuming $\psi_e=\psi_\mu=\psi\gg1$, as

$$\rho_\nu=\rho_\gamma\frac{15}{4\pi^3}\left(\frac{T_\nu}{T_r}\right)^4|\psi|^4=3.2\cdot10^{12}E_F^4\ \mathrm{eV/cm^3}, \tag{2·18}$$

where E_F is the Fermi energy defined by $E_F=kT_\nu\psi$. As the maximum energy density at present is limited as $\rho<10^{-28}\ \mathrm{g/cm^3}$, the Fermi energy is limited as

$$E_F<10^{-2}\ \mathrm{eV} \quad \text{or} \quad |\psi|<50. \tag{2·19}$$

Therefore the number density of neutrinos is limited as

$$300\ \mathrm{cm^{-3}}<n_\nu<10^6\ \mathrm{cm^{-3}}. \tag{2·20}$$

As the expansion proceeds, the neutrinos decouple from the matter. The decoupling time of the muon neutrino is estimated from Eq. (2·6) as

$$t_{D\nu_\mu}\simeq10^{-2.1}\ \mathrm{sec}, \tag{2·21}$$

taking $f=5\cdot10^{-15}$ for the weak interaction. The decoupling time for the electron neutrino is estimated as

$$t_{D\nu_e}\simeq0.2\ \mathrm{sec}, \tag{2·22}$$

which cannot be given by Eq. (2·6) because $kT_{D\nu_\mu}>mc^2$. If the universal Fermi interaction does not hold, the electron neutrino may be coupled with matter only through such interactions as

$$\mu+\nu_{e,\mu}\rightleftarrows e+\nu_{e,\mu}\,, \quad \mu\rightleftarrows e+\bar\nu_e+\nu_\mu$$

and the decoupling time of ν_e may be the same order of that of given by Eq. (2·21).

Here, we notice that the electron pairs annihilate after the decoupling of neutrinos. Therefore, the annihilation energy is shared only with photons but not with the neutrinos, and the photon temperature becomes slightly larger than the neutrino temperature; the difference of the temperatures is given as[68)]

$$T_\nu/T_r=(4/11)^{1/3}. \tag{2·23}$$

The detection of these primordial neutrinos will bring us information about the structure of the universe as early as $t=10^{-2}$ sec.[70] Several authors have discussed a possible existence of the degenerate neutrino sea[71)~74)] and its superfluidity.[75] One possibility of its detection is a slight modification of the Kurie plot of the β-decay[72),73),76)] and the other is to observe the energetic neutrinos produced by the high energy metagalactic cosmic rays:[77)~79)]

$$\nu^{\text{soft}}+N(\text{cosmic ray})\rightarrow N+(\text{leptons})+(\text{mesons})$$
$$\qquad\qquad\qquad\qquad\qquad\qquad\qquad\qquad\qquad \lfloor\!\rightarrow \nu^{\text{energetic}}.$$

If the energy spectrum of $\nu^{\text{energetic}}$ is much less steep than that of the atmospheric neutrinos, such neutrino may be detectable by observing large bursts underground.[80] Above the energy of 10~100 TeV, the probability of the neutrino bursts dominate over that of muon bursts, if $E_F>1$ eV.

§3. Formation of nuclear elements

Assuming an asymmetrical population of matter and antimatter, we consider the evolution after the very early stage. After about 10^{-6} sec since the start of the cosmic expansion, only nucleons survive among baryons.

Following the $\alpha\beta\gamma$ theory,[4] Fermi and Turkevich[8] and Alpher and Herman[9] calculated the formation of elements from primordial neutrons and showed that the main product is helium whose mass fraction is about 30%. However, Hayashi[10] showed that the induced beta-processes caused by hot electrons, positrons, neutrinos and antineutrinos must have proceeded and have a severe effect on the composition of the primordial nucleons. About the proton-neutron ratio of the primordial matter and the synthesis of elements, we give a brief explanation in this section.

(i) *Proton-neutron ratio*[10),23),24),68)]

At the stage when a large number of mesons are produced thermally, protons and neutrons are converted mutually through the strong interaction such as

$$p+\pi^{-}\rightleftarrows n+\gamma,\quad n+\pi^{+}\rightleftarrows p+\gamma. \tag{3·1}$$

The ratio of the time scale of strong interaction τ_{st} to that of the cosmic expansion τ_{ex} is given as

$$\tau_{st}/\tau_{ex}\simeq 10^{-12}/(T/10^{12}\,{}^{\circ}\mathrm{K})\qquad \text{for}\quad T>10^{12}\,{}^{\circ}\mathrm{K}. \tag{3·2}$$

As the temperature decreases below 10^{11} °K, the number of mesons decreases rapidly and the mutual conversion through Eq. (3·1) stops. However, the mutual conversion is maintained thereafter through the weak interaction such as

$$n+e^{+}\rightleftarrows p+\bar{\nu}_e,\quad n+\nu_e\rightleftarrows p+e^{-} \tag{3·3a}$$

and

$$n \rightleftarrows p + e^- + \bar{\nu}_e \,. \tag{3·3b}$$

The time scale of the weak interaction τ_w is given by the ratio to τ_{ex} as

$$\tau_w/\tau_{ex} \simeq 10^{-3}/(T/10^{11}\,{}^\circ\mathrm{K})^3 , \tag{3·4}$$

which shows that the mutual conversion stops at about $T \simeq 10^{10}\,{}^\circ\mathrm{K}$ and the proton-neutron ratio begins to deviate from the equilibrium value.

The evolution of the neutron concentration is given in general by the equations

$$\frac{d}{dt}\left(\frac{n_n}{n}\right) = \frac{1}{\tau_0}\left(K_p \frac{n_p}{n} - K_n \frac{n_n}{n}\right), \tag{3·5}$$

$$K_n = \int_1^\infty \frac{\epsilon(\epsilon^2-1)^{1/2}}{1+e^{\epsilon z_r}} \left[\frac{(\epsilon+q)^2}{1+e^{-(\epsilon+q)z_\nu-\psi_e}} + \frac{(\epsilon-q)^2 e^{\epsilon z_r}}{1+e^{(\epsilon-q)z_\nu-\psi_e}}\right] d\epsilon$$

and K_p is given by replacing q and ψ_e by $-q$ and $-\psi_e$ in the expression of K_n, where $\tau_0 = 1.01 \cdot 10^3$ sec,*) $q = (m_n - m_p)/m_e$, $z_r = m_e c^2/kT_r$ and $z_\nu = m_e c^2/kT_\nu$. In the stage of $\tau_w/\tau_{ex} \ll 1$, the ratio is given by the thermal equilibrium value as

$$n_n/n_p \simeq K_p/K_n \simeq \exp\left[\frac{(m_n - m_p)c^2}{kT_r}\right]. \tag{3·6}$$

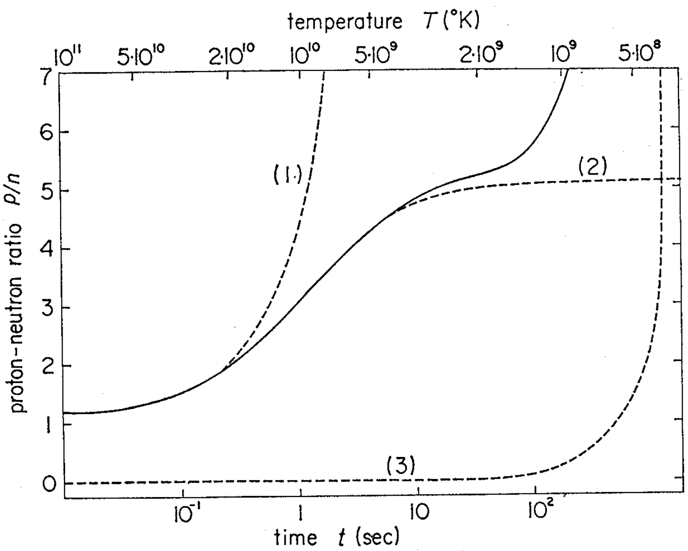

Fig. 1. Temporal change of the proton-neutron ratio p/n. The solid curve represents the real behaviour. The dotted curves (1) and (2) represent the thermal equilibrium curve between proton and neutron and the behaviour when the free neutron decay of Eq. (3·3b) is neglected, respectively. For comparison, we show the behaviour on the assumption that all baryons are initially neutrons and they transmute to protons only through free decay.

*) About the decay life of the neutron, see Ref. 82).

As temperature decreases, this ratio begins to deviate from the equilibrium value of Eq. (3·6) as shown in Fig. 1. After about 10 sec, the induced beta-process has stopped and the ratio changes only through the free decay of neutrons as

$$n_p/n_n = [(n_p/n_n)_{\mathrm{d}\nu} - 1] \cdot e^{1.632(t - t_{\mathrm{d}\nu})/\tau_0} + 1, \qquad (3\cdot7)$$

where $t_{\mathrm{d}\nu}$ and $(n_p/n_n)_{\mathrm{d}\nu}$ are the decoupling time of the reactions of (3·3a) and the ratio at $t_{\mathrm{d}\nu}$, respectively. For a case of $\psi_e = 0$, we have $t_{\mathrm{d}\nu} = 10$ sec and $(n_p/n_n)_{\mathrm{d}\nu} = 4.8$.

(ii) *Formation of helium element**)

In the mixture of protons and neutrons, the radiative capture and the photo-dissociation of deuterons, the time scales of these reactions being taken as τ_{rac} and τ_{pd} respectively, are balanced as

$$n + p \rightleftarrows \mathrm{D} + \gamma, \qquad (3\cdot8)$$

and the time scales are given as

$$\tau_{\mathrm{rac}}/\tau_{\mathrm{ex}} \simeq 10^{-3.6}/(T/10^9\ {}^\circ\mathrm{K})$$

and

$$\tau_{\mathrm{pd}}/\tau_{\mathrm{ex}} \simeq (T/10^9\ {}^\circ\mathrm{K})^{1/2}\, 10^{-16.34 + 11.18 \cdot 10^9/T}, \qquad (3\cdot9)$$

where the capture reaction rate is taken as $\langle \sigma v \rangle = 4.1 \cdot 10^{-20}$ cm^3/sec. For $T > 5.8 \cdot 10^8\ {}^\circ$K, the equilibrium is maintained and the density of deuterons is given by

$$\left(\frac{n_{\mathrm{D}}}{n_n n_p}\right)_{\mathrm{eq}} = \frac{3}{4}\left(\frac{4\pi\hbar^2}{m_p k T}\right)^{3/2} e^{Q/kT}, \qquad (3\cdot10)$$

where $Q = 2.22$ MeV is the binding energy of the deuteron. This equilibrium density of deuterons, n_{D}, increases rapidly as temperature decreases. The increase of the deuteron density is immediately followed by the following nucleon reactions.

$$\mathrm{D} + \mathrm{D} \rightarrow \mathrm{T} + p, \quad \mathrm{He}^3 + n,$$

$$\mathrm{T} + \mathrm{D} \rightarrow \mathrm{He}^4 + n, \quad \mathrm{He}^3 + n \rightarrow \mathrm{T} + p$$

and

$$\mathrm{He}^3 + \mathrm{D} \rightarrow \mathrm{He}^4 + p. \qquad (3\cdot11)$$

As the binding energies of T, He^3 and He^4 are larger than that of D, the photo-dissociation of these nuclei is no longer effective. By the reactions of Eq. (3·11), a part of free neutrons is transformed into bound neutrons in helium nuclei. If we define the ratio of the two elimination rates of neutrons,

*) Discussion in this subsection is due to C. Hayashi (unpublished, 1965).

i.e., free decay rate and the D–D reaction rate, by

$$\mathcal{R}=\frac{n_D^2\langle\sigma v\rangle_{DD}}{n_n/\tau_0}, \quad (3\cdot12)$$

$\mathcal{R}$ increases rapidly with the decrease of temperature as anticipated from Eq. (3·10). Therefore, most of the free neutrons remainning up to the temperature T_c, T_c being defined by $\mathcal{R}(T_c)=1$, may be consumed to form helium nuclei after the epoch of T_c; we can estimate the final abundance of helium by the fraction in weight as

$$Y=\frac{2}{1+(n_p/n_n)_{T_c}}, \quad (3\cdot13)$$

where $(n_p/n_n)_{T_c}$ is the p/n ratio at T_c. For example, $T_c=1.02\cdot10^9$ °K and $(n_p/n_n)_{T_c}=6.8$, taking the model of $\Omega=0.1$ and $\langle\sigma v\rangle=10^{-16.5}\text{cm}^3/\text{sec}$ at $T=100$ keV, and Y becomes 0.26.

Recently, more detailed calculations have been made by several authors.[83),84),23)~25)] The evolution of abundances is shown in Fig. 2. The final abundance of helium is represented in Fig. 3. The astronomical meaning of the final abundance has been discussed in §1, in Appendix B and in Refs. 46), 84)~88).

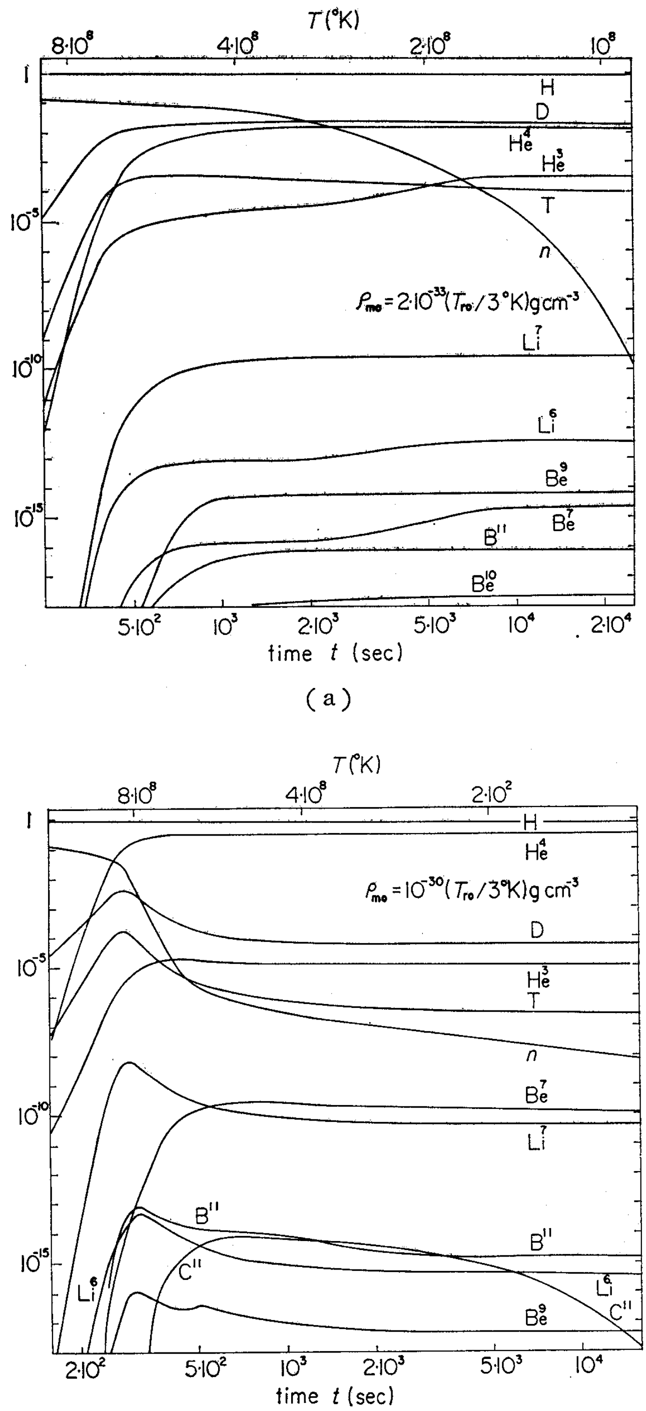

Fig. 2. Evolution of abundances during the element formation. The figures (a) and (b) are the typical examples of low and high density models of universe, respectively. ρ_{m0} and T_{r0} represent the average matter density and the radiation temprature of the present universe, respectively.

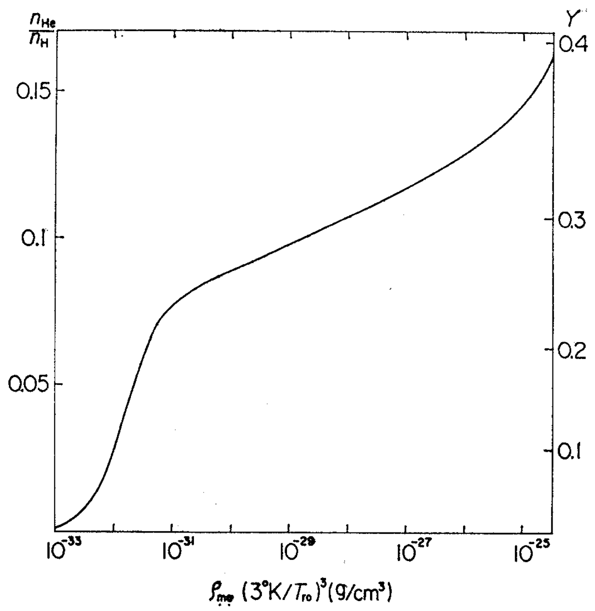

Fig 3. Final abundance of helium by the ratio to the remaining hydrogens n_{He}/n_H and by the mass fraction Y. ρ_{m0} is the present matter density.

(iii) *Formation of elements heavier than helium*

This problem consists of two parts; one is concerned with elements heavire than carbon and the other with Li, Be and B. The formation of the former was studied early in 1956 by Hayashi and Nishida.[11] In order to secure an appreciable amount of carbon and other heavier elements, the three-alpha reaction is indispensable, which is frequent at high density. As the characteristic temperature T_N, around which the formation of helium is most frequent, is nearly independent of density, we have to adopt a very cold universe model to secure a high density in comparison with temperature T_N; the present radiation temperature of the universe was adopted in Ref. 11) as low as $T_r \simeq 10^{-1.5\sim-2.5}$ °K, which is much smaller than $T_{r0}=2.7$°K of the current observable value. In Fig. 4, the evolutions of the density and the temperature for various models characterized by the parameter (ρ/T_r^3) are shown. The temperature T_N is roughly given by the temperature at which the equilibrium value of Eq. (3·10) shifts in favour of deuterons. The hatched region in Fig. 4 shows the 3α-reaction region where $\tau_{3\alpha}<\tau_{ex}$, $\tau_{3\alpha}$ being the time scale of 3α-reaction estimated under the assumption of pure helium composition. As seen from this figure, the 3α-reaction is frequent only if we adopt the models of a large value of (ρ/T_r^3).

Without the 3α-reaction, massive elements could be formed in succession through Li, Be and B.[25] In Fig. 5, the route of such element formation is given. Since the destruction of Li, Be and B takes place by the bombardment of protons in these reactions, only a small amount of nuclei are formed. For example, the formation rate and the destruction rate of Li^7 are given as

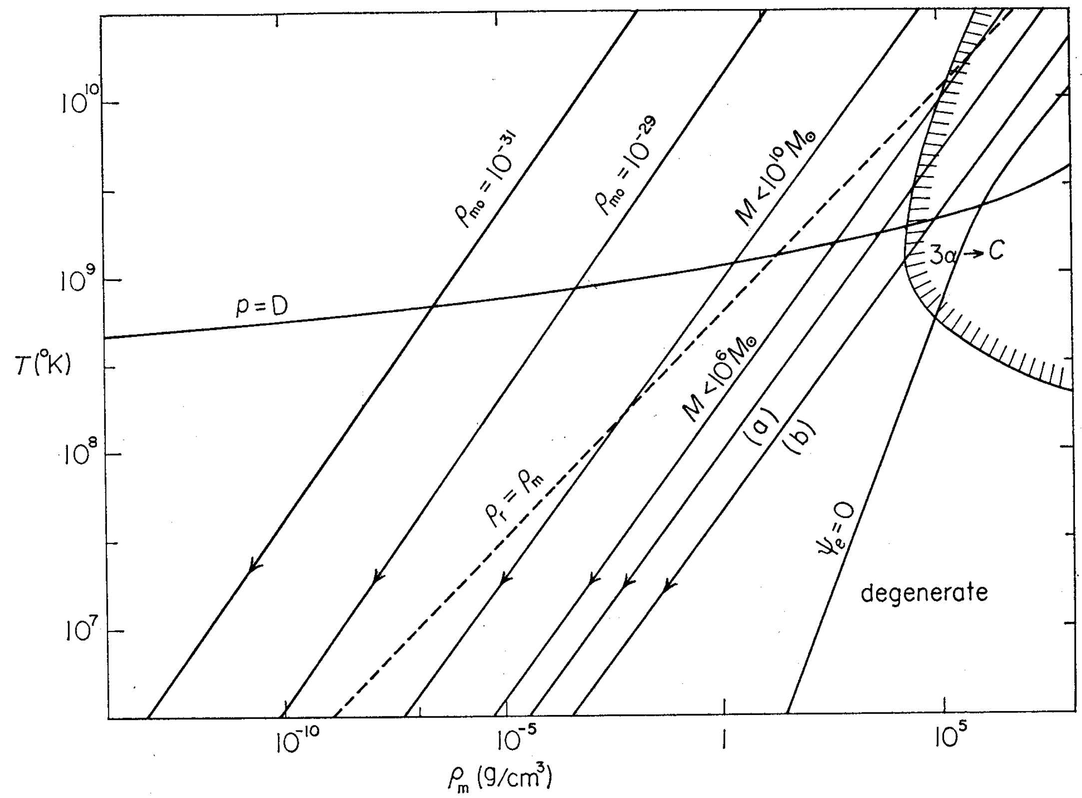

Fig. 4. The density-temperature region where helium formation occurs. The curve denoted by p=D represents the temperature where the equilibrium value of deuteron given by Eq. (3·10) equals the proton number. Production of helium occurs around this critical temperature. In the hatched region, a time scale of three-alpha reaction is smaller than τ_{ex}, if most of nucleons has been transformed into He already. The arrowed lines are the evolutionary pathes; ρ_{m0} is the density at $T=2.7$°K and M is the mass of supermassive object. The lines denoted by (a) and (b) are the evolutionary pathes taken by Hayashi and Nishida.[11] ψ is chemical potential of electron divided by kT.

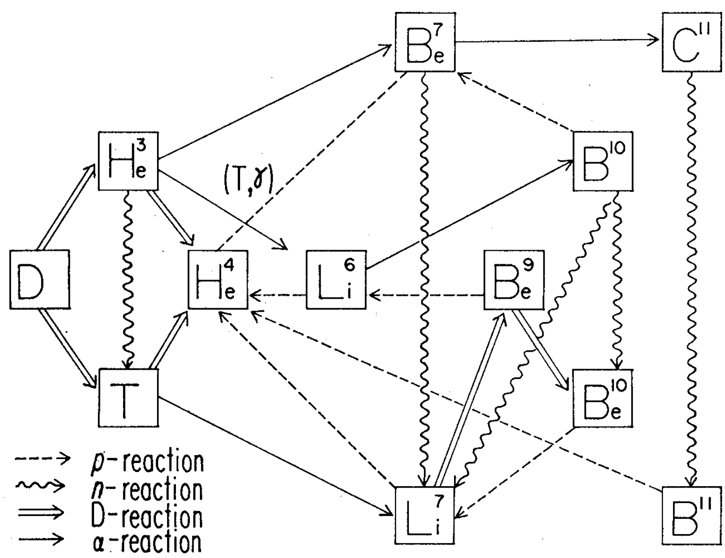

Fig. 5. Flow diagram to illustrate a main route of element formation of Li, Be and B.

$\langle\sigma v\rangle_{\mathrm{Li}\,p}=10^{-22.0}$ cm^3/sec and $\langle\sigma v\rangle_{\alpha\mathrm{D}}=10^{-17.6}$ cm^3/sec respectively, and the amount of Li^7 is estimated as

$$\frac{n_{\mathrm{Li}^7}}{n_p}\simeq\frac{\langle\sigma v\rangle_{\alpha\mathrm{T}}}{\langle\sigma v\rangle_{\mathrm{Li}\,p}}\frac{n_\alpha n_{\mathrm{T}}}{n_p^2}\sim10^{-8.4\sim-10.4}, \tag{3·14}$$

taking $n_\alpha/n_p\sim10^{-1}$ and $n_{\mathrm{T}}/n_p\sim10^{-3\sim-5}$.

The rate of $He^4(D,\gamma)Li^6$ is much smaller than that of $He^4(T,\gamma)Li^7$ by a factor of more than $10^{6.5}$, because the capture of deuterons takes place only through *d*-wave and E2 transition. Therefore the produced amount of Li^6 is much smaller than that of Li^7. The amounts of Be^9 and B^{10} are still smaller. The calculated final abundances are given in Fig. 6. Except of Li^7, the abundances are incomparatively smaller than the observed ones.[25)]

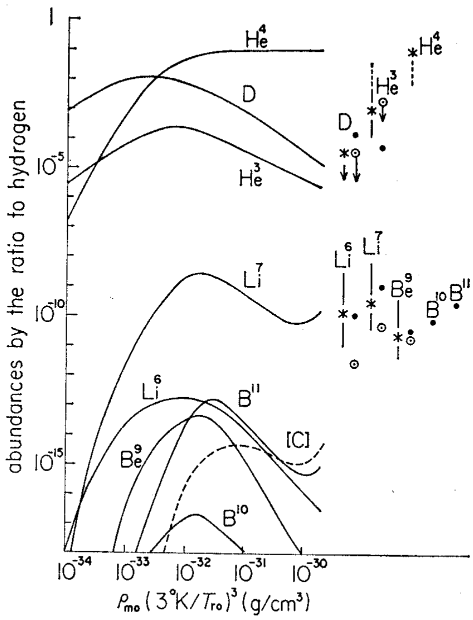

Fig. 6. Final abundances of the elements by the ratio to the remaining hydrogens. On the right-hand side, we represent the observed abundances of the meteorite ●, the sun ⊙ and the stars *. [C] denotes $C^{12}+N^{14}$.

Element synthesis in the expanding medium with a large value of (ρ/T_r^3) is considered to be realized in an expanding supermassive object; such explosion is named a little bang.[24)] The calculation by Hayashi et al.[11)] corresponds to this little bang, and Wagoner has throughly calculated the abundances of elements formed thereby for various models and various initial states.[24,89)]

(iv) *Formation of elements in the other universe models*

Hitherto, the universe models have been restricted to the conventional model with isotropy, homogeneity and non-degenerate neutrinos. Several authors have studied the synthesis of elements in other modified models. These models are classified as follows: (a) an anisotropic-homogeneous model,[90),91)] (b) a model which contains degenerate neutrinos,[24)] (c) a model with strong magnetic field,[92),93)] (d) a model based on the Brans-Dicke theory.[94)] In the models (b) and (c), the reaction rates of Eq. (3·5) change through the modification of energy spectra of neutrinos for (b) and of electrons for (c), respectively. Another effect in these models is a decrease of τ_{ex} at $T\sim T_N$ in comparison with that in the conventional model. Usually, the final abundance of He increases with the decrease of τ_{ex} because the neutron is more abundant in the earlier state; the stage of the element synthesis is shifted to earlier time. Of course, the final abundance of helium becomes smaller again if τ_{ex} decreases below the time scale of D–D reaction into helium. According to Peebles,[23] the helium abundance becomes as large as $Y=0.8$ for the case of $\tau_{ex}(T_N)/[\tau_{ex}(T_N)]_0 \simeq 10^{-2}$, $[\tau_{ex}(T_N)]_0$ being the time scale in the conventional model. For most cases of these modifications, the final abundances become larger than that in the conventional model because of the decrease of $\tau_{ex}(T_N)$. To reduce a helium abundance, we have to assume a high degeneracy of neutrinos[24] and a high degree of anisotropy whose effect remained to a stage as late as 10^4 years.[91] The abundance of helium in the cold model is small, since the density of electron-positron pairs is so small compared with that of nucleons that the p/n ratio is much smaller than that in the conventional model.[58]

§4. Thermal radiation in the expanding medium

In contrast to the thermal neutrinos which decouple at the epoch as early as 10^{-1} sec, the coupling of the thermal photons with the matter is maintained to the later stages. According to the types of interactions, the coupling stage of photons is devided into four stages; (1) *free-free* stage, where an equilibrium is maintained in each frequency range by free-free transition, (2) *free-free and Compton* stage, where photons are produced in the low frequency range by free-free emission and the energy equilibrium is preserved by the Compton scattering, (3) *Compton* stage, where the emission and absorption of photons do not take place and the energy equilibrium is preserved by inelastic scattering, (4) *scattering* stage, where photons suffer only elastic scattering. After the scattering stage, most of photons decouple completely from the matter and they propagate along the geodesic lines suffering red-shift by the cosmic expansion. These primordial photons survive up to the present and are observed as the isotropic background radiation. Therefore, the microwave background radiation discovered by Penzias and Wilson[21] can be interpreted to be a relic of the primordial thermal photons, which may bring us various information about the stage of decoupling.

(i) *Establishment of thermal equilibrium*

As shown in Fig. 7, an evolutionary path of the universe goes through four stages of different interaction types successively.

During the *free-free* stage, an equilibrium is maintained through the pair annihilation-creation process and the free-free transition. The time scales of them are given for the pair-electron interaction as

$$\begin{aligned}\tau_{pair}/\tau_{ex} &= 10^{-17.5}(T/10^9\,{}^\circ\mathrm{K}) && \text{for } T>6\cdot 10^9\,{}^\circ\mathrm{K},\\ &= 10^{-15.3}(T/10^9\,{}^\circ\mathrm{K})e^{2.57\cdot 10^9/T} && \text{for } T<6\cdot 10^9\,{}^\circ\mathrm{K},\end{aligned} \tag{4·1}$$

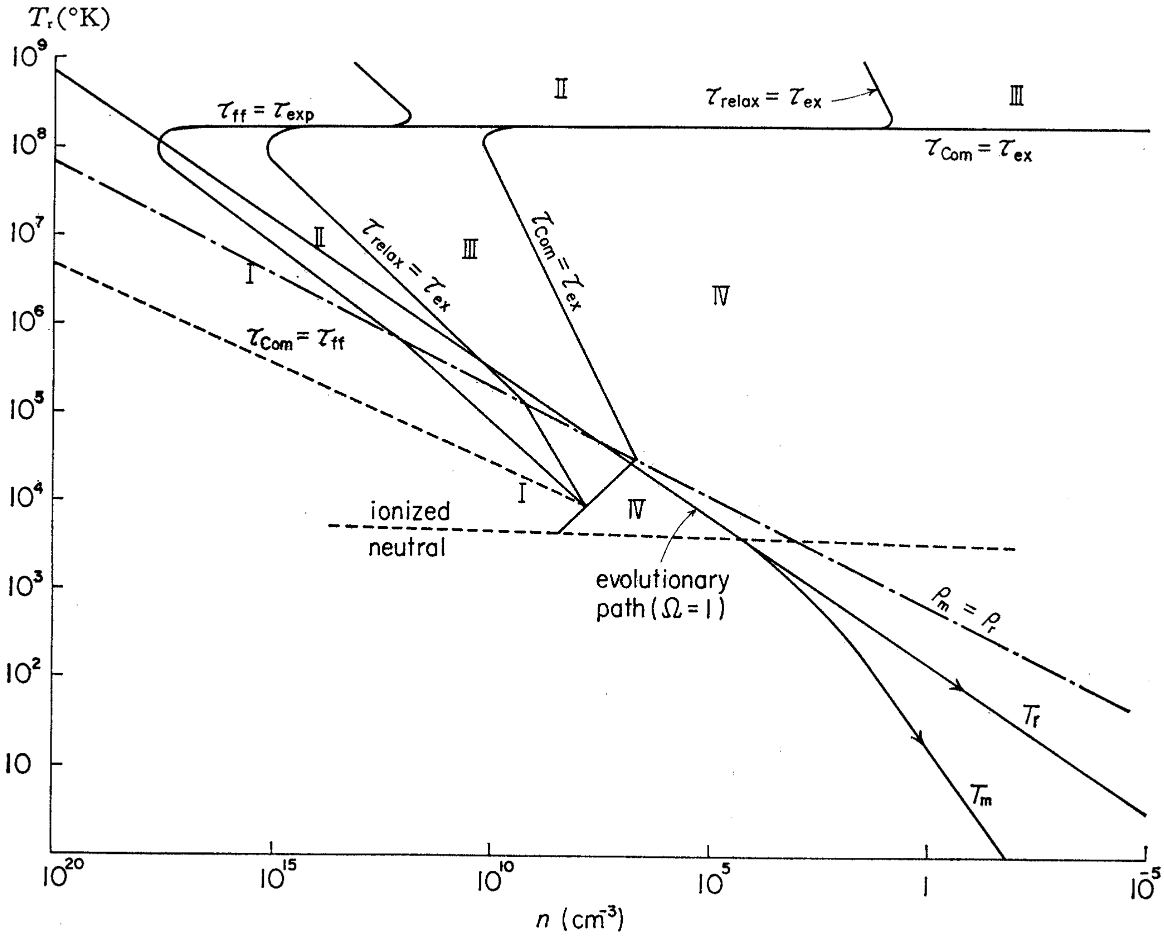

Fig. 7. Interaction between radiation and matter, as a function of density and temperature. The regions denoted by I∼IV correspond to *free-free* region ($\tau_{Com}<\tau_{relax}<\tau_{ff}<\tau_{ex}$), *free-free and Compton* region ($\tau_{Com}<\tau_{relax}<\tau_{ex}<\tau_{ff}$) *Compton* region ($\tau_{Com}<\tau_{ex}<\tau_{relax}<\tau_{ff}$) and *Scattering* region ($\tau_{ex}<\tau_{Com}<\tau_{relax}<\tau_{ff}$), respectively, where τ_{Com}, $\tau_{ff}(=\tau_{ff}(1))$ and τ_{relax} are given in Eqs. (D·7), (D·8) and (D·22). The curves denoted by T_r and T_m and evolutionary path of the universe model with $\Omega=1$.

and for the free-free interaction as

$$\tau_{ff}/\tau_{ex}=\frac{10^{-0.12}}{\Omega^2}\left(\frac{10^9\,°K}{T}\right)^{1/2}\frac{K_0(x/2)\,(e^x-1)}{x^3e^{x/2}} \quad \text{for } T<6\cdot10^9\,°K \qquad (4\cdot2)$$

from Eq. (D·9). These relations are also shown in Fig. 8, from which one sees that the complete equilibrium condition, i.e., $(\tau_{pair}^{-1}+\tau_{ff}^{-1})^{-1}\ll\tau_{ex}$, is not satisfied for most of the photons soon after the annihilation of pair electrons.

During the *free-free and Compton* stage and the *Compton* stage, the energy exchange is mainly due to the Compton interaction,[95] whose time scale of interaction is given as

$$\tau_{Com}/\tau_{ex}\simeq\frac{10^{-1.1}}{\Omega}\left(\frac{10^5\,°K}{T}\right)^2 \qquad (4\cdot3)$$

from Eq. (D·8) and is shown also in Fig. 8. Even after the annihilation of pair electrons, the energy equilibrium is maintained until about $10^{4.5}$ °K. However, in the *Compton* stages, the photon number equilibrium is not generally attained and a chemical potential of photons can be different from zero, though its initial value is zero. A characteristic of these two stages will appear only if we consider a heating or a cooling of matter by some causes.[96)~98)]

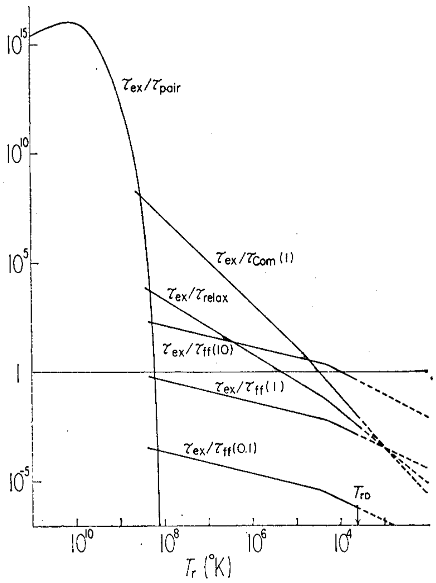

Fig. 8. Variation of τ_{pair}, $\tau_{ff}(x)$, τ_{Com} and τ_{relax} by the ratio to τ_{ex}, for the universe model with $\Omega=1$. x is frequency of photon divided by kT.

(ii) *Recombination of plasma*[99)~102)]

When the number of ionizing photons, whose energies are larger than the ionization energy, is sufficiently large, the ionization equilibrium by radiative processes is attained through the reactions such as

$$He^{++}+e \rightleftarrows He^{+}+\gamma, \qquad He^{+}+e \rightleftarrows He+\gamma$$

and

$$H^{+}+e \rightleftarrows H+\gamma. \tag{4·4}$$

As the temperature of the radiation decreases, the equilibrium abundance shifts to neutral atoms at some temperature, which is given in Table I as the recombination temperature. This recombination process is not so simple because the photons emitted by the recombination themselves suppress the further recombination.[99),100)] Taking the recombination into He^+ as an example, we shall explain the recombination process in some details.[102)] As shown in Table I, the density of ionizing photons n_I is much smaller than that of helium nuclei n_α and the mean-free path of the ionizing photons is also much smaller than c/H. Therefore, the direct capture of an electron into the ground state of He^+ is followed by the ionization of another He^+. The Lyman series photons are also recaptured. Through the repeat of emission and absorption of the recombination photons, they split gradually into the Lyman-α photons and the lower energy photons. The Lyman-α photons accumulated in this way suppress the allowed transition from $2p$ to $1s$, and the forbidden transition from $2s$ to $1s$ through the two-photon emission becomes more frequent than the allowed one, the equilibrium between $2s$ and $2p$ being maintained by the collision of protons.

Considering these effects, the equation of recombination is given from

Table I. Characteristic quantities of recombination of plasma in the expanding universe. n_a, n_I and $n_I(2)$ are number densities of nuclei, ionizing photons from the ground state and ionizing photons from the first excited state, respectively, at the temperature of recombination. $(\sigma_I n_a)^{-1}$ represents mean-free path of the ionizing photons.

Atom	He^+	He	H
Ionization energy B_i(eV)	54.40	24.59	13.60
Temperature of recombination (°K)	18,000	8,000	4,000
Lyman α emission rate A(sec^{-1})	$1.0\cdot10^{10}$	$2.3\cdot10^{9}$	$6.2\cdot10^{8}$
Tow-photon emission rate Λ(sec^{-1})	526.5[a]	46[b]	8.23[c]
n_a/n_I	$4.9\cdot10^{3}$	$8.6\cdot10^{3}$	$3.1\cdot10^{6}$
$(H/c)/(\sigma_I n_a)$	$1.6\cdot10^{-10}$	$1.3\cdot10^{-10}$	$4.4\cdot10^{-11}$
$n_I(2)/n_a$	$3.4\cdot10^{6}$	$2.9\cdot10^{7}$	$7.3\cdot10^{4}$
(Lyman α rate)/(Tow-photon rate)	$4.0\cdot10^{-2}$	$1.5\cdot10^{-1}$	$1.8\cdot10^{-2}$

a) M. Lipeles, R. Novick and N. Tolk, Phys. Rev. Letters **15** (1965), 690.
b) A. Dalgarno, Month. Notices Roy. Astron. Soc. **131** (1966), 311.
c) L. Spitzer, Jr. and J. L. Greenstein, Astrophys. J. **114** (1951), 407.

Eq. (E·16) as

$$-\frac{d}{dt}\left(\frac{n_{He^{++}}}{n_\alpha}\right)=\left\{\frac{\alpha n_e n_{He^{++}}}{n_\alpha}-\frac{\beta n_{He^+}}{n_\alpha}\exp(-B_\alpha/kT)\right\}C, \tag{4·5}$$

where C is an inhibition factor to reduce the direct capture to the ground state. The time scale of the recombination τ_{rec} is given as

$$\tau_{rec}=(\alpha n_e C)^{-1} \tag{4·6}$$

whose value is given in Fig. 9 in comparison with a time scale given by

$$\tau_{eq}=n_{eq}/(dn_{eq}/dt), \tag{4·7}$$

n_{eq} being the equilibrium values of He^+, He or H. Further, the ratio of the suppressed allowed transition rate to the two-photon emission rate is given from Eq. (E·12) as

$$\frac{(\text{Lyman-}\alpha\text{ transition})}{(\text{two-photon emission})}=\frac{1}{K\Lambda n_{He^+}} \tag{4·8}$$

whose value is given also in Table I. In the case of the recombination into He, we must notice that 2^1s-state is not degenerate with 2^1p-state and the inhibition factor becomes as

$$C=\frac{1+K\Lambda n_{He}e^{\Delta E/kT}}{1+K(\Lambda+\beta)n_{He}}, \tag{4·9}$$

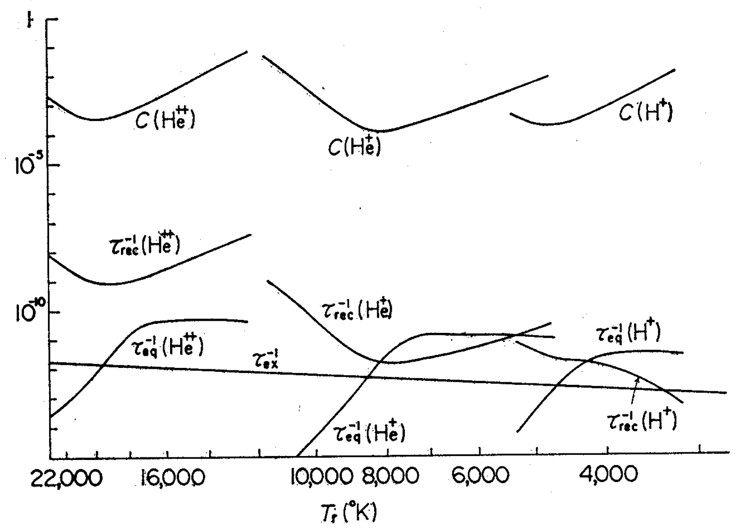

Fig. 9. Variation of the characteristic quantities of the recombination process in the universe model with $\Omega=1$. Inhibition factor of the direct capture C refers to a non-dimensional unit of the ordinate value. The inverses of the time scales τ_{rec}, τ_{eq} and τ_{ex} refer to unit of sec^{-1} of the ordinate value.

where the energy difference $\varDelta E$ between 2^1s-and 2^1p-states is 0.61 eV. The thermal equilibrium between the two spin states is attained through the spin flip reaction by particle bombardment.

The calculated evolution of ionization degree is shown in Figs. 10 and 11. As the recombination proceeds, the coupling between matter and radiation completely stops. Afterward the temperature of matter, T_m, decreases more rapidly than that of radiation, T_r, as shown in Fig. 7. The decrease of T_m is due to an adiabatic cooling in an usual meaning but that of T_r is due to the red-shift of freely travel-ing photons as will be ex-plained in §4 (iv).

If we consider a heating of matter, the epoch of the recombination is postponed later than that given in this section. We shall consider such a problem in §6.

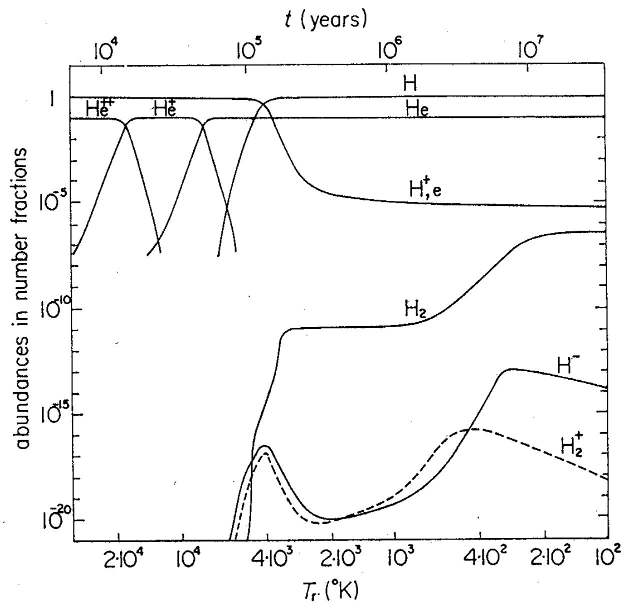

Fig. 10. Evolution of the abundances in the uniform medium for the universe model with $\Omega=1$.

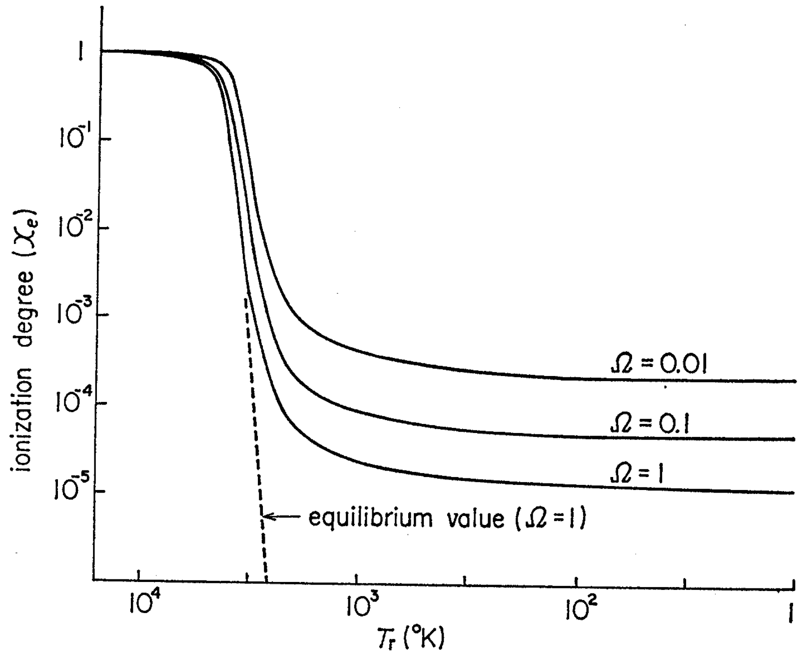

Fig. 11. Evolution of the ionization degree of hydrogen for the universe models with Ω=0.01, 0.1 and 1.

(iii) *Formation of hydrogen molecules*

After the recombination, hydrogen molecules begin to be formed through the reactions such as[103),104)]

$$H+e \rightleftarrows H^- + \gamma, \quad (4\cdot 10a)$$

$$H^- + H \rightleftarrows H_2^- \rightarrow H_2 + e, \quad (4\cdot 10b)$$

$$H+H^+ \rightleftarrows H_2^+ + \gamma$$

and

$$H_2^+ + H \rightleftarrows H_2 + H^+. \quad (4\cdot 11)$$

Electrons and protons which have been remained without recombination work as a kind of catalyzer. Dissociation of hydrogen molecules is mainly due to photo-dissociation such as

$$H_2 + \gamma \rightarrow H_2^* \rightarrow H+H. \quad (4\cdot 12)$$

The reaction rates of these reactions are given in Appendix G. However, the photo-dissociation rates of Eqs. (4·11) and (4·12), which are sharply dependent on the population among the vibrational levels, have a large ambiguity. If most of the synthesized atom were in the vibrationally ground state, an amount of H_2^+ produced through Eq. (4·11) might be as large as $H_2^+/H \sim 10^{-4}$. However, it may be much smaller by a factor of the order 10^{10} for a reasonable population.

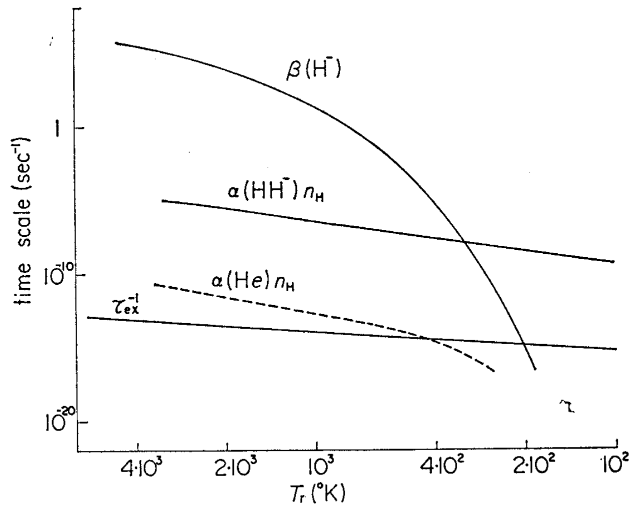

Fig. 12. Reaction rates for $H+e \to H^- + \gamma (\alpha(H, e))$, $H^- + H \to H_2 + e(\alpha(H, H^-))$ and $H^- + \gamma \to H + e(\beta(H^-))$. This comparison shows that formation of H_2 is effective only after the epoch of $T_r = 300°K$.

The time scales of the reactions are given in Fig 12, from which one sees that the equilibrium between H and H^- through the reaction of Eq. (4·10a) is maintained until the stage of $T_r \simeq 300°K$, this value is related to the binding energy of H^-, i.e., 0.75 eV. The equilibrium value of H^- is very small for $T_r > 300°K$ and the formation of H_2 is postponed until the stage of $T_r < 300°K$. The evolution of H_2 abundance is given in Fig. 11 and the final abundance is of the order of $H_2/H \simeq 10^{-6.5}$.[101] Thus, the abundance of H_2 in a uniform medium is not so large but that in the contracting pregalactic cloud becomes large enough to cool the matter.[102),105),106]

(iv) *Origin of the microwave background radiation*

The temporal change of the collision mean-free time around the stage of the recombination is given in Fig. 13. The mean-free time due to the Thomson scattering becomes suddenly larger than the length of horizon at the epoch of recombination. After then, the Rayleigh scattering is the main source of

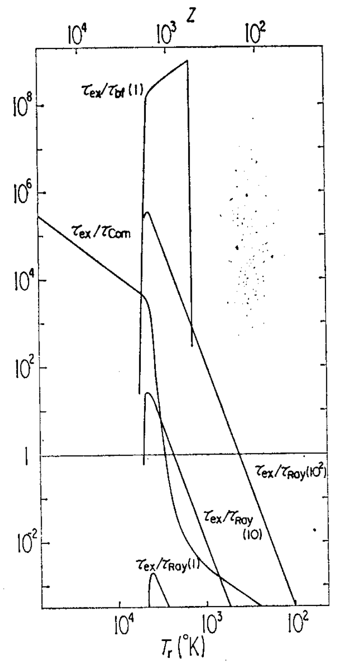

Fig. 13. Variation of τ_{Com}, $\tau_{bf}(x)$ and $\tau_{Ray}(x)$ by the ratio to τ_{ex}, where $\tau_{bf}(x)$ is defined by Eq. (D·10) for hydrogen and $\tau_{Ray}(x)$ is a time scale of Rayleigh scattering by the hydrogen atom.

scattering except the bound-bound absorption for some lines and the bound-free absorption for the ionizing photons. Though some photons may be coupled with matter through the b–b and b–f absorptions only during a short period, most of the thermal photons become free the matter after the recombination. In other words, the universe which has been cloudy until the recombination clears up after the recombination. If the heating of matter is strong enough to maintain ionized states of matter, the clearing-up of the universe is postponed to the epoch of $z \simeq 7 \sim 70$ for $\Omega \simeq 1 \sim 10^{-2}$.[108]

After the decoupling, the photons propagate freely and reach us at the present epoch as the isotropic microwave radiation. Putting the radiation flux at the coordinate $\boldsymbol{r}$ and the decoupling time t_D as $B(\nu, \boldsymbol{l}, \boldsymbol{r}, t_D)$, the observed flux at $\boldsymbol{r}=0$ and $t=t_0$ in the direction $\boldsymbol{l}_0$, $\boldsymbol{l}_0=\boldsymbol{r}/r$ being the unit vector in the direction of observation, is given as

$$I_\nu(\boldsymbol{l}_0) = \frac{B(\nu(\overline{z_D+1}), \boldsymbol{l}_0, \boldsymbol{r}, t_D)}{(\overline{z_D+1})^3}, \tag{4·13}$$

where $\overline{z_D}$ has been given by Eq. (C·16). If the radiation flux is the isotropic-uniform Planck spectrum,

$$I_\nu = \frac{2h\nu^3/c^2}{\exp(h\nu/kT_r(t_0))-1}, \tag{4·14}$$

where $T_r(t_0) = T_D(a(t_D)/a_0)$ and the decoupling temperature T_D is $\sim 4000°K$.

As anticipated from Eq. (4·13), there are two causes of anisotropy; an intrinsic anisotropy resulting from $B(\nu, \boldsymbol{l}, \boldsymbol{r}, t)$ and an apparent anisotropy resulting from the inhomogeneity of the metric, the red-shift parameter $\overline{z_D}$ being dependent on the direction of observation $\boldsymbol{l}_0$. The intrinsic inhomogeneity may result from the primordial inhomogeneity or from the local heating by decay of turbulence, release of gravitational energy, matter-antimatter annihilation and some other mechanisms.[98),107)~114)] By the heating in the *Compton* stage of the coupling stage, the energy spectrum is modified from the Planck spectrum into the Bose-Einstein spectrum with a finite chemical potential of photons.[98),114)] The inhomogeneous metric may result from the local gravitational field and the peculiar motion of matter,[115),116)] the apparent anisotropy being essentially due to the gravitational shift and the doppler shift (see Appendix C). Through the modification by the inhomogeneous metric, the spectrum is preserved. Even if an anisotropic flux is once established its anisotropy may be smeared out by the electron scattering[110)] or by the random deflection by gravitational field.[117)]

Observationally, any distinct anisotropy has not yet been detected in a relatively large angular size such as $10' \sim 1''$, as described in Appendix A. Theoretical estimation of the angular size and the degree of anisotropy has been given in Refs. 107), 108), 112) and 113).

In any way, the distribution of this background radiation is considerably isotropic and homogeneous, though some ideas of an isotropic inhomogeneous structure of the whole universe have been proposed.[118),119),119a)] In this meaning, this radiation can be regarded as a kind of ether, by which the inertia reference system is defined.[120)~123)] Therefore, the peculiar velocity of our sun and our galaxy can be determined from the weak anisotropy of this background, the degree of which may be of the order of 0.1%. However, this analysis has not yet succeeded until now.

§5. Inhomogeneous motions of the cosmic fluid and formation of galaxies

Though we have assumed the isotropic-homogeneous model of the universe, the actual universe is quite lumpy and stirring in the distribution and the motion of matter respectively. However, any significant departure of the space-time metric from the isotropic-homogeneous metric have not been detected observationally.[124)] Therefore, we may assume such inhomogeneities of density and velocity do not significantly distort the metric. This restriction will be satisfied if their sizes and the velocities of peculiar motions are much smaller than the radius of curvature of the space and the light velocity, respectively.[125),126)]

The evolution of the weak inhomogeneities has been studied by Lifshitz[34)] and many other authors.[127)] In their treatment, the cosmic fluid has been regarded as an ideal fluid. In the hot universe, however, effects of the dissipative process due to thermal neutrinos and thermal photons cannot be neglected for the fluid motions with small sizes.[128),129)] One consequence of the dissipation is to reduce the anisotropy of the metric by neutrino viscosity[130)] (see also a criticism in Ref. 130a)), and another consequence is to reduce the inhomogeneity of small scales by viscosity and thermal conductivity.[131),132)] As the small-scale inhomogeneities are considered to be the seeds of galaxies or galaxy clusters, the minimum mass of these objects can be explained by the dissipative process.[40),41),132)] Dissipative decay of the inhomogeneous motions leads to a heating of the cosmic medium,[42)] about which we consider in the next section.

(i) *Dissipative process in the radiative gas*

According to Lifshitz,[34)] small departures from the strictly isotropic-homogeneous model consist of scalar, vector and tensor perturbations, those are called more intuitively density fluctuations or acoustic motions, vortical fluctuations or eddy motions and gravitational waves, respectively. In the linear approximation, these three modes of perturbation are independent, but they are coupled with each other by non-linear effects, e.g., the coupling of acoustic motion with vortical motion being discussed in Ref. 133). A reasonable theory to estimate the absolute value of amplitude for each mode of perturbation has not been given except for some speculation.[134] As a fluid dynamical analysis is represented in Ref. 35) in this issue, our aim is to clarify physical properties of the cosmic fluid in the hot model.

In order to verify a fluid approximation of the inhomogeneous motion, we estimate the mean-free pathes for individual processes in the cosmic gas. After the annihilation of electron pairs, the mean-free path of photons is given as

$$l_{rr}=10^{13}/(T/10^8\,{}^\circ\mathrm{K})^9\ \mathrm{cm} \qquad \text{for photon-photon collision}$$

and

$$l_{re}=m_p/(\rho_m\sigma_T)=2.5/\rho_m\ \mathrm{cm} \qquad \text{for photon-electron collision,}$$

where the cross section of photon-photon collision is taken as $\sigma_{rr}=4.1\cdot 10^{-32}(E_r/m_ec^2)^6\ \mathrm{cm}^2$, E_r being photon energy. The mean-free path due to free-free absorption is much larger than l_{re}. On the other hand, the mean-free pathes of electrons and protons are much smaller than that of photons, e.g., $l_{ep}/l_{re}\sim 5\cdot 10^{-7}(T/10^8\,{}^\circ\mathrm{K})^2$, l_{ep} being the mean-free path for electron-proton collisions. The fluid approximation for photons is valid only for the relatively large-scale motions with $\lambda \gg l_r \equiv (l_{rr}^{-1}+l_{re}^{-1})^{-1}$, λ being the scale of the inhomogeneous motions. To acquire a more intuitive meaning about the scale of motions in the expanding universe, it is preferable to employ the mass M_λ defined by

$$M_\lambda=\rho_m\lambda^3=\rho_m\left(\frac{2\pi a}{k}\right)^3, \tag{5·2}$$

where k is wave number corresponding to λ. The mean-free path of photons is also given by the mass $M_l=\rho_m l_r^3$ in Fig. 14, from which we notice that the fluid approximation for photons is only valid in the coupling stage and the mean-free path of photons is not negligibly small compared with the size in which the mass of a galaxy is contained.

As photons run straightly between two collisions, the photons cannot tightly follow the motion of matter unless $\lambda \gg l_r$, the gravitational bend being neglected in our problem. As the ratio l_r/λ for some fixed M_λ increases with the cosmic expansion, the collective motion of photons will disappear at the stage of $l_r/\lambda \simeq 1$ at latest, and the larger inhomogeneities of photons survive longer than the smaller. In fact, the collective motion of photons is reduced before this stage, because of a drag force which results from the relative motion between the matter and the radiation decreases. Under the assumption of the fluid approximation, this drag-effect can be described in terms of viscosity and thermal conductivity as shown in Appendix G. Taking $l_r=l_{re}$, the kinematic viscosity of radiation ν_r is given by Eq. (G·22) as

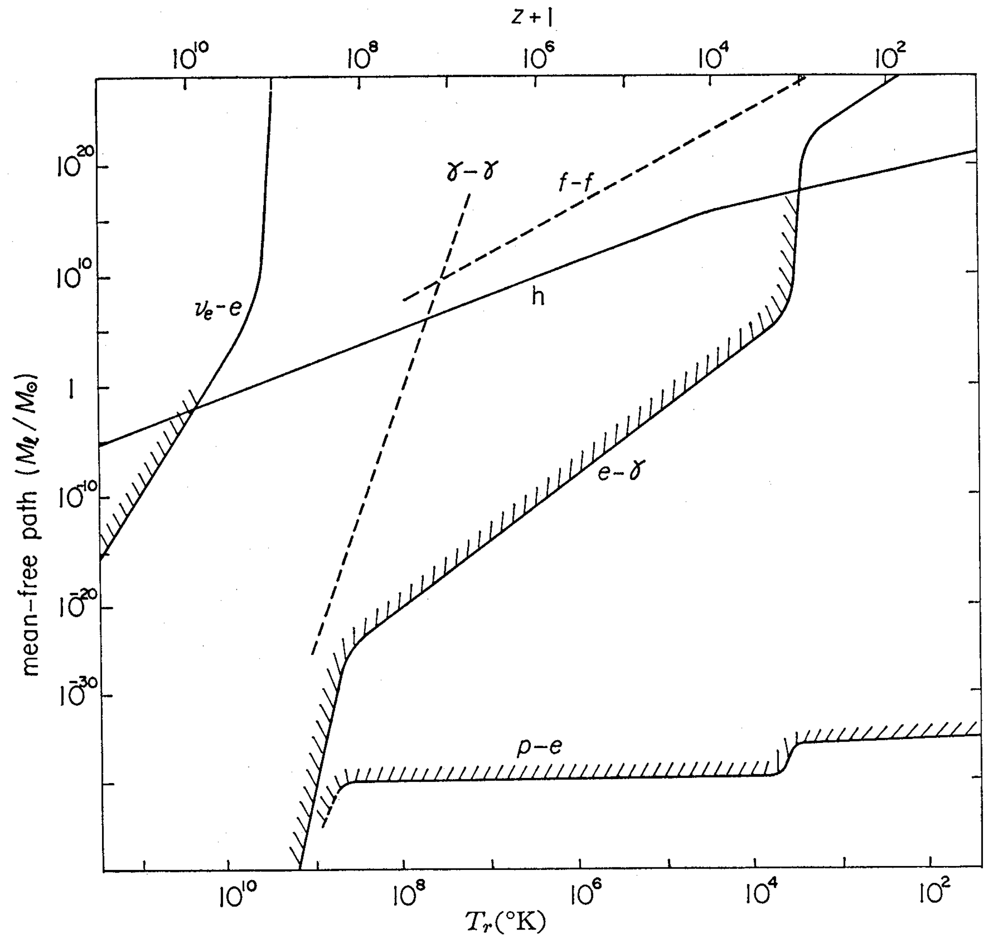

Fig. 14. Mean-free pathes for neutrino-electron collision (ν_e-e), photon-photon collision (γ-γ), collision due to free-free transition (f-f), collision due to Thomson scattering (e-γ) and ion-electron or atom-atom collision (p-e). In stead of the mean-free pathes themselves, we give them by the mass defined as $M_e=\rho_m$ (mean-free path)^3. The line denoted by (h) represents the mass involved within the horizon defined by $\rho_m(C\tau_{ex})^3$. z is redshift parameter defined as $z+1=a_0/a(t)$ in Eq. (C·5).

$$\nu_r=\frac{8}{27}cl_r\frac{\rho_r}{(\rho_m+\frac{4}{3}\rho_r)}\,. \tag{5·3}$$

The viscosity of radiation is much larger than the viscosity ν_g due to ion-ion collision; $\nu_g/\nu_r<10^{-17}$ at the epoch of decoupling.

(ii) *Dissipative decay of acoustic and vortical motions*[41)]

Formulation of the fluid dynamics with dissipation is given in Eqs. (G·7) ~(G·9).

For the acoustic fluctuation of $\nabla\cdot\boldsymbol{V}\neq 0$, a small departure from the uniform quantity, e.g., $\delta\rho/\rho$ for density, evolves the following relation:

$$\frac{\partial^2}{\partial t^2}\left(\frac{\delta\rho}{\rho}\right)+c_s^2\frac{k^2}{a^2}\left(1-\frac{k_J}{k^2}\right)\left(\frac{\delta\rho}{\rho}\right)+2\frac{1}{\tau_d}\frac{\partial}{\partial t}\left(\frac{\delta\rho}{\rho}\right)=0, \tag{5·4}$$

where k is a wave number of the fluctuation such as $\nabla^2(\delta\rho/\rho) = -k^2(\delta\rho/\rho)$, proper wave length being given as $\lambda = 2\pi a/k$, the sound velocity c_s is defined as

$$c_s = c\sqrt{\frac{4}{3}\frac{P}{\mathcal{E}+P}}\,, \tag{5·5}$$

Jeans wave number k_J is defined as

$$\frac{k_J}{a} \equiv \frac{2\pi}{\lambda_J} = \sqrt{4\pi G\left(\rho_m + \frac{8}{3}P_r\right)}\Big/c_s \tag{5·6}$$

and τ_d is the decay time by dissipation. In deriving Eq. (5·4), we have assumed that

$$\tau_{ex} \gg \tau_s \quad \text{and} \quad \tau_d \gg \tau_s\,, \tag{5·7}$$

τ_s being a period of acoustic wave defined by

$$\tau_s \equiv \lambda/c_s = 2\pi a/(kc_s). \tag{5·8}$$

For a large wave length such as $\lambda \gg c_s t$, the evolution is completely non-dissipative because of $\tau_d \gg \tau_{ex}$ and the adiabatic perturbation theory is applicable. The decay time τ_d is expressed in terms of a viscous decay time τ_{dv} and a conductive decay time τ_{dc} as

$$\tau_d^{-1} = \tau_{dv}^{-1} + \tau_{dc}^{-1}, \tag{5·9}$$

where

$$\tau_{dv} = \frac{9}{4}\left(\frac{c}{c_s}\right)^2 \tau_{diff}(k), \tag{5·10}$$

$$\tau_{dc} = 6\{1 - 3(c_s/c)^2\}^{-2}\tau_{diff}(k) \tag{5·11}$$

and $\tau_{diff}(k)$ is a diffusion time given by

$$\tau_{diff}(k) = a^2/(l_r k^2 c). \tag{5·12}$$

Later, we express $\tau_d = \tilde{\alpha}\tau_{diff}$, where $\tilde{\alpha} = 7.5 \sim 6.0$.

For the subsonic eddy motions of $\nabla \cdot \boldsymbol{V} = 0$ but $\nabla^2 \boldsymbol{V} = -k^2 \boldsymbol{V}$, the density, the temperature and the Newtonian gravitational potential do not deviate from the uniform background. The small departure of velocity from the general expansion evolves the following relation:

$$\frac{1}{c^2 a^2}\frac{\partial}{\partial t}[a^4(\mathcal{E}+P)\boldsymbol{V}] + \frac{\mathcal{E}+P}{c^2 a}\boldsymbol{V}\cdot\nabla\boldsymbol{V} - \frac{\eta_r}{a^2}\nabla^2\boldsymbol{V} = 0. \tag{5·13}$$

As seen from this equation, an evolution of the velocity field is characterized by three time scales: a time scale of evolution due to the non-linear inertia term given by

$$\tau_v \sim \lambda/v, \tag{5·14}$$

a decay time by viscosity τ_{dv}, and an expansion time scale $\tau_{ex} \sim t$. As the ratio τ_{dv}/τ_v represents the Reynolds number, the motions with $\tau_{dv}/\tau_v \gg 1$ may be generally in a turbulent state, but a pattern of velocity field remains constant for large eddies satisfying the condition $\tau_v/\tau_{ex} \gg 1$, that is, these large eddies are frozen.

Now, we introduce characteristic masses,

$$\text{Jeans mass} \quad M_J(t) = \rho_m \lambda_J^3, \tag{5·15}$$

$$\text{frozen mass} \quad M_v(t) = \rho_m (vt)^3 \tag{5·16}$$

and

$$\text{dissipation mass} \quad M_{dis}(t) = \rho_m \lambda_{dis}^3, \tag{5·17}$$

where λ_{dis} is defined by $\tau_d(\lambda_{dis}) = t$ and given by

$$\lambda_{dis} = \frac{2\pi}{\sqrt{\tilde{\alpha}}} \sqrt{l_r ct}\ . \tag{5·18}$$

When we consider the evolution of fluctuations with a given mass M_λ, we meet characteristic times, $t_J(M_\lambda)$, $t_v(M_\lambda)$ and $t_{dis}(M_\lambda)$, which are defined by

$$M_J(t_J) = M_v(t_v) = M_{dis}(t_{dis}) = M_\lambda\ . \tag{5·19}$$

In the case of turbulence, we use a dissipation mass M_{dis} defined by k_{dis}, where $\tau_{dv}(k_{dis}) = t$. Variations of these masses are given in Figs. 15 and 16. Reffering to these figures, we can get a gross evolutionary feature of the fluctuations until the decoupling. We denote the epoch of decoupling by t_D. The evolution of an accustic fluctuation whose wave length is given by a definite mass M_λ smaller than $M_{dis}(t_D)$ consists of the following three

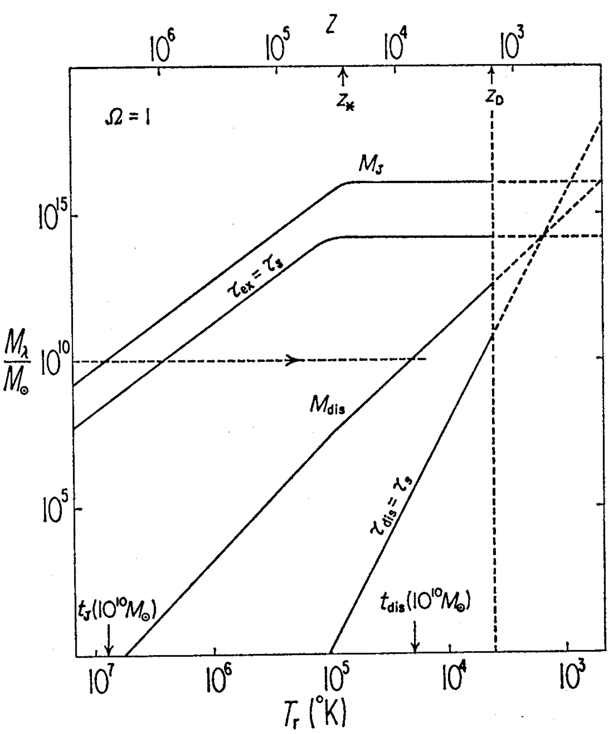

Fig. 15. Variations of Jeans mass M_J and dissipation mass for acoustic motions M_{dis} defined by Eqs. (5·15) and (5·17), respectively. τ_{sound} is period of acoustic wave defined by $\tau_{sound} = 2\pi a/c_s k$. Density fluctuation with a definite size, e.g., $M_\lambda = 10^{10} M_\odot$, grows monotonously up to t_J, oscillates between t_J and t_{dis}, and decays after t_{dis}.

stages; (1) Until t_J, the density contrast $\delta\rho_m/\rho_m$ shows monotonous growing by self-gravity. (2) Between $t_J(M_\lambda)$ and $t_{dis}(M_\lambda)$, $M_\lambda(t)$ becomes larger than M_λ and the density contrast begins to oscillate as the acoustic wave by radiation pressure. (3) After $t_{dis}(M_J)$, a reduction of the density contrast by the dissipation becomes severe until the radiation decouples from the matter at t_D. The evolution of the eddy motion containing a definite mass M_J smaller than $M_{dv}(t_D)$ also consists of three stages: (1) Until $t_v(M_\lambda)$, the eddy motion is frozen, that is, the size is increasing with the cosmic expansion but the magnitude of velocity remains constant for $t<t_*$. (2) Between $t_v(M_\lambda)$ and $t_{dis}(M_\lambda)$, the energy outflow to smaller eddies due to the non-linear inertia term becomes dominant but, soon, the energy inflow from the larger eddies begins also. The energy transported into such small eddies as $M_\lambda<M_{dis}$ is dissipated eventually into heat. (3) After $t_{dis}(M_\lambda)$, a dissipative decay of the eddy motion becomes severe.

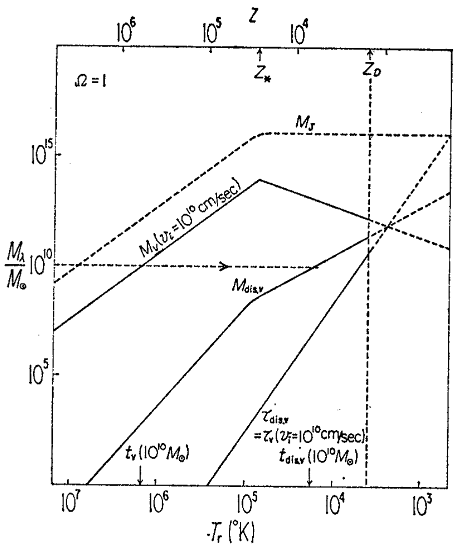

Fig. 16. Variation of M_J, $M_{dis,v}$ and frozen mass M_v for $v=10^{10}$ cm/sec. Velocity of the turbulent eddy with a definite size, e.g., $M_\lambda=10^{10}M_\odot$, is frozen up to t_v, decays into smaller eddies between t_v and $t_{dis,v}$, and dissipates into thermal motions.

Thus, the local inhomogeneities in density and velocity suffer eventually a strong reduction if their sizes are smaller than the critical size, i.e., $M_{dis}(t_D)$ or $M_{dis,v}(t_D)$. This reduction affects two phenomena; one is the mass spectrum of galaxies and the other is the thermal history of the universe.

(iii) *A possible origin of magnetic field*

As the drag force by radiation works more effectively on the electrons, a difference in velocity arises between the electrons and the ions. In the absence of interactions between radiation and ions, the angular velocity of an eddy motion changes with the expansion as $\omega_r \propto a^{-1}$ and $\omega_i \propto a^{-2}$, and the angular velocity of radiation ω_r becomes faster than that of matter ω_i. As the electron-photon coupling is tight in the radiation dominant stage, the electron-photon gas rotates faster than the ion gas. As pointed out by Harrison,[136] this expanding eddy generates magnetic field, whose strength is approximately given by

$$B \simeq \frac{m_p c}{e} \tilde{\zeta}, \tag{5·20}$$

where $\tilde{\zeta}$ is vorticity, i.e., $\tilde{\zeta}=|\nabla\times\boldsymbol{V}|$. To sustain the eddy motion, the rotational energy must be smaller than the gravitational energy. This condition put the upper limit of $\tilde{\zeta}$ as

$$\tilde{\zeta}<\left(\frac{3}{8\pi G\rho}\right)^{1/2}\sim\frac{1}{t}. \tag{5·21}$$

As $\tilde{\zeta}<10^{-12}$ sec at the end of the radiation dominant stage, $B<10^{-16}$ gauss. Thus, weak seed of magnetic field can be generated if the primordial eddy motion is assumed in the hot universe.

The decay of the magnetic field is determined by the magnetic viscosity $\nu_{\rm m}$ defined by[137)]

$$\nu_{\rm m}=\frac{c^2}{4\pi}\frac{m_e}{e^2}\left[\frac{1-x_e}{x_e}96a_{\rm B}^2+\frac{2}{3}\left(\frac{e^2}{kT_{\rm m}}\right)^2\ln\Lambda\right]\left(\frac{2\pi kT_{\rm m}}{m_e}\right)^{1/2}, \tag{5·22}$$

where $a_{\rm B}$ is the Bohr radius. Similar to Eq. (5·17), the magnetic dissipation mass is defined as

$$M_{\rm dis.m}(t)=\rho_{\rm m}(\nu_{\rm m}t)^{3/2} \tag{5·23}$$

and given in Fig. 17. As seen from this figure, the dissipative decay of the magnetic field is negligible even after the recombination except for very small eddies. Under the condition of $\nu_{\rm r}\gg\nu_{\rm m}$, a weak seed field is amplified by the turbulent dynamo mechanism up to the strength of $B^2/8\pi<\rho v^2/2$. The scales of the amplified field may be in the range of $M_{\rm dis.v}<M_\lambda<M_v$. If such magnetic fields are generated in the turbulent gas, the cosmic ray may be generated also in the pre-galactic era.[137),138)]

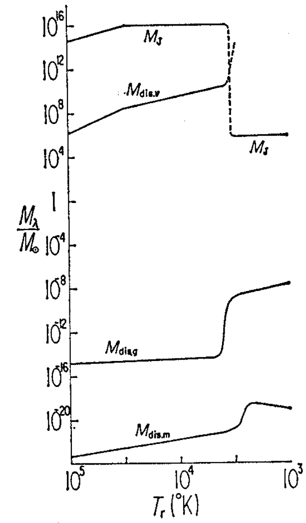

Fig. 17. Comparison of the magnetic dissipation mass $M_{\rm dis.m}$ defined by Eq. (5·23) with the dissipation mass for radiation viscosity $M_{\rm dis.v}$ and the dissipation mass for gaseous viscosity $M_{\rm dis.g}$.

(iv) *Size spectrum of inhomogeneities*[41),42),112),113)]

The size spectrum may be determined by the initial spectrum and its modification. In the case of the acoustic fluctuation, the weak density contrast of a definite M_λ evolves independently of others. Now, we define the Fourier components $(\delta\rho/\rho)_{\boldsymbol{k}}$ of the density contrast in such a way as

$$\frac{\delta\rho(\boldsymbol{r},t)}{\rho(t)}=\int\left(\frac{\delta\rho}{\rho}\right)_{\boldsymbol{k}}e^{i\boldsymbol{k}\cdot\boldsymbol{r}}d\boldsymbol{k}. \tag{5·24}$$

Evolution of these components can be summarized as follows: in the stage of $t \ll t_*$

$$\left(\frac{\delta\rho}{\rho}\right)_{\boldsymbol{k}} \propto a(t)^2 \qquad \text{for } k<k_J, \qquad (5\cdot25)$$
$$\propto \exp\left(-\int_{t_J}^{t}\frac{dt}{\tau_d}\right)\sin\left(k\int_{t_J}^{t}\frac{c_s}{a}d_t+\varphi\right) \qquad \text{for } k>k_J,$$

and in the stage of $t \gg t_*$

$$\left(\frac{\delta\rho}{\rho}\right)_{\boldsymbol{k}} \propto a(t) \qquad \text{for } k<k_J, \qquad (5\cdot26)$$
$$\propto a(t)^{-1/4}\exp\left(-\int_{t_J}^{t}\frac{dt}{\tau_d}\right)\sin\left(k\int_{t_J}^{t}\frac{c_s}{a}dt+\varphi'\right) \quad \text{for } k>k_J,$$

where φ and φ' are phases determined from the condition of joining solutions at t_J. As seen from the above relations, the growth rate in the stage of adiabatic perturbation, i.e., $t_{\text{dis}} \gg t$ is independent of k, but the epoch when the growth has stopped is dependent on k. The other effect which depends on k arises from the dissipative decay. Through these wave-number dependent effects, the initial spectrum will be modified.

For example, an initial spectrum $F(k, t_i)$ is modified in the stage of $t<t_*$ to

$$F(k,t)=F(k,t_i)\left(\frac{a}{a_i}\right)^4 \qquad \text{for } k<k_J(t), \qquad (5\cdot27)$$
$$=F(k,t_i)\left(\frac{a}{a_i}\right)^4\frac{k_J^4}{k^4}\sin^2\left(k\int_{t_J}^{t}\frac{c_s}{a}dt+\varphi\right)\exp\left(-\frac{2k^2}{k_d^2(t)}\right) \qquad \text{for } k>k_J(t),$$

where the spectrum $F(k,t)$ is normalized in such a way as

$$\left\langle\left(\frac{\delta\rho(\boldsymbol{r},t)}{\rho(t)}\right)^2\right\rangle=\int_0^\infty F(k,t)\frac{dk}{k}=\int_{\boldsymbol{k}}\left\{\left(\frac{\delta\rho}{\rho}\right)_{\boldsymbol{k}}\right\}^2 d\boldsymbol{k}, \qquad (5\cdot28)$$

$\langle\ \rangle$ represents the spatial average, and k_d is defined as

$$k_d^2=k^2\Big/\int_{t_J}^{t}\frac{dt}{\tau_d}. \qquad (5\cdot29)$$

Corresponding to k_d, we consider the mass defined as

$$M_d(t)=\rho_m(2\pi a/k_d)^3, \qquad (5\cdot30)$$

where $M_d(t)$ is the same order of magnitude as in Eq. (5·17) and is given later by Eq. (5·46). As seen from Eq. (5·28), the spectrum oscillates with

k*), but we are not concerned with such an oscillatory feature, because the spectrum of the localized inhomogeneities may be obtained by averaging this oscillatory spectrum over some range of k and the oscillatory feature may be smeared out.

According to these discussions, we may obtain a gross shape of the spectrum as shown in Fig. 18, where the initial spectrum is assumed to be the white noise spectrum such as

$$F(k, t_i) \equiv A\left(\frac{\delta\rho}{\rho}\right)_{k\mathrm{i}} k^3 = A'k^3. \qquad (5\cdot 31)$$

Peebles and Yu have advocated the spectrum such as $(\delta\rho/\rho)_{k\mathrm{i}} \propto k^{1/2}$, in order to avoid the deformation of metric by a large-scale inhomogeneity.[112] Generally, the spectrum has a broad maximum around k_J for $0 > m > -4/3$ and around k_d for $m < -4/3$, where m is a spectral index of the initial spectrum such as $F(M_\lambda, t_\mathrm{i}) \propto M_\lambda^m$.

Next, we consider the size spectrum of the eddy motions. Following the statistical theory of the incompressible homogeneous turbulence, the evolution of the energy spectrum is given by the relation;[42]

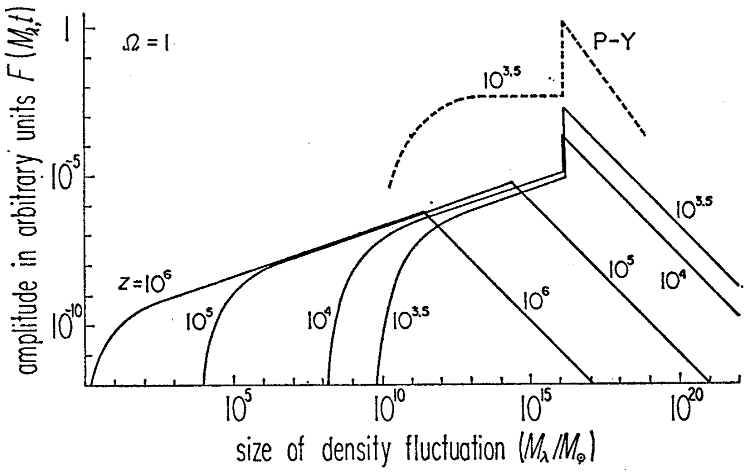

Fig. 18. Behaviour of size spectrum of acoustic inhomogeneous motion or density inhomogeneity. The abscissa represents the size of density inhomogeneities by masses involved within the sizes of inhomogeneities, and the ordinate does the amplitudes of the inhomogeneities in an arbitrary unit. Assuming that the initial inhomogeneity is the white noise, i.e., $F(k, t_\mathrm{i}) \propto k^3$, the spectra at $z = 10^6$, 10^5, 10^4, $10^{3.5}$ are shown for the universe model with $\Omega = 1$. The dotted curve denoted by P−Y is the shape of the spectrum taken from the initial spectrum of $F(k, t_\mathrm{i}) \propto k^4$.

*) According to Zeldovich and Sunyaev,[113] the zeros of the spectrum is given for masses M_0 satisfying

$$M_0/M_J = 1/(n\pi - \varphi_1)^3,$$

φ_1 being given as $\varphi_1 = \varphi - \int_0^{t_J} (kc_s/a)dt$ and $n = 1, 2, 3, \cdots$.

$$-\frac{\partial E(k,t)}{\partial t}=T(k,t)+2\left[\frac{\eta}{(\mathcal{E}+P)}\frac{k^2}{a^2}+\frac{d\{(\mathcal{E}+P)a^4\}/dt}{(\mathcal{E}+P)a^4}\right]E(k,t), \tag{5·32}$$

where $E(k,t)$ is the energy spectrum defined as $V^2=\int_0^\infty E(k,t)dk$ and $T(k,t)$ is a transfer term of energy among other wave numbers. Solving Eq. (5·32) under a suitable assumption on $T(k,t)$ is a very tedious problem and we give only a rough discussion in Appendix H, in order to illustrate the effect of the cosmic expansion. According the discussion, the evolution of the spectrum is given in Fig. 19, where we have used the spectrum $F(M_\lambda,t)$, normalized as $v^2/c_s^2=\int_0^\infty F dM_\lambda/M_\lambda$, instead of $E(k,t)$. A general characteristics is the turnings of slope at $M_v(t)$ and $M_{\mathrm{dis.v}}(t)$. The three regions of this spectrum, i.e., the frozen eddies $M_\lambda>M_v(t)$, the cascading eddies $M_v(t)>M_\lambda>M_{\mathrm{dis.v}}(t)$ and the dissipating eddies $M_\lambda<M_{\mathrm{dis.v}}(t)$ are corresponding the three stages of the evolution of a definite mass as stated in §5 (ii), respectively.

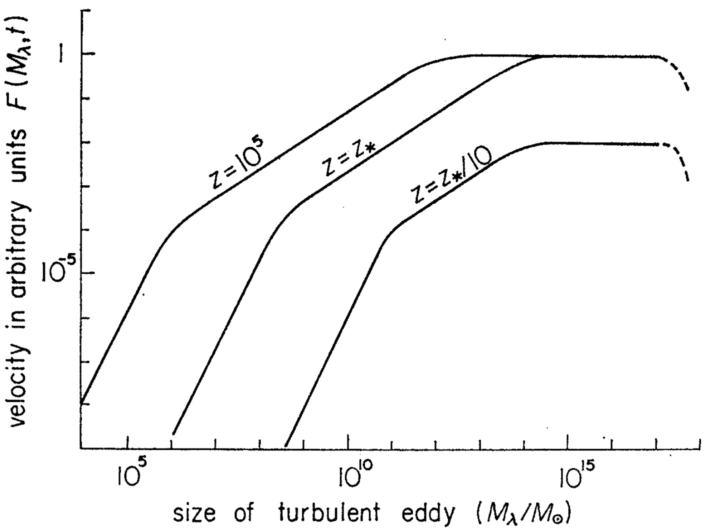

Fig. 19. Behaviour of size spectrum of vortical motions or turbulent motions, obtained from the discussion in Appendix H. The abscissa and the ordinate represent size of vortex and magnitude of velocity, respectively. Assuming that the initial spectrum is given by Eq. (H·4) with $m=1$, i.e., flat spectrum, and $v_0=10^{10}$ cm/sec, the spectram at $z=10^5$, z_* and $z_*/10$ are given for the model with $\Omega=1$.

(v) *Heating rates by dissipation*[41),42)]

A reduction of the inhomogeneity by dissipation accompanies necessarily the production of heat. For the density fluctuation, the heating rate per unit volume is given as

$$\epsilon_d=\frac{4}{27}\left\{\frac{10}{9}+\left(1-\frac{3c_s^2}{c^2}\right)^2\frac{c^2}{c_s^2}\right\}\frac{\mathcal{E}_r c l_r \overline{k^2}}{a^2}\frac{v^2}{c^2} \tag{5·33a}$$

and

$$\overline{k^2}=\int_0^\infty kF(k,t)dk\Big/\int_0^\infty k^{-1}F(k,t)dk \tag{5·33b}$$

which has been obtained taking a spatial average of Eq. (G·7) under the assumption of an isotropic inhomogeneity. If we take the spectrum as shown in Fig. 18, $\overline{k^2}$ is given as

$$\overline{k^2}=0.47k_d k_J \qquad \text{for} \quad t \ll t_*, \tag{5·34}$$

assuming $k_d \gg k_J$. Substituting Eq. (5·34) into Eq. (5·33a) and using Eq. (5·29), we get

$$\epsilon_d \simeq 0.55\frac{\mathcal{E}_r}{c^2}\frac{v^2}{t}\frac{k_J}{k_d}. \tag{5·35}$$

For the eddy motions, the heating rate has been discussed in Ref. 35) taking into account the law of turbulence in the non-expanding medium. In this theory, the decay of velocity is written as

$$v^2(t)=\left[\frac{\{(\mathcal{E}+P)a^4\}_{\rm i}}{(\mathcal{E}+P)a^4}\right]^2\left(\frac{\beta_{\rm i}}{t/t_{\rm i}-1+\beta_{\rm i}}\right)^s v_{\rm i}^2, \tag{5·36}$$

with

$$\beta_{\rm i}=\overline{\lambda}_{\rm i}/v_{\rm i}t_{\rm i}.$$

This expression is applicable for $\beta_{\rm i} \lesssim 1$, where $\overline{\lambda}_{\rm i}$ is a mean scale of the vortical motions and s is taken as 1, 10/7 or 5/2. From this, we can get the heating rate per unit volume as

$$\epsilon_d=\frac{(\mathcal{E}+P)}{2c^2}\left[\frac{\{(\mathcal{E}+P)a^4\}_{\rm i}}{(\mathcal{E}+P)a^4}\right]^2\frac{s\beta_{\rm i}^2 v_{\rm i}^2/t_{\rm i}}{(t/t_{\rm i}-1+\beta_{\rm i})^{s+1}}. \tag{5·37}$$

(vi) *Formation of condensed objects and their masses*[40),41)]

Strong inhomogeneities in matter distribution on the scale of a galaxy and/or a galaxy cluster are generally considered to result from the evolution of the primordial weak inhomogeneity. However, it has been pointed out that the instability due solely to the self-gravity is ineffective to form the strong density contrast. In order to get rid of this defect, several mechanisms have been proposed: the hydrodynamical instability,[39),41),139)] the thermal instability,[36),38)] the composition instability between matter and antimatter,[65)] and so on. Among them, we consider the hydrodynamical instability is the most promissing one, because this mechanism can explain, in a natural way, the mass of a galaxy.

Complete analysis of the hydrodynamical instability has not been given. Qualitatively, this instability is due to a dynamical compression by supersonic fluidal motions, which arise not from an acceleration of the fluid but from a sudden decrease of the sound velocity. By the decoupling of the matter from the thermal radiation, the sound velocity decreases from c_s, defined by Eq. (5·5), to $c_{sm}=\sqrt{5P_m/3\rho_m}$, P_m being a pressure of matter. Then, the fluidal velocity v changes from subsonic one to supersonic if $c_s>v>c_{sm}$ at the decoupling time, as shown schematically in Fig. 20 (see also Fig. 24). In the supersonic medium, a strong density contrast of the order of $\delta\rho/\rho \simeq (v/c_{sm})^2$ will be formed by the compression in the time scale of τ_V. The density contrast can be formed not only from the acoustic motions but also from the eddy motions, because the potential flow such as $\nabla\cdot \boldsymbol{V} \neq 0$ arises from the vortical flow also in the time scale τ_V. Once the density contrast is formed in this way, the self-gravity becomes strong enough to detouch the condensed object from the ambient expanding medium.

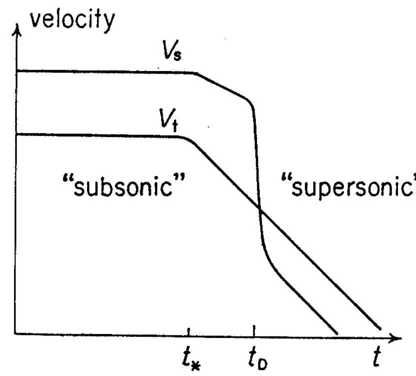

Fig. 20. Ozèrnoi-Chernin's idea to explain the origin of density inhomogeneity by the supersonic dynamical pressure after the decoupling time t_D. (See also Fig. 24.)

From the above discussions, we can find two necessary conditions of the hydrodynamic instability,

$$\lambda/v(<M_\lambda)<t \qquad (5\cdot 38)$$

and

$$v(<M_\lambda)>c_{sm} \qquad (5\cdot 39)$$

at the decoupling. The condition Eq. (5·38) gives the maximum mass of inhomogeneities which evolve into condensed objects. Because of the dissipative decay before the decoupling, the size spectrum has a sharp cut-off around $M_d(t_D)$ or $M_{dis.v}(t_D)$ as shown in Figs. 18 and 19. The condition Eq. (5·39) gives the minimum mass, if the amplitude around the peak of the spectrum is large enough to satisfy the condition Eq. (5·34) at the decoupling. Thus the maximum mass M_{max} and the minimum mass M_{min} can be estimated from the above discussions, if the size spectrum is known.

For an example, if we assume a spectrum of density fluctuations such as

$$F(M_\lambda, t)=g(t)(M_\lambda/M_J(t))^\gamma \quad \text{for} \quad M_d<M_\lambda<M_J, \qquad (5\cdot 40)$$

the velocity is given as

$$v(<M_\lambda)=(3g(t)/\gamma)^{1/2}(M_\lambda/M_J)^{\gamma/2}c_s \qquad (5\cdot 41)$$

and we have from Eq. (5·38)

$$M_{max} \simeq (3g(t)/\gamma)^{3/(2-3\gamma)} \cdot 10^{-5.0/(2-3\gamma)} M_J(t_D), \tag{5·42}$$

assuming $\gamma < 2/3$ and $\gamma \neq 0$. The numerical value of M_J at t_D is given as

$$\begin{aligned} M_J(t_D) &= 10^{16.1} \Omega^{-2} M_\odot \quad \text{for} \quad \Omega > 10^{-1.4}, \\ &= 10^{19.9} \Omega M_\odot \quad \text{for} \quad \Omega < 10^{-1.4}. \end{aligned} \tag{5·43}$$

On the other hand, Eq. (5·39) gives

$$\delta\rho/\rho > (\delta\rho/\rho)_{min}, \tag{5·44}$$

where $(\delta\rho/\rho)_{min} = \sqrt{\Omega}\, 10^{-4.1}$ for $\Omega > 10^{-1.4}$ and $10^{-4.6}$ for $\Omega < 10^{-1.4}$, and the minimum mass can be given by the relation such as

$$g(t_D)(M_{min}/M_J(t_D))^\gamma \exp[-2(M_d(t_D)/M_{min})^{2/3}] \simeq (\delta\rho/\rho)^2_{min}, \tag{5·45}$$

where $M_d(t_D)$ is given as

$$\begin{aligned} M_d(t_D) &= 10^{12.6} \Omega^{-5/4} M_\odot \quad \text{for} \quad \Omega > 10^{-1.4}, \\ &= 10^{13.4} \Omega^{-1/2} M_\odot \quad \text{for} \quad \Omega < 10^{-1.4}. \end{aligned} \tag{5·46}$$

As seen from Fig. 19, Eq. (5·45) gives roughly

$$M_{min} \simeq 10^{-2} M_d(t_D), \tag{5·47}$$

if g is not too small. For example,

$$M_{max} \simeq 10^{11.6} M_\odot \quad \text{and} \quad M_{min} \simeq 10^{10.9} M_\odot, \tag{5·48}$$

if we take $\gamma = 1/3$ or initial spectral index $m = -1$, $g = 1/10$ and $\Omega = 1$.

For the eddy motions whose spectrum is similar to Eq. (5·40), M_{max} is given also by Eq. (5·42), though the case of $\gamma = 2/3$ is excluded. If we assume $F \propto M_\lambda^2$ for $M_{dis.v} > M_\lambda$ as in Eq. (H·8), the minimum mass is given by

$$M_{min} \simeq \frac{1}{\sqrt{3g(t_D)}} \left(\frac{c_{sm}}{c_s}\right) \left(\frac{M_J(t_D)}{M_{dis.v}(t_D)}\right)^{\gamma/2} M_{dis.v}(t_D). \tag{5·49}$$

Based on these discussions, it may be permissible to conclude that the mass of a galaxy is determined by the mecahanism stated above.

§6. Thermal history of the hot universe

In §5, we have assumed the primordial existence of the inhomogeneous motions of the cosmic medium, in order to explain the formation of condensed objects such as galaxies. On the other hand, the energy of these motions dissipates into heat energy through the collision between electrons and photons, and the inhomogeneous motions affect the thermal history. An exchange of heat energy between matter and radiation is determined mainly by the Compton scattering. As the heat capacity of the radiation is large compared with that of matter, the matter temperature becomes larger than the radiation temperature and the heat energy flows from the matter into the radiation, that is a cooling of matter. If the matter temperature rises sufficiently, the radiation flux from the matter modifies the primordial spectrum of the radiation, that is observed now as the metagalactic background radiation. For simplicity, we have assumed a spatially homogeneous heating in this section. If the heating is inhomogeneous, the background radiation will have an anisotropy of small angular sizes as discussed in §4 (iv).

The heating due to the primordial inhomogeneous motions is different from the heating of the metagalactic matter due to an activity of galaxies such as proposed by Ginzburg and Ozernoi.[140] The former is a pre-galactic heating and the latter is a post-galactic one. We consider mainly the pre-galactic heating in this section.

(i) *Heating of matter before the decoupling*

Time variation of matter temperature is governed by the following equation,

$$\frac{dT_m}{dt} = -2\frac{\dot{a}}{a}T_m + \frac{2}{3}\frac{m_p}{k\rho_m}(\epsilon_d - \epsilon_c), \tag{6·1}$$

where ϵ_d and ϵ_c are heating rate and cooling rate of matter per unit volume. The cooling mechanism consists of the Compton scattering and the radiative processes such as bound-bound, bound-free and free-free transitions. A comparison between the cooling rates is given in Fig. 21. Undedr the condition in the universe, however, the Lyman-α emission is suppressed by the factor in Eq. (E·11), and the two-photon emission becomes larger than the allowed emission. Thus, the Compton scattering is found to be most dominant before the decoupling time. The cooling rate by the Compton scattering is given as

$$\epsilon_{Com} = \frac{4\sigma_T n_e}{m_e c}\mathcal{E}_r k(T_m - T_r), \tag{6·2}$$

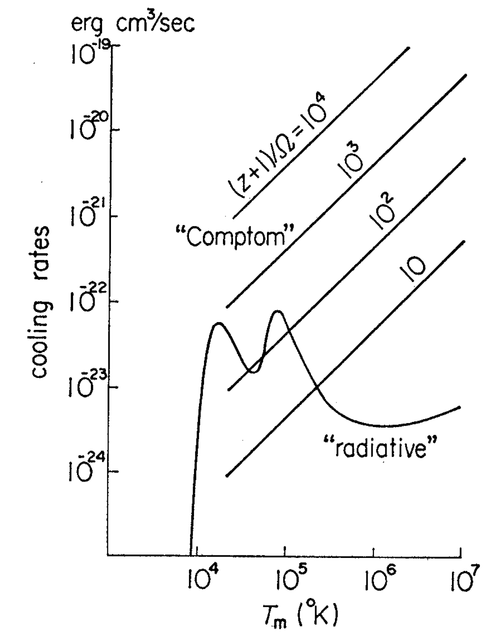

Fig. 21. Comparison of radiative cooling rate with Compton cooling rate. The radiative cooling rate, which includes those due to bound-bound, bound-free and free-free transitions of hydrogen and helium with He/H=1/10, is taken from Ref. 147).

where $\mathcal{E}_r$ is radiation energy density. This expression is correct only for the radiation field in a thermal equilibrium, i.e., the radiation with Bose-Einstein spectrum including Planckian one.[141] As discussed later in §6 (v), a distortion of the radiation spectrum from the Planckian is very small for the thermal history considered in the present paper.

In an early stage, $\epsilon_{\rm Com}$ is much larger than the adiabatic cooling rate defined by $\epsilon_{\rm adi}=3(\dot{a}/a)(k\rho_{\rm m}/m_{\rm p})T_{\rm m}$, and the heating has been balanced with the Compton cooling, i.e., $\epsilon_c=\epsilon_d$, which gives the following relations,

$$
\begin{aligned}
(T_{\rm m}-T_{\rm r})/T_{\rm r} &= \frac{m_e c}{4\mathcal{E}_{\rm r}\sigma_T n_e}\frac{\epsilon_d}{kT_{\rm r}} \\
&\simeq \frac{10^{-3.3}}{\Omega}\left(\frac{10^3}{z+1}\right)^2\left(\frac{\epsilon_d\tau_{\rm ex}}{\mathcal{E}_{\rm r}}\right) \quad \text{for } t\ll t_*, \qquad (6\cdot3)\\
&\simeq \frac{10^{-2.6}}{\Omega}\left(\frac{10^3}{z+1}\right)^{2.5}\left(\frac{\epsilon_d\tau_{\rm ex}}{\mathcal{E}_{\rm r}}\right) \quad \text{for } t\gg t_*,
\end{aligned}
$$

where $(\epsilon_d\tau_{\rm ex})$ represents roughly an amount of heat energy generated at the stage of $t\simeq\tau_{\rm ex}$. As we have assumed that the energy of heating is supplied by the weakly inhomogeneous motions as discussed in §5 (v), the condition $(\epsilon_d\tau_{\rm ex}/\mathcal{E}_{\rm r})\ll1$ is satisfied always, and therefore, the departure of $T_{\rm m}$ from $T_{\rm r}$ is found to be small in the coupling stage. After the recombination, however, the cooling time increases suddenly, so the flow of energy stagnates at the matter energy and the matter temperature rises suddenly in the presence of heating source. Because of a large heat capacity of the radiation, the accumulation of the energy in the radiation has little effect on $T_{\rm r}$.

(ii) *Evolution of heating rate*

In this subsection, we discuss an evolutionary property of the heating rate given in §5 (v). As is seen from the time variation of the size spectrum of the inhomogenegous motions, the source of heat energy is small-scale motions in early stages and large-scale motions in later stages. Therefore, the evolution of the heating rate may be dependent on the size spectrum.

At first, we consider the case of acoustic motions. Using Eq. (5·33a) for $t\ll t_*$, we can deduce the time variation of ϵ_d. If we write a time variation of the heating rate as $\epsilon_d\propto a^{-\alpha}$ for the initial size spectrum of $F(M_\lambda, t_i)\propto M_\lambda^m$, α varies from 6 to 0, when m does from $-4/3$ to $1/3$, e.g., $\alpha=4.5$ for $m=-1$ (a white noise spectrum) and $\alpha=1$ for $m=0$ (a flat spectrum). As physically expected, ϵ_d decreases with time faster if the energy of small-scale motions is larger than that of the larger ones in the initial spectrum. An effect of the heating on the thermal history cannot be represented by ϵ_d itself but can be done by such quantities as

$$(T_m - T_r)/T_r \propto a^7 \epsilon_d$$

and $$(\epsilon_d \tau_{ex})/\mathcal{E}_r \propto a^6 \epsilon_d\,. \tag{6·4}$$

Therefore, the heating is more ineffective in earlier stages if $m > -4/3$, though ϵ_d itself is larger in earlier stages.

In the case of turbulence, the size of eddy effective for the heating is larger than that in the case of acoustic motions. As expected from Fig. 20, available eddies for the heating is restricted to the eddies of sizes smaller than $2\pi a/k_I(t_*)$. If we put the initial spectrum as $F(M_\lambda, t_i) = (v_0/c_s)^2 (M_\lambda/M_0)^m$, Eq. (H·9) gives

$$\epsilon_d \simeq \frac{\mathcal{E}_r}{c^2} \frac{v_0}{t} \left(\frac{M_I(t)}{M_0}\right)^m, \tag{6·5}$$

where $M_I(t)$ is defined by $M_I(t) = (M_I(t)/M_0)^{3m/2} \rho_m (v_0 t)^3$. For the stage of $t \ll t_*$, ϵ_d is proportional to $a^{12\cdot(2m-1)/(2-3m)}$. For some choice of m except for $0 < m < 2/3$, the effect of heating is larger in the earlier stage but $a/k_I(t)$ decreases with time in such cases; only a small portion of the total turbulent energy has been consumed. Therefore, we can conclude that the effect of the heating is also more ineffective in earlier stages.

As the largest and the most energetic eddy in the stage $t \gtrsim t_*$ is the eddy with mass of $M = \rho_m \{2\pi a/k_I(t_*)\}^3$, we use Eq. (5·37) with $t_i = t_*$ and $\beta_i = 1$ as the heating rate for $t > t_*$.

(iii) *Thermal history after the decoupling*[43)]

As a result of the discussion in §6 (ii), we may consider only later stages to clarify the thermal history. As an example, we show a solution of Eq. (6·1) with the heating due to the decay of the turbulence in the stage $t > t_*$, ϵ_d being taken from Eq. (5·37) with $s = 1$. As a cooling rate, we include not only the Compton scattering but also the radiative processes. The results of numerical integration for several values of the initial turbulent velocity v_i are shown in Figs. 22∼25. To calculate the time variation of degree of ionization, Eq. (E·16) in Appendix E has been used.

Even in the case with the heating, the recombination of hydrogen commences at $T_r \simeq 4000$°K because the rate of photo-ionization decreases suddenly (see Fig. 23). As the energy flow stagnates in the matter energy, T_m begins to rise, the population of 2s-and 2p-states increases through collisional excitation by the heated electrons, the collisional-ionization rate increases and the recombination is suppressed. This effect is represented by the factor D in Eq. (E·18), which becomes as large as 10^{39}. As an increase of the ionization degree results in an increase of the cooling rate, T_m cannot exceed some critical temperature about $10^{4.3}$°K. This self-controlled mechanism works as a kind of a thermostat to check the rise of the temperature of matter.

As T_m increases, the radiative cooling becomes efficient and the most effective mechanism is always the Compton scattering as seen in Fig. 21. The turbulent velocity decreases very rapidly in comparison with the adiabatic deceleration by the cosmic expansion as shown in Fig. 24. As the recombination proceeds, the sound velocity decreases suddenly and the turbulent velocity becomes supersonic at some stage. For the decay law of supersonic turbulence, we have assumed as

$$\epsilon_d \simeq \rho_m \frac{v_t^2}{t}. \qquad (6\cdot6)$$

Though this assumption is rather unfounded, our result is not so sensitive to this assumption.

As time goes on, the energy source is consumed as seen in Fig. 24 and T_m begins to decrease adiabatically after the epoch with the

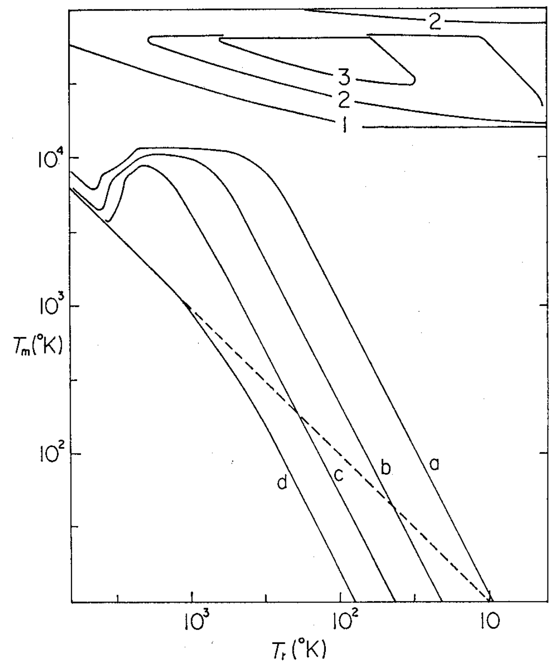

Fig. 22. Variation of matter temperature by the heating due to the decay of turbulence for the universe model with $\Omega=0.1$. The initial velocity, that is the velocity before t_*, is taken as (a) $3\cdot10^9$ (b) 10^9, (c) $3\cdot10^8$, (d) 0 in an unit of cm/sec. On the contour curves denoted by 1, 2 and 3, the growth time of thermal instability is equal to $10^{-1}\tau_{ex}$, $10^{-2}\tau_{ex}$ and $10^{-3}\tau_{ex}$ respectively.

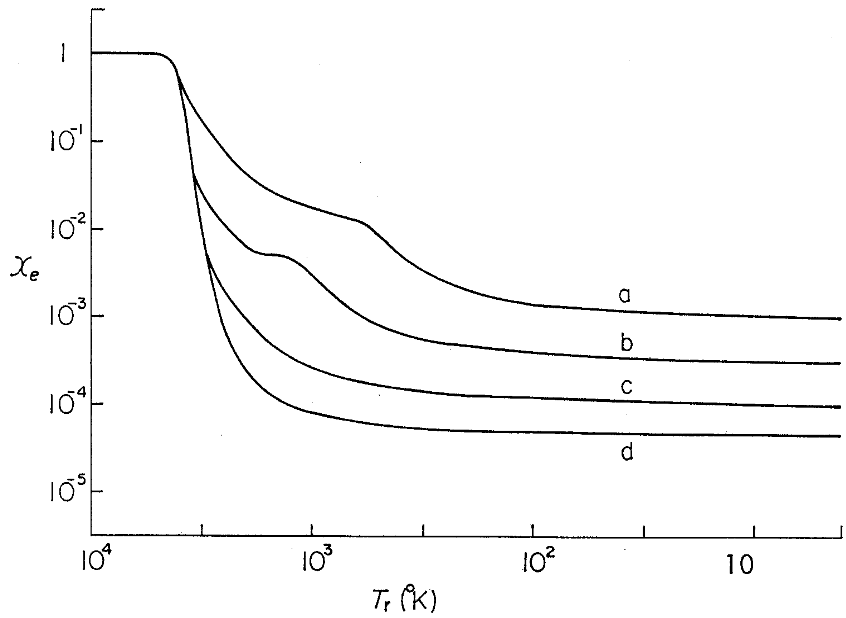

Fig. 23 Variation of ionization degree of hydrogen for the cases in Fig. 22.

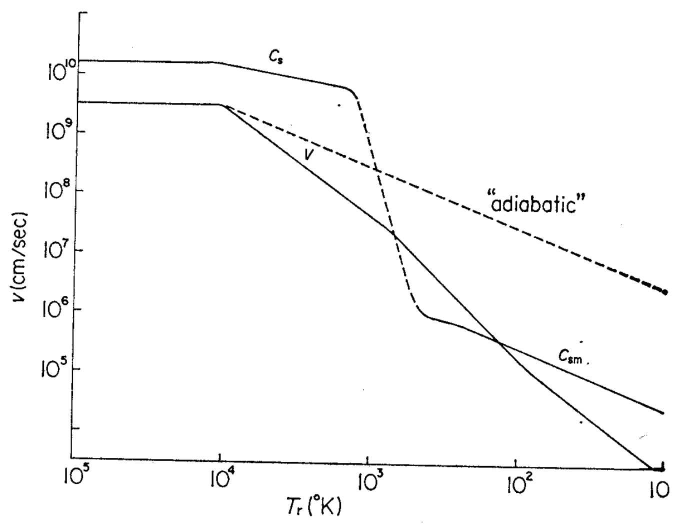

Fig. 24. Variations of turbulent velocity and sound velocity for the case (a) in Fig. 23. A sudden transition of sound velocity from c_s into c_{sm} is taken at the epoch when the mean-free path equals the horizon defined by $c\tau_{ex}$. Without the decay of turbulence, the velocity would change along the line denoted by "abiabatic".

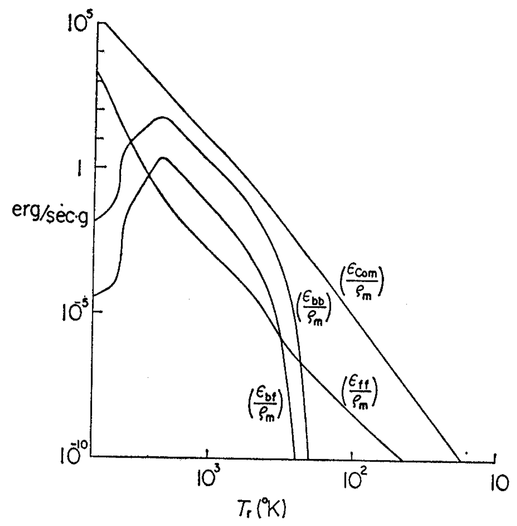

Fig. 25. Variation of cooling rates of matter for the case (a) in Fig. 22.

maximum temperature. A larger amount of electrons does not recombine and T_m is larger even after the stop of heating in comparison with the case without heating. This condition is preferable to form hydrogen molecules as stated in §4 (iii), and the amount of hydrogen molecules produced may attain as large as $H_2/H \sim 10^{-3.5}$.

In the dense universe model with larger Ω, the rise of temperature is smaller for the same value of v_1, because the velocity has been damped out until the epoch of recombination. In the thin universe model, the collision between electrons and photons becomes more scarce in later stages, and the viscosity becomes meaningless. Under a teneous medium, it is questionable whether the fluidal velocity of radiative gas is available for a source of heating. Therefore, the heating may also be suppressed in very thin universe models. In these cases, the radiation field may remain to be anisotropic even after the decoupling. This problem, however, has not been solved.

(iv) *Heating by galactic activity and thermal instability*

The energy source of heating due to the primordial inhomogeneous motions has been consumed soon after the decoupling, and the temperature of the present metagalactic matter becomes as low as $T_{m0} < T_{r0} = 2.7°K$, even if we take into account the pre-galactic heating. However, there are some observational evidences to suggest that the present metagalactic matter is hot enough to be ionized. These evidences include the low opacity of Lyman-α line from QSO,[142] the detected upper limit of the 21 cm radiation from the metagalactic matter[143),144] and others.[145] Ginzburg and Ozernoi[140] and others[146]~[149] have advocated a hypothesis that the metagalactic matter has been heated by the activity of galaxies through energetic particles, shock waves, turbulent motions and others. Their hypothesis is different from ours given in §6 (iii) in the points of its energy source and its epoch of heating. Our aim is to investigate the state of the pre-galactic stage. As our heating is most effective in the period soon after the decoupling, the presence of the primordial radiation is essential to our discussion; our heating is different from the heating proposed by Ginzburg et al.

An estimate of the heating rate by galaxies is difficult, and now we take a rather arbitrary assumption. To overcome the large cooling rate around $T_m = 10^{4.3}$ °K and $10^{4.8}$ °K, the heating rate ϵ_d has to be larger than $10^{-22.2} n_H^2$ erg/sec cm^3. An expectation of the overall thermal history is given in Fig. 26, combining our result with Weymann's result for the post-galactic heating,[147] where the period of the post-galactic heating stage is assumed rather arbitrary. Following the discussion in Ref. 96), it is not plausible that the metagalactic matter is ionized throughout the whole history, because such hypothesis conflicts with the observed flux of the background radio wave around $\lambda = 1.7$ m. Therefore, there may be two discrete periods of heating as shown in Fig. 26.

As seen from Fig. 21, the radiative cooling process dominates over the Compton cooling for $T_m > 10^4$ °K, if T_r is sufficiently low. Under such a stage, the condition of thermal instability, that is written as $(\partial\epsilon_c/\partial T)_p < 0$ assuming $(\partial\epsilon_d/\partial T)_p = 0$, is satisfied for $T_m > 10^{4.3}$ °K except for $10^{4.7}$ °K $< T_m < 10^{4.9}$ °K. A detailed analysis of thermal instability in such condition has been given by Kondo et al.[38] Referring to their result, the instability region where the growth time of instability is sufficiently shorter than τ_{ex} is depictated in Fig. 22. This instability region depends on a size of the unstable region and it shifts to the low density part if the size is increased.

If the evolutionary path of T_m goes through this instability region, density contrasts appear here and there by the compression by the pressure of surrounding medium, and they may evolve into condensed gas clouds. In our evolutionary paths of T_m, however, this thermal instability seems difficult to occur, because the maximum temperature is a little smaller than that required for the instability. Although this instability may occur by the heating due to the galactic activity at later stages, we must notice that this heating

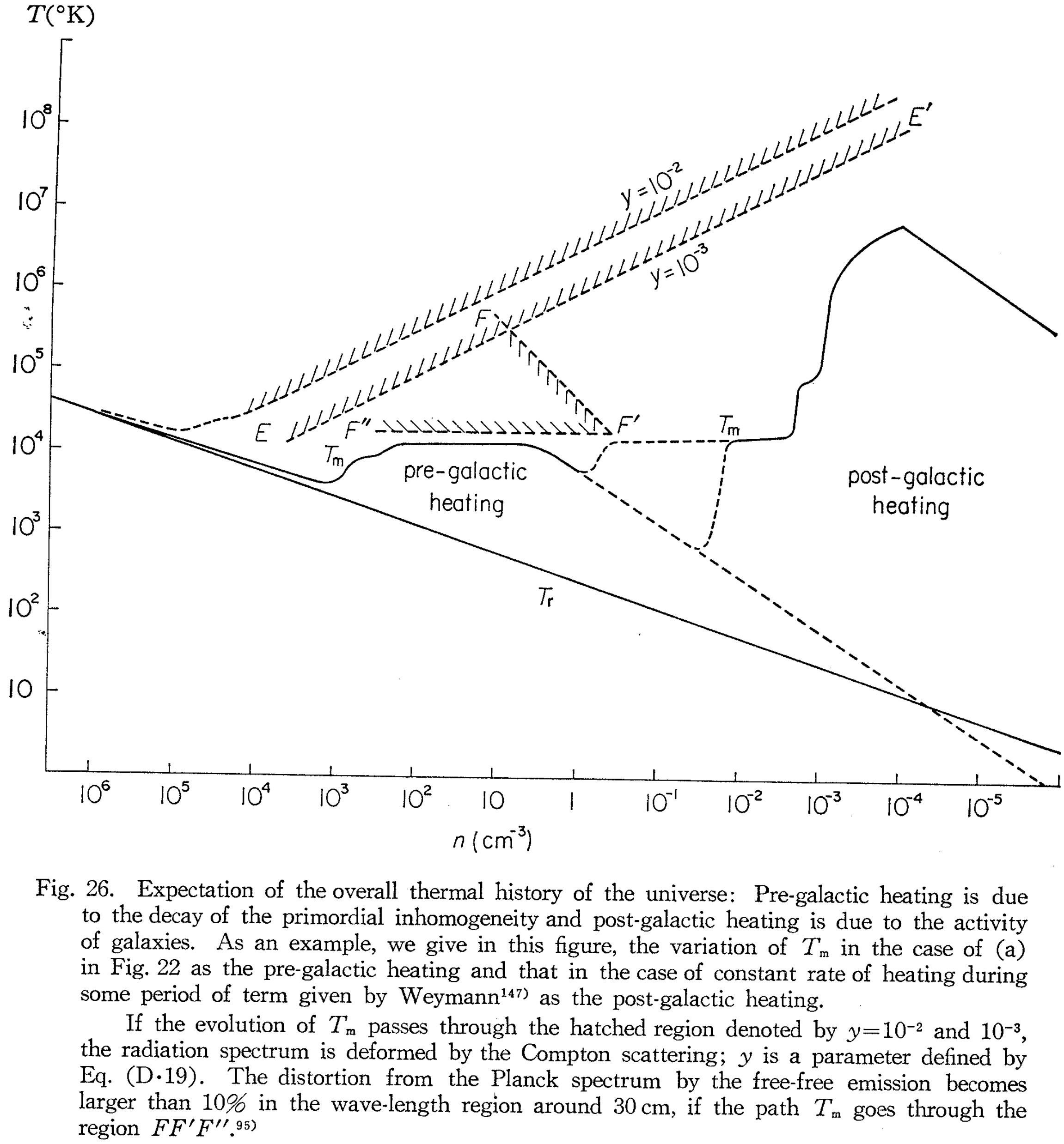

Fig. 26. Expectation of the overall thermal history of the universe: Pre-galactic heating is due to the decay of the primordial inhomogeneity and post-galactic heating is due to the activity of galaxies. As an example, we give in this figure, the variation of T_m in the case of (a) in Fig. 22 as the pre-galactic heating and that in the case of constant rate of heating during some period of term given by Weymann[147] as the post-galactic heating.

If the evolution of T_m passes through the hatched region denoted by $y=10^{-2}$ and 10^{-3}, the radiation spectrum is deformed by the Compton scattering; y is a parameter defined by Eq. (D·19). The distortion from the Planck spectrum by the free-free emission becomes larger than 10% in the wave-length region around 30 cm, if the path T_m goes through the region $FF'F''$.[95]

mechanism is possible only after the formation of galaxies. Hence, the thermal instability cannot work as a mechanism to form the initial galaxy itself, and we have proposed in §5 (vi) the hydrodynamic instability. The thermal instability, however, has not been denied completely even in the pre-galactic stage.

(v) *Heating of matter and background radiation*

In the presence of heating of matter, the primordial Planck spectrum is modified in various ways[95),96),98] (see Appendix D). The heating in the coupling stage mainly distorts the Planck spectrum by the Compton scattering. If the spectrum is distorted into the Bose-Einstein spectrum, the chemical potential ψ in Eq. (E·12) is of the order of

$$-\psi \simeq \left(\frac{\varepsilon_d \tau_{\mathrm{ex}}}{\mathcal{E}_{\mathrm{r}}}\right)\frac{\tau_{\mathrm{relax}}}{\tau_{\mathrm{ex}}}\,, \tag{6·7}$$

which is easily found to be small. In more general distortion of the spectrum, the parameter y defined in Eq. (D·19) represents a magnitude of deformation, and it is estimated to be

$$y \simeq \left(\frac{\varepsilon_d \tau_{\mathrm{ex}}}{\mathcal{E}_{\mathrm{r}}}\right). \tag{6·8}$$

The terms in the right-hand side of Eqs. (6·7) and (6·8) coincide with Eq. (6·4) and the distortion of the spectrum is concluded to be smaller in the earlier stages. If the evolutionary path in the later stage is restricted to the lower right region of the line EE' in Fig. 26, the distortion is smaller. From this figure, it is apparent that the distortion is small in our evolutionary path. Therefore, the expression of Eq. (6·2) is verified.

Spectral modifications through the radiative processes arise in the frequency regions outside the hump of the Planck spectrum. As an example, if the evolutionary path goes through the region $FF'F''$ in Fig. 26, the modification by free-free transition is larger than 10% at $\lambda = 30$ cm.[95] Now,

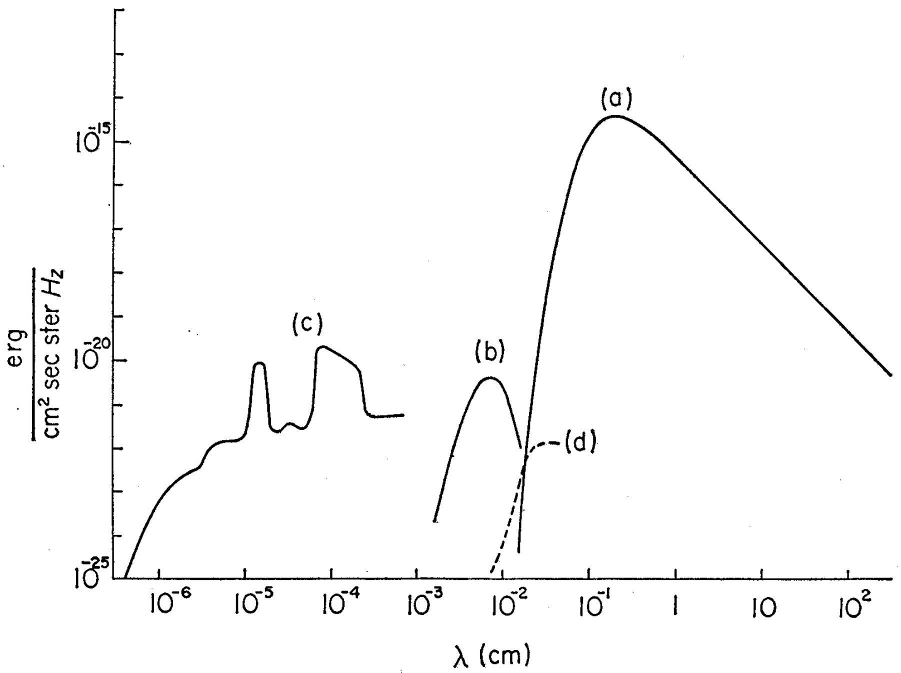

Fig. 27. Background radiation expected from the thermal history such as given in Fig. 26; (a) The primordial black-body radiation, (b) The flux emitted by two-photon emission during the pre-galactic heating, (c) The flux of emitted by bound-bound and free-free transitions during the post-galactic heating. The curve (d) represents the flux emitted by two-photon emission in the absence of heating.

we consider the expected background radiation resulting from our evolutionary path in Fig. 26. As seen from Fig. 25, the free-free transition is dominant in the coupling stage. However, this radiation at this stage does not make any appreciable deformation, because T_m is nearly equal to T_r and the universe is opaque to the low frequency photons such as $h\nu/kT_m<0.1$. After the decoupling, the bound-bound transition becomes dominant and a hump of red-shifted photons of two-photon emission appears around 100 μ in the background spectrum (see Fig. 28). However, this flux seems too small to be detected.

§7. Evolutions of the whole universe and of a galaxy

From §2 to §6, we have studied the evolution of the expanding hot universe. In Table II, we give a chronological table of the universe, in which marked events in each stage of the evolution are listed up. As seen from this table, the evolutionary sequence is divided into three ages; early era,

Table II. A chronological table of the expanding hot universe. Evolution of the cosmic matter in its composition and distribution is summarized.

Time	Composition	Distribution
10^{-43}sec		(Quantum fluctuation?)
	....	
10^{-8}sec	Formation of elementary particles	....
	(Separation of matter and anti-matter?)	
	Decoupling of neutrino	
10^{3}sec	Formation of helium	Uniform distribution
	....	
10^{5}years	Recombination of plasma Decoupling of the radiation	Growth and decay of inhomogeneity in density and velocity (Origin of magnetic field?)
		Formation of clouds ↓ Galaxies → Extra-galactic clouds
10^{8}years	Formation of H_2 / Heating of gas	Collapse ↓
	Formation of heavy elements on Pop. II stars ←	(Little bang?) ↓
10^{10}years	Formation of elements on Pop. I stars ←	Formation and evolution of stars
		Galactic nuclear activities

middle era and late or galactic era. The contents of this paper have been concerned with the early era in §§2～3 and the middle era in §§4～6. In this section, we comment upon the galactic era only briefly, though a detailed study has not been worked yet.

(i) *Importance of the middle era for the galactic era*

In the following, we summarize a character of each era mentioned above.

Early era: Elementary particles and primordial nuclei have their origin in this era, and we may call it the era of formation of matter.

Middle era: Coupling between the primordial radiation and the matter ceases in this era. After this decoupling, density fluctuations are generated here and there in the cosmic medium whose distribution is nearly uniform up to this epoch. Dense regions contract into individual gas clouds due to the gravitational forces by themselves, overcoming the expansion of the whole universe.

Galactic era: Each gas cloud begins to evolve independently of each other. Formations of stars and various elements start meanwhile, and the metagalactic matter may be heated again by the activity of galaxies.

Transfiguration of the universe from the nearly uniform configuration in the early era into the uneven configuration in the galactic era has occured in the middle era. Physical behaviour in the middle era is inherent to the hypothesis of the hot universe model. In the middle era, the atomic state and the fluid-dynamical state of matter are correlated intimately through the primordial radiation. Now, we stress that this agency of the primordial radiation is indispensable for the beginning of the galactic era. A similar effect may be expected to occur at the epoch where the thermal neutrinos decouple with the matter by the annihilation of electron pairs. However, the effect on the fluid-dynamical state by this decoupling is not eminent, because the neutrino pressure and the radiation pressure are nearly equal.

(ii) *Evolution of galaxies*

The evolution of galaxies from the gas clouds into the star-gas systems at the present has been studied by many authors from various points of view.[15),150)~152)] In this problem, evolutions of stars, chemical composition, thermal state of the galactic matter and the dynamical structure have been entangled with each other. We do not discuss this problem now, but only mention the initial condition of the clouds that is succeeded from the evolution of the whole universe.

Chemical composition

As discussed in §3, the primordial matter does not contain heavy elements exceeding $Z \simeq 10^{-15}$, where Z denotes the mass fraction of elements as heavy as and heavier than carbon. On the other hand, the population II stars, which are considered to be the first generation of stars,[15),150)] contain an appreciable amount of heavy elements as large as $Z=10^{-4}$.[152] Therefore, it is plausible to conclude that there existed a stage of the formation of heavy elements prior to the formation of the population II stars. Therefore, a rapid formation of heavy elements during a period shorter than $10^8 y$ may be required. Some authors have proposed a hypothesis that the primary formation of heavy elements may be due to the explosion of supermassive stars.[89),102] In the pre-stellar galactic matter, cooling of the matter required in the process of the star formation may be ineffective because of absence of cryogens composed from heavy elements, and only massive stars may be produced.[102] Recently, unconventional interpretation of the population II stars has been proposed by Unsöld,[86] though many objections have already been raised.[154] In Unsöld's hypothesis, the explosion of supermassive stars in galaxy is also assumed.

Concerning this problem, the observation of heavy elements in the extragalactic high velocity clouds observed by 21 cm radio wave[155] may bring us very important information, because they might be the pre-galactic clouds without stellar component.

Dynamical parameters of the pre-galactic clouds

In §5 (vi), we have discussed about a mechanism to determine the mass of the pre-galactic cloud. The hypothesis of primordial turbulence is convenient to explain the other dynamical parameters of the clouds such as angular momentum and peculiar velocity of galaxies. At first, such an idea was proposed by Weizsäcker[29] and Gamow,[30] and some authors have revived this idea in connection with the hot universe model.[156),157] This assumption enables us to estimate a magnitude of the initial turbulent velocity from the velocity observable for galaxies.

After t_*, the velocity decreases monotonously as seen in Figs. 21 and 25. In the bound systems, however, this deceleration does not occur. After the decoupling the decay mechanism of turbulence may be different from that before the decoupling, because the motion is supersonic in general. Though the decay law after the decoupling is unknown to us, we can estimate the order of magnitude of the initial velocity. Assuming that the formation of gravitationally bound systems has completed up to the epoch $\rho_m=10^{-24}\text{g/cm}^3$, v_i is estimated roughly as

$$10^{5.5}\Omega^{7/3}v_g > v_i > 10^{3.1}\Omega^{4/3}v_g\,, \qquad (7\cdot 1)$$

where the characteristic velocity of galaxies v_g may be the order of $10^7 \sim 10^8$ cm/sec, the upper value is given by assuming the decay law of Eq. (5·36) even after the decoupling, and the lower one is done by assuming the adiabatic deceleration. Thus, the initial velocity must be large enough to be comparable to the light velocity. On the other hand, the velocity must be small enough to preserve the Friedmann model of the universe. Therefore, we have assumed the values such as $10^{10}\sim10^{9}$ cm/sec in §§5 and 6. If we assume higher values for $v_{\rm i}$, we should consider a chaotic universe with relativistic turbulence as the initial state of the universe. It is noticeable that our consideration on the local structure of the universe seems to force a revisions of the conventional model for the global structure. The origin of the primordial turbulence might be discussed in relation to the global structure of the universe. These questions, however, have remained unsolved.

Acknowledgements

We would like to express our thanks to Professor C. Hayashi, who suggested the investigation of cosmology to one of the authors (H. S.) as early as in 1964 and has encouraged us continuously, and to Professors K. Aizu, S. Hayakawa, H. Nariai, M. Taketani, Drs. M. Kondo and K. Tomita for their discussions and comments. We also express our thanks to Professor S. Hayakawa for his advices on the English composition. One of the authors (T. M.) is grateful to Professor T. Sakurai for his encouragement.

Appendix A

——*Microwave background radiation*——

Since the discovery of the background radiation at wave length $\lambda=7.35$ cm,[21] many observations have been made over such a wide range of wave length as $\lambda=73$ cm$\sim$0.2 cm,[158)~173)] they are summarized in Table III. Observations of the anisotropies are also summarized in Table IV,[174)~180a)] but any noticeable anisotropy has not been detected. The observed fluxes at various wave lengths agree well with the Planck spectrum of 2.7°K, except those at $\lambda<0.2$ cm. Especially, the flux observed by Harwit et al.[171),172)] deviates appreciably from the Planckian spectrum. At present, however, it may be premature to conclude this flux as the metagalactic radiation because properties about the radiation around these wave bands, i.e., sub-mm and far-infrared bands, are obscure.

Many interpretations about this isotropic radiation have been given.[181)~188)] Some of them are classified as follows: (a) A relic of the black-body radiation in the condensed stage of the universe.[5),22),181),182)] (b) A superposition of the flux from discrete sources such as active galaxies.[183)~185)] (c) A black-(or grey) body radiation in the universe filled with dense dust particles.[186)]

The interpretation (a) is orthodox and has been explained in §4. The hot universe model is based on this interpretation. According to (b), such an anisotropy as large as 1% in angular size of about 1′ is expected[189)~191)] but the observation has failed to find such fluctuations as shown in Table IV. The (c) has been advocated by Hoyle et al.[186)] based on the view of the steady

Table III. Observational data of the isotropic background radiation. The observed intensity is represented by black-body temperature at each wave length.

Wave length (cm)	Observed intensity (°K)	Authors
73.5	3.7 ±1.2	Howel & Shakeshaft[158]
49.1		
21.0	3.2 ±1.0	Penzias & Wilson[159]
20.7	2.6 ±0.6	Howel & Shakeshaft[160]
7.35	3.3 ±1.0	Penzias & Wilson[21]
3.2	$2.69^{+0.16}_{-0.21}$	Roll & Wilkinson[161]
3.2	3.0 ±0.5	Stokes, Partridge
1.58	$2.78^{+0.12}_{-0.17}$	& Wilkinson[162]
1.5	2.0 ±0.8	Weleck, Keachie, Thornton & Wrixon[163]
0.924	3.16±0.26	Ewing, Burke & Staelin[164]
0.856	$2.56^{+0.17}_{-0.22}$	Wilkinson[165]
0.80	2.9 ±0.7	Pyzanov, Salomonovich & Stankevich[166]
0.33	$2.46^{+0.4}_{-0.44}$	Boynton, Stokes and Wilkinson[167]
	2.61±0.25	Millea, McColl, Pendersen & Vernon[167a]
0.263	<7.0	Field & Hitchcock[168]
		Thaddeus & Clauser[169]
0.263	<2.91	Bortolot, Clauser & Thaddeus[170]
0.131	<4.74	
0.0599	<5.43	
0.035	<8.11	
0.04~0.13	8.3	Shivanandan, Houch & Harwit[171),172]
>0.1	3.6	Muehlner & Weiss[173]
>0.08	7.0	
>0.055	5.5	

Table IV. Observational data of the anisotropy of the background radiation.

Angular size	Observed wave length	Degree of anisotropy	Authors
2°	3.2 cm	< 0.2%	Partridge & Wilkinson[174]
40′	7 cm	<0.006°K	Penzias & Wilson[177]
10′	2.8 cm	<0.004°K	Conklin & Bracewell[176]
80″	3.5 mm	<0.024°K	Penzias, Schraml & Wilson[89]

state cosmology. They notice that solidification of hydrogen in the metagalactic space occurs at temperature about 3°K and consider the energy of star light absorbed by the metalic core of dust particles is changed to the radiation energy with 3°K and is reemitted to the intergalactic space. Further, if the optical thickness in the universe is sufficiently large, the universe is filled with the black-body radiation with 3°K. The optical depth τ can be estimated as

$$\tau < 9\pi \frac{\rho_{m0}}{\bar{\rho}} \frac{1}{\lambda} \frac{c}{H_0}, \qquad (A\cdot 1)$$

where $\bar{\rho}$ is the mean density of the dust particles and is taken as $\rho_{m0}/\bar{\rho}=10^{-29}$. Putting $\lambda=1$ cm, we get $\tau=27$. For the larger wave length, however, the universe is apparently transparent in contradiction to their hypothesis. Further, it is very questionable that the absorption coefficient has a flat value over the wide band such as 0.2 cm∼73 cm. Therefore, this interpretation is also unpromising. Thus, the interpretation (a) is the most promising.

Appendix B

——Observation of helium abundance——

As regards the spectroscopic measurements of helium abundance published, excellent reviews have been given in Refs. 85)∼87) and 192). A brief summary of the observation is given in Table V. Most of the observed abundances lie in the range $Y=0.20\sim0.40$, the most probable values clustering in $Y=0.25\sim0.30$. As for the measurements of low abundance, a more extensive analysis seems to be needed.

As for the stellar origin of helium, two difficulties have been pointed out; one is that an amount of helium produced by the stars in a galaxy, ΔY_s, is estimated to be the order of 10^{-2} and the other is that an amount of heavy elements to be produced by the stars, ΔZ_s, is nearly the same as that of helium, i.e., $\Delta Y_s \simeq \Delta Z_s$.[46] These points, however, should be investigated more carefully from the theory of stellar evolution and that of galaxy evolution.[151]

According to the cosmological origin of helium, the present abundances of elements, denoted as X, Y and Z, are expressed by the primordial abundance, denoted as X_p, Y_p and $Z_p(=0)$, as follows:

$$X = X_p - \Delta Y_s - X_p \Delta Z_s,$$

$$Y = Y_p + \Delta Y_s - \Delta Z_s Y_p$$

and

$$Z = \Delta Z_s.$$

If we assume $Y_p=0.26$ and $\Delta Y_s=\Delta Z_s=0.02$, we have $X=0.7$, $Y=0.28$ and $Z=0.02$.

Table V. Observational data of helium abundance by the ratio of helium density to hydrogen density.

Objects		Abundances He/H
The Sun	Prominence	0.07[a]
	Wind	0.02 ~0.05[b]
	Cosmic rays	0.09[c], 0.063[d]
	Neutrino	<0.05[e],[87]
Hot stars*)		0.20~0.11[85],[86],[88]
He deficient stars		~10^{-3} [85],[86],[88]
Galactic nebula**)		
(optical)		0.18~0.08[192]
(radio)		~0.084[f]
Extragalactic nebula***)		0.13~0.096[g],[192]
QSO****)		0.13~0.005[h]
Galactic cosmic rays		0.17[i]

*) They include population II stars as well as population I.
**) Planetary nebula, Orion nebula and other HII regions.
***) M33, M101, NGC449, LMC, SMC, etc.
****) 3C273, 3C2491, PKS225+11, Tom1542, etc.

a) T. Hirayama, Solar Phys., **17** (1971), 50.
b) K. W. Ogilvie, L. F. Barloga and T. D. Wilkerson, J. Geophys. Res. **73** (1968), 6809.
S. J. Bame, A. J. Hundhausen, J. R. Asbvidge and J. B. Strong. Phys. Rev. Letters **20** (1968), 393.
c) S. Biswas and C. E. Fichtel, Astrophys. J. **139** (1963), 941.
C. E. Fichtel and F. B. McDonald, Ann. Rev. Astron. and Astrophys. **5** (1967), 351.
d) D. L. Lambert and B. Warner, Month. Notices Roy. Astron. Soc. **140** (1968), 197.
e) R. Davis, D. S. Harmer and K. C. Hoffman, Phys. Rev. Letters **20** (1968), 1205.
J. N. Bahcall, N. A. Bahcall and G. Shaviv, Phys. Rev. Letters **27** (1968), 1209.
f) R. Palmer, B. Zuckerman, H. Penfield, A. E. Lilley and P. G. Mezger, Astrophys. J. **156** (1969), 857.
g) M. Peimbert and H. Spinrad, Astrophys. J. **159** (1970), 809.
h) J. N. Bahcall and B. Kozlovsky, Astrophys. J. **155** (1969), 1077; **158** (1970), 529.
i) S. Biswas, S. Ramadurai and N. Srenivasan, Can. J. Phys. **46** (1968), 593.

Appendix C

——*Cosmic expansion and red-shift parameter*——

Throughout this paper, we have assumed the isotropic-homogeneous model based on the Einstein theory of general relativity.[1] This model is called the Friedmann model. The space-time metric is taken as

$$ds^2=c^2dt^2-\frac{a^2(t)}{(1+\kappa r^2/4)^2}(dr^2+r^2d\theta^2+\sin^2\theta d\varphi^2), \qquad (C\cdot 1)$$

where $a(t)$ is a scale factor and other notations are usual ones. In the hot universe model, the density ρ and the pressure p are given as

$$\rho=\rho_{\rm m}+\rho_{\rm r} \quad \text{and} \quad P=P_{\rm r}=\rho_{\rm r}c^2/3, \tag{C·2}$$

where the suffices m and r denote matter and radiation, respectively. The Einstein's field equation gives a rate of the cosmic expansion as

$$\frac{1}{a}\frac{da}{dt}=H_0(z+1)^{1.5}\sqrt{\psi} \tag{C·3}$$

with

$$\psi=\left[2q_0\left(1+\frac{z+1}{z_*+1}\right)+\left\{(1-2q_0)+(1-q_0)\frac{2}{z_*+1}\right\}\frac{1}{z+1}\right]\frac{z_*+1}{z_*+3}, \tag{C·4}$$

$$z+1=a_0/a, \quad z_*+1=\rho_{\rm m0}/\rho_{\rm r0}, \tag{C·5}$$

$$H_0=\left(\frac{da}{dt}\Big/a\right)_0 \tag{C·6}$$

and

$$2q_0=-2\left(\frac{d^2a}{dt^2}\Big/a\right)_0=\frac{\rho_{\rm m0}}{\rho_0}\frac{z_*+3}{z_*+1}, \tag{C·7}$$

where the suffix 0 denotes the values at the present, and ρ_c is defined as

$$\rho_c=3H_0^2/8\pi G. \tag{C·8}$$

The values of H_0 and q_0 are determined observationally based on the dynamics of the cosmic expansion. According to Sandage,[193),19a)] these values are now given as

$$49\ \text{km/sec Mpc}<H_0<130\ \text{km/sec Mpc} \tag{C·9}$$

and

$$q_0=1.2\pm0.4,$$

though we should not take the above value of q_0 very seriously. From Eq. (C·9), we have

$$4.7\cdot10^{-30}\ \text{g/cm}^3<\rho_c<3.2\cdot10^{-29}\ \text{g/cm}^3. \tag{C·10}$$

From the observation of microwave background radiation (see Appendix A), the radiation temperature is found to be $T_{\rm r0}=2.7°$K and z_* is given as

$$z_*+1=10^{4.45}\Omega/[1+N(\psi_e,\psi_\mu)], \tag{C·11}$$

where $N(\psi_e,\psi_\mu)$ is given in Eq. (2·17) and Ω is a parameter to denote the matter density as

$$\Omega=\rho_{\rm m0}/(2\cdot10^{-29}\ \text{g/cm}^3). \tag{C·12}$$

Denoting the epoch of $\rho_r=\rho_m$ by t_*,

$$z_*+1=a_0/a(t_*). \tag{C·13}$$

Now, we define an expansion time scale τ_{ex} as

$$\tau_{ex}\equiv a/(da/dt), \tag{C·14}$$

$$=2t=2\left(\frac{T_r}{10^{10.14}\,°\mathrm{K}}\right)^{-2}\ \mathrm{sec} \qquad \text{for } t<t_*, \tag{C·14a}$$

$$=\frac{2}{3}t=\frac{2}{3}\frac{10^{9.98}}{(1+z)(1+\Omega z)^{1/2}}\ \text{years} \qquad \text{for } t>t_*. \tag{C·14b}$$

The red-shift of a photon in the expanding universe is generally given as[124)]

$$\lambda_0/\lambda_e=(k_a U^a)_e/(k_a U^a)_0, \tag{C·15}$$

where λ is wave length of photon, U^a is a world velocity, k_a is a tangent vector to the light-like geodesics and suffices e and 0 represent the values at the emitter and the observer, respectively. If the metric is strictly homogeneous as in Eq. (C·1), $\lambda_0/\lambda_e=a_0/a_e=z_e+1$ and z is called red-shift parameter. In weakly inhomogeneous metric, however, the red-shift is modified as[107),115)]

$$\lambda_0/\lambda_e=\overline{z_e+1}$$
$$=(z_e+1)\left[1-\boldsymbol{l}_0\cdot\frac{(\boldsymbol{V}_e-\boldsymbol{V}_0)}{c}+\frac{(\varphi_0-\varphi_e)}{c^2}+\frac{1}{2c^2}(v_0^2-v_e^2)+\tilde{\varphi}\right], \tag{C·16}$$

where $\boldsymbol{V}$ and φ represent the proper velocity and the gravitational potential respectively, and $\tilde{\varphi}$ is given as

$$\tilde{\varphi}=-\int_{t_e}^{t_0}\frac{\partial\varphi}{\partial t}dt.$$

Appendix D

——*Interaction of radiation with matter in the hot universe*——

In the expanding universe, the change of the radiation spectrum is given as[141)]

$$\frac{\partial U_\nu}{\partial t}=H\left(\nu\frac{\partial U_\nu}{\partial \nu}-3U_\nu\right)+\epsilon_c(\nu), \tag{D·1}$$

where U_ν is the energy density per unit volume and per unit frequency, $\epsilon_c(\nu)$ is a net energy production rate. Considering that the frequency changes as $\nu/\nu_0=a_0/a$, we introduce the occupation number N_ν defined by

$$N_\nu=U_\nu(\nu_0(a/a_0),t))/\{8\pi h\nu_0^3(a_0/a)^3/c^3\}. \tag{D·2}$$

Substituting Eq. (D·2) into Eq. (D·1), we have

$$\frac{\partial N_\nu}{\partial t}=\bar{\epsilon}_c(\nu) \tag{D·3}$$

with

$$\bar{\epsilon}_c(\nu)=\epsilon_c(\nu)/(8\pi h\nu^3/c^3).$$

Generally, $\bar{\epsilon}_c(\nu)$ is expressed as follows,

$$\bar{\epsilon}_c(\nu)=\bar{\epsilon}_{\rm Com}(\nu)+\bar{\epsilon}_{\rm ff}(\nu)+\bar{\epsilon}_{\rm bf}(\nu)+\bar{\epsilon}_{\rm bb}(\nu), \tag{D·4}$$

where respective terms are expressed as follows:

for Compton scattering

$$\bar{\epsilon}_{\rm Com}(\nu)=\frac{1}{\tau_c}\frac{1}{x^2}\frac{\partial}{\partial x}\left\{x^4\left(\frac{\partial N_\nu}{\partial x}+N_\nu+N_\nu^2\right)\right\}, \tag{D·5}$$

for free-free transition

$$\bar{\epsilon}_{\rm ff}(\nu)=\frac{1}{\tau_{\rm ff}(\nu)}\{(1+N_\nu)-N_\nu e^x\} \tag{D·6}$$

and

for bound-free transition

$$\bar{\epsilon}_{\rm bf}(\nu)=\frac{1}{\tau_{\rm bf}(\nu)}\{(1+N_\nu)-N_\nu e^x\}. \tag{D·7}$$

In the above expression, the time scales are given as

$$\tau_{\rm Com}=\frac{m_e c}{n_e\sigma_{\rm T}kT_{\rm m}}, \tag{D·8}$$

$$\tau_{\rm ff}(\nu)=\frac{3}{32}\sqrt{\frac{2m_e^3}{\pi^3}}\frac{(kT_{\rm m})^{3.5}}{n_e n_i e^6\hbar^2}\frac{x^3e^{x/2}}{K_0(x/2)} \tag{D·9}$$

and

$$\tau_{\rm bf}(\nu)=\frac{32}{3}\sqrt{\frac{2}{3\pi m^5}}\frac{B_1}{(kT_{\rm m})^{1.5}}\frac{g_{\rm bf}}{n^3}\exp\left(\frac{B_1}{n^2kT}-\frac{h\nu}{kT_{\rm m}}\right), \tag{D·10}$$

where $x=h\nu/kT_{\rm m}$, $\sigma_{\rm T}$ is the Thomson cross section, B_1 is the ionization energy, $g_{\rm bf}$ is the gaunt factor, n is the principal quantum number and K_0 is the modified Bessel function of order zero. Among various types of the bound-bound transition, the two-photon emission from $2s$ into $1s$ plays an important role at the stage of recombination (see Appendix E).

On the other hand, the change of matter temperature is given as

$$\frac{ds_{\rm m}}{dt}=\frac{\epsilon_d-\epsilon_c}{T_{\rm m}\rho_{\rm m}}, \tag{D·11}$$

where $s_{\rm m}$ is specific entropy of matter, ϵ_d is heating rate and $\epsilon_c=\int_0^\infty\epsilon_c(\nu)d\nu$.

In nonrelativistic temperature, the above relation reduces to Eq. (6·1).

(i) *The case without heating*

If the thermal equilibrium has been attained only through the Compton scattering, we have the occupation number as

$$N_\nu = \frac{1}{e^{x-\psi}-1}, \qquad \text{(D·12)}$$

by solving the equation $\bar{\epsilon}_{\mathrm{Com}}(\nu)=0$, where ψ is chemical potential divided by temperature. If the radiation spectrum has such a form as Eq. (D·12) but $T_\mathrm{r} \neq T_\mathrm{m}$, ϵ_c is given as shown in Eq. (6·2). The change of T_r in this assumption is found from Eq. (D·3) as

$$\frac{dT_\mathrm{r}}{dt} = -HT_\mathrm{r} - T_\mathrm{r}\frac{\sigma_T n_e}{m_e c}k(T_\mathrm{r}-T_\mathrm{m}). \qquad \text{(D·13)}$$

Before the decoupling, Eq. (D·13) is approximately solved as

$$\frac{T_\mathrm{r}-T_\mathrm{m}}{T_\mathrm{r}} = \frac{3}{8}\frac{m_e c}{\sigma_\mathrm{T}\mathcal{E}_\mathrm{r}}\frac{1+x_e}{x_e}H \ll 1. \qquad \text{(D·14)}$$

After the decoupling, the energy exchange due to ϵ_{Com} ceases and the temperature changes like $T_\mathrm{r} \propto 1/a$ and $T_\mathrm{m} \propto 1/a^2$ (see Fig. 7).

(ii) *The "Compton" region*

As seen from Fig. 7, the evolutionary path of the universe goes through the *Compton* region defined in §4 (i). In this case, the radiation spectrum in the frequency range of $\tau_{\mathrm{ff}}(x) \gg \tau_{\mathrm{Com}}$ is essentially given by Eq. (D·12). Now, we consider that the radiation of Planck spectrum with temperature T_{r1} is heated to $T_\mathrm{m}(>T_{\mathrm{r1}})$ instantaneously. Then, the chemical potential and the energy density are given by solving the following relations:

$$\left(\frac{T_\mathrm{m}}{T_{\mathrm{r1}}}\right)^3 \int_0^\infty \frac{x^2 dx}{e^{x-\psi}-1} = 2\zeta(3) \qquad \text{(D·15)}$$

and

$$\mathcal{E}_\mathrm{r}(T_\mathrm{m},\psi)/\mathcal{E}_\mathrm{r}(T_{\mathrm{r1}},0) = \left(\frac{T_\mathrm{m}}{T_{\mathrm{r1}}}\right)^4 \frac{1}{6\zeta(4)} \int_0^\infty \frac{x^3}{e^{x-\psi}-1}dx, \qquad \text{(D·16)}$$

where $\zeta(n)$ is Rieman's Zetha-function. Some solutions of the above problem are exemplified in Fig. 28. If the heat supply is large enough, ψ has a large negative value and

$$\mathcal{E}_\mathrm{r}(T_\mathrm{m},\psi)/\mathcal{E}_\mathrm{r}(T_{\mathrm{r1}},0) \simeq 1.15(T_\mathrm{m}/T_{\mathrm{r1}}).$$

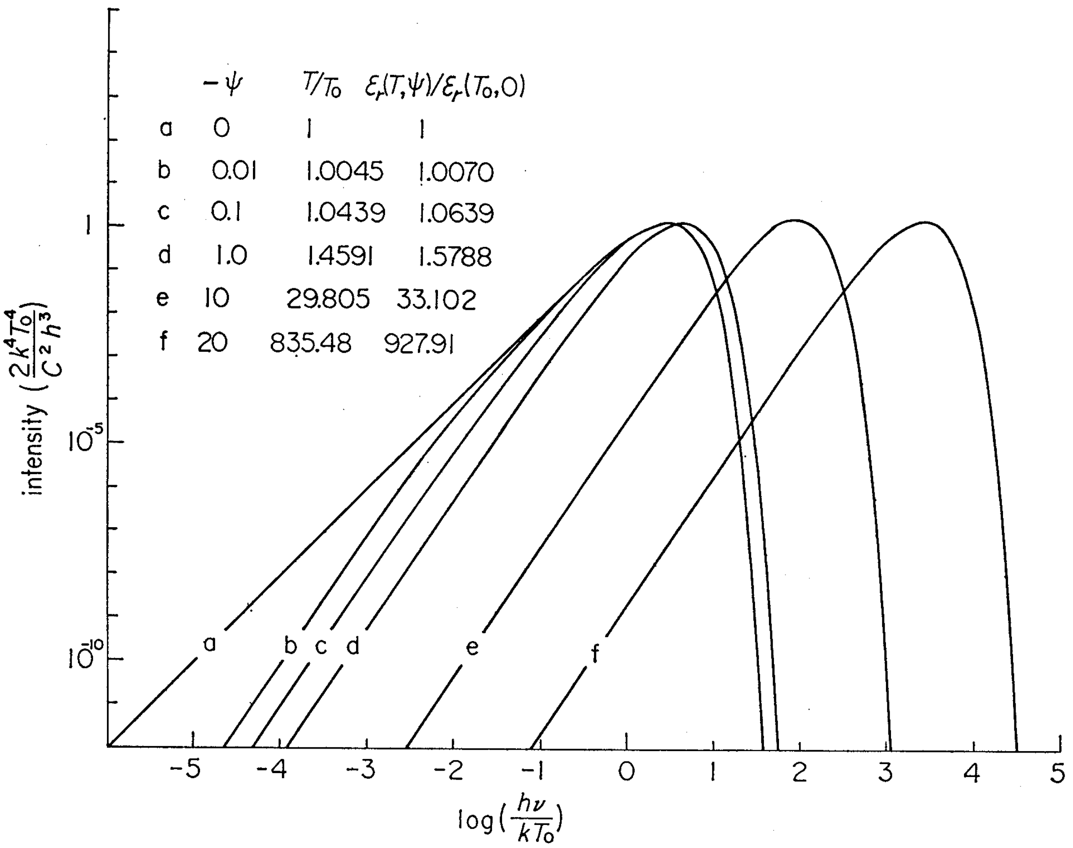

Fig. 28. Energy spectrum of the radiation heated preserving the number of photons. (See Eqs. (D·15) and (D·16).)

(iii) *Zeldovich-Sunyaev's treatment*[96),98a)]

Without assuming the thermal equilibrium, a small departure from the Planck spectrum can be obtained in an analytical form. Putting $\bar{\epsilon}_c(\nu) = \bar{\epsilon}_{\rm Com}(\nu)$ in Eq. (D·3) and $N_\nu = 1/(e^{x'}-1)$ in Eq. (D·5), we have

$$\frac{\partial N_\nu}{\partial y} = \frac{x' e^{x'}}{(e^{x'}-1)^2}\left\{\frac{x'}{\tanh(x'/2)} - 4\right\} \tag{D·17}$$

with

$$y = \int^t \frac{n_e \sigma_{\rm T}}{m_e c} k(T_{\rm m} - T_{\rm r})\, dt, \tag{D·18}$$

where $x' = h\nu/kT_{\rm r}$. Therefore, a parameter y, whose definition is a little different from that of Zeldovich and Sunyaev, represents a degree of the spectral deformation. In the Rayleigh-Jeans region

$$N_\nu \simeq \frac{1}{x' e^{2y}}, \tag{D·19}$$

which means that the radiation temperature is effectively reduced by the factor e^{-2y}.

(iv) *Relaxation time for the Planck spectrum*[98)]

As seen from Eq. (D·9), a production of photons by the free-free emission is more effective in the lower frequency region. The time scale for the equilibrium by the free-free transition is given as

$$\bar{\tau}_{ff}(x) = \tau_{ff}(x)(e^x - 1) \tag{D·20}$$

and the condition of $\bar{\tau}_{ff} \simeq \tau_{Com}$ gives a critical frequency as

$$x_0 = \sqrt{\frac{\tau_{Com}}{\tau_{ff}^0}}\,, \tag{D·21}$$

where we have assumed $x \ll 1$ and $\tau_{ff}(x) = \tau_{ff}^0 x^3$. The production of photons is possible in the frequency region of $x > x_0$, because the emission balances with the absorption in $x < x_0$. Averaging the $\bar{\tau}_{ff}(x)$ over $x > x_0$, we have a relaxation time τ_{relax} as

$$\tau_{relax} \simeq 1 \Big/ \int_{x_0}^{\infty} \frac{x^2 dx}{\tau_{ff}(e^x - 1)} \simeq \sqrt{\tau_{ff}^0 \tau_{Com}}\,. \tag{D·22}$$

Appendix E

——*Recombination of hydrogen in the hot universe*——

For hydrogen atoms, we consider only two levels, i.e., the ground state (1*s*) and the first excited state (2*s* and 2*p*), because the relative populations of the other levels are given simply by thermal equilibrium values. Then number densities of the atom in the ground state, the first excited state and the ionized state are expressed by n_1, n_2 and n_p respectively. For simplicity, a statistical equilibrium through the particle collision between 2*s*-and 2*p*-states is assumed; $n_2 = 4n_{2s}$.

The equations governing the change of their population are given as

$$\frac{d}{dt}\left(\frac{n_1}{n}\right) = B(p \to 1) + B(2 \to 1), \tag{E·1}$$

$$\frac{d}{dt}\left(\frac{n_p}{n}\right) = -B(p \to 1) - B(p \to 2), \tag{E·2}$$

$$B(p \to i) = \left[\left(\alpha_i n_p n_e - \frac{\beta_1}{i^2} n_i\right) + \left(\gamma_{pi} n_e^2 n_p - \frac{\gamma_{ip}}{i^2} n_e n_i\right)\right] \Big/ n \tag{E·3}$$

and

$$B(2 \to 1) = \left[R + A\left\{\frac{n_2}{4} - n_1 \exp(-B_\alpha/kT_r)\right\} + \frac{\gamma_{21}}{4} n_e \{n_2 - 4n_1 \exp(-B_\alpha/kT_r)\}\right] \Big/ n, \tag{E·4}$$

where $i = 1$ or 2, $n = n_p + n_1 + n_2$, B_α is the Lyman-α energy, α_i, β_1 and $\gamma_{jj'}$

denote the rates of radiative recombination into i-state, photo ionization from i-state and collisional reaction from j-state into j'-state respectively, Λ is the two-photon emission rate from $2s$ into $1s$ and R is the net emission rate of Lyman-α photon per unit volume defined in Eq. (E·5) later. In the following, we shall neglect a direct radiative recombination into $1s$-state, i.e., $\alpha_1 n_e n_p - \beta_1 n_1 = 0$.

The net emission rate of Lyman-α is defined as

$$R = A\left[\frac{3}{4} n_2 (1+N_\alpha) - 3 n_1 N_\alpha\right], \tag{E·5}$$

where A is the spontaneous emission rate from $2p$ into $1s$ and N_α is the occupation number of Lyman-α photons. As the number of Lyman-α photons is a summation of the Planck value $N_{\alpha P} = 1/\{\exp(-B_\alpha/kT_r) - 1\}$ and the accumulated Lyman-α photons emitted, we can write

$$N_\alpha \Delta\nu_\alpha = N_{\alpha P} \Delta\nu_\alpha + R\frac{\lambda_\alpha^3}{8\pi}\Delta t, \tag{E·6}$$

where Δt is a time duration of accumulation within the line width $\Delta\nu_\alpha$. In the expanding universe, $\Delta t = (a/\dot{a})(\Delta\nu_\alpha/\nu_\alpha)$ and Eq. (E·6) becomes as

$$N_\alpha = N_{\alpha P} + RK \tag{E·7}$$

and

$$K = (\lambda_\alpha^3/8\pi) a/\dot{a}. \tag{E·8}$$

From Eqs. (E·5) and (5·7), we have

$$R = N_{\alpha P}\frac{3A\{n_2 \exp(B_\alpha/kT_r)/4 - n_1\}}{1 + 3AK(n_1 - n_2/4)}. \tag{E·9}$$

Substituting Eq. (E·8), Eq. (E·2) becomes as

$$B(2\to 1) \simeq \left(\frac{3A}{1+3AKn_1} + \Lambda\right)\frac{n_2}{4} - \gamma_{21} n_e n_1 \exp(-B_\alpha/kT_m), \tag{E·10}$$

where we have approximated for the case of $\exp(B_\alpha/kT_r) \gg 1$ and $\gamma_{21} n_e \ll 1$. The Lyman-α emission is found to be suppressed by the factor

$$(1+3AKn_1)^{-1} \tag{E·11}$$

and the ratio of the suppressed allowed transition to the two-photon emission is given as

$$\frac{(\text{Lyman-}\alpha)}{(\text{two-photon})} = \frac{3A}{(1+3AKn_1)\Lambda}. \tag{E·12}$$

The transition is mainly due to the two-photon emission if $n_1 > (K\Lambda)^{-1}$, due to the suppressed Lyman-α emission if $(K\Lambda)^{-1} > n_1 > (KA)^{-1}$ and due to the free Lyman-α emission if $n_1 < (KA)^{-1}$, where

$$(K\Lambda)^{-1} = 4.2\cdot 10^{-3}(1+z)(1+\Omega z)^{1/2}\ \mathrm{cm}^{-3}$$

and

$$(KA)^{-1} = 7.4\cdot 10^{-11}(1+z)(1+\Omega z)^{1/2}\ \mathrm{cm}^{-3}. \tag{E·13}$$

(a) *Equation of recombination*

Because of low density of the universe, the collisional recombination and the collisional de-excitation are always neglected. The most drastic effect of the heating is the collisional excitation from the ground state into the first excited state. Putting

$$B(2\to 1) = B(p\to 2), \tag{E·14}$$

we have

$$\frac{n_2}{4n_1} = \frac{(1+Kn_1\Lambda)\exp(-B_\alpha/kT_r) + K\alpha_2 n_e^2 + K\gamma_{21} n_e n_1 \exp(-B_\alpha/kT_m)}{1+Kn_1(\Lambda+\beta_2)}, \tag{E·15}$$

where only dominant terms are retained. Substituting Eq. (E·15) into Eq. (E·2), we have the equation of recombination as

$$-\frac{d}{dt}\left(\frac{n_e}{n}\right) = [\alpha_2 n_e^2 C - (\beta_2+\gamma_{2c} n_e)\exp(-B_\alpha/kT_r) n_1 D - \gamma_{1c} n_1 n_e]/n, \tag{E·16}$$

where

$$C = \frac{1+K(\Lambda n_1 + \alpha_2 n_e^2)}{1+K(\Lambda+\beta_2)n_1 + K(\alpha_2 n_e^2 + \gamma_{2c} n_e n_1)}, \tag{E·17}$$

$$D = \frac{1+K\{\Lambda + \gamma_{21} n_e \exp(B_\alpha/kT_r - B_\alpha/kT_m)\} n_1}{1+K(\Lambda+\beta_2)n_1 + K(\alpha_2 n_e^2 + \gamma_{2c} n_e n_1)}. \tag{E·18}$$

If γ_{21} is neglected, D reduces to C, which is the inhibition factor of recombination defined by Peebles,[99] and Eq. (E·16) does to Eq. (4·5).

(b) *Neutral atoms in the heated metagalactic space*

Assuming the steady heating, we put

$$B(p\to 1) \simeq -B(p\to 2)$$

and

$$B(p\to 1) \simeq -B(2\to 1). \tag{E·19}$$

Neglecting the radiative ionization because of low T_r, we have from the above relation

$$\frac{n_1}{n_p} = \frac{\alpha_2}{\gamma_{1p} + \gamma_{2p} n_2/4n_1}, \tag{E·20}$$

$$\frac{n_2}{4n_1}=\frac{\gamma_{1p}n_e}{A+3A/(1+3AKn_1)}\ . \tag{E·21}$$

If $\gamma_{2p}n_e/A\ll 1$, we have

$$\frac{n_1}{n_p}=\frac{\alpha_2}{\gamma_{1p}}=\frac{\exp(1.57\cdot 10^5/T_m)}{2T_m}\ . \tag{E·22}$$

Appendix F

——*Atomic processes of hydrogen*——

Reaction rates of atomic processes including hydrogen are summarized in Table VI. In our calculation in §§4 and 6, we have used these values.

Table VI. Reaction rates involving hydrogen atom and hydrogen molecule.

Reaction	Q-value (ev)	Capture rate (cm³sec⁻¹)
$H+e\to H(2)+\gamma$	3.40	$2.84\cdot 10^{-11}T_m^{-1/2}$
$H(2)+e\to H^++2e$	−3.40	$5.46\cdot 10^{-11}T_m^{1/2}\exp(-38827/T_m)\Gamma_{2c}$ [a]
$H(2)+e\to H(1)+e$	10.2	$5.47\cdot 10^{-11}T_m^{1/2}\Gamma_{12}$ [b]
$H+e\to H^-+\gamma$	0.754	$6.06\cdot 10^{-19}T_m$
$H^-+e\to H+2e$	−0.754	$1.6\cdot 10^{-6}(1+34T_m^{-5/4})\exp(-65/T_m^{1/3})$
$H+H^+\to H_2^++\gamma$	2.648	$5\cdot 10^{-24}T_m^2$
$H+H\to H_2+\gamma$	4.476	$4.0\cdot 10^{-27}$ at 100°K
$H+H^-\to H_2+e$	3.722	$1.3\cdot 10^{-9}$
$H^++H^-\to 2H+\gamma$	12.84	$1.6\cdot 10^{-6}T_m^{-0.45}$
$H+D\to HD+\gamma$	4.476	10^{-22}
$H_2^++e\to 2H+\gamma$	10.95	10^{-7}
$H_2+e\to H+H^-$	−3.722	$2.7\cdot 10^{-8}T_m^{-3/2}\exp(-4.3\cdot 10^4/T_m)$
$H_2^++H\to H_2+H^+$	1.828	$1.3\cdot 10^{-9}$
$H_2^++H^-\to H_2+H$	14.67	——
$H_2+H^+\to H_2^++H$	−1.828	$2.6\cdot 10^2T_m^{-1/2}\exp(-2.12\cdot 10^4/T_m)$
$H_2+H\to 3H$	−4.476	$2.0\cdot 10^{-6}T_m^{-1/2}\exp(-5.19\cdot 10^4/T_m)$
$H_2+H^-\to H_2+H+e$	−0.754	——
$H_2+H_2^+\to H_3^++H$	1.462	$2.1\cdot 10^{-9}$
$H_2+H_2\to H_2+2H$	−4.476	$3.0\cdot 10^{-4}T_m^{-3/2}\exp(-5.2\cdot 10^3/T_m)$
		photo reaction rate (sec⁻¹)
$H(2)+\gamma\to H^++e$	−10.2	$2.46\cdot 10^8E(-B_\alpha/4T_r)$ [c]
$H^-+\gamma\to H+e$	−0.754	$1.5\cdot 10^{-2}T_r^{2.4}\exp(-8750/T_r)$
$H_2^++\gamma\to H+H^+$	−0.861	$1.1\cdot 10^{-13}T_r^{5.34}\exp(-10000/T_r)$
$H_2+\gamma\to H+H$	−12.40	$5.1\cdot 10^7\exp(-1.44\cdot 10^5/T_r)$
	−7.91	$2.1\cdot 10^7\exp(-9.19\cdot 10^4/T_r)$

a) $\Gamma_{2c}=20.0-5.90\cdot 10^{-5}T_m-2.82\cdot 10^4/T_m+5.44\cdot 10^7/T_m^2$

b) $\Gamma_{12}=-30.2+3.86\cdot\log T_m+305.6/(\log T_m)^2$

c) $E(-x)=\frac{e^{-x}}{x}\,\frac{x^2+2.33x+0.250}{x^2+3.33x+1.68}$

As the primordial gas contains not only hydrogen but also deuteron and helium, it is possible to form hydrogen molecules via the following reactions in addition to these in Eqs. (4·10) and (4·11);

$$He+H^+\to HeH^+ +\gamma, \quad HeH^+ +H\to He+H_2^+, \tag{F·1}$$

$$H+D\to HD+\gamma, \tag{F·2}$$

$$D+e\to D^- +\gamma, \quad D^- +H\to HD+e, \tag{F·3}$$

$$D+H^+\to HD^+ +\gamma, \quad HD^+ +H\to HD+H^+. \tag{F·4}$$

The reaction rates of Eqs. (F·3) and (F·4) are approximately equal to those of Eqs. (4·10) and (4·11). As the rotational excitation energy of HD molecule is smaller than that of H_2, the cooling is more effective for HD at lower temperature. Even if the abundance of D is as small as $D/H\simeq 3.10^{-5}$, the cooling by HD becomes more effective for $T_m < 20°K$.

Appendix G

——Hydrodynamic equation of radiative fluid——

Following the relativistic formulation of hydrodynamics with dissipation,[195),196)] the energy-momentum tensor is written as

$$T^{ab}=\mathcal{E}U^aU^b-Ph^{ab}+\tau^{ab}+(q^aU^b+q^bU^a)/c, \tag{G·1}$$

where $\mathcal{E}$ is energy density $(\rho_r+\rho_m)c^2$, P is pressure, $h^{ab}=g^{ab}-U^aU^b$, q^a is heat flow vector, U^a is the four velocity such as $U^aU_a=1$ and τ^{ab} is the viscous tensor defined as

$$\tau^{ab}=\eta\{h^{ac}h^{bd}(U_{c;d}+U_{d;c})-\tfrac{2}{3}h^{ab}h^{cd}U_{c;d}\}+\zeta h^{ab}h^{cd}U_{c;d}, \tag{G·2}$$

η and ζ being coefficients of viscosity. Divergence of T^{ab} can be written as

$$T^{ab}{}_{;b}\equiv\Phi U^a+\Psi^a=0. \tag{G·3}$$

If q^a is taken as $q^aU_a=0$, Φ and Ψ^a must be zero. Thus, we have hydrodynamic equations as follows:

$$D\mathcal{E}+(\mathcal{E}+P)U^b{}_{;b}+U^b{}_{;c}\tau^c_b+(q^b{}_{;b}+q_bDU^b)/c=0, \tag{G·4}$$

$$(\mathcal{E}+P)DU^a+h^{ab}(P_{,b}+\tau^c_{b;c})+(h^{ab}q_b+U^a{}_{;b}q^b+U^b{}_{;b}q^a)/c=0, \tag{G·5}$$

where $D\mathcal{E}=U^a\mathcal{E}_{,a}$, $DU^a=U^bU^a{}_{;b}$ and so on. Further, the second law of thermodynamics requires to put q^a as

$$q_a=-Kh^b_a(T_{,b}+TDU_b), \tag{G·6}$$

where K is a coefficient of thermal conductivity.[195)] A full set of the fundamental equations completed by Eqs. (G·4), (G·5) and (G·6), the equation of state and the equation of particle number conservation. The linealized equations of Eqs. (G·4), (G·5) and (G·6) in the expanding universe are given as[41)]

$$\frac{1}{a^3}\frac{\partial a^3\mathcal{E}_1}{\partial t}+(\mathcal{E}+P)\nabla\cdot\boldsymbol{u}+3P_1\frac{\dot{a}}{a}+\nabla\cdot\boldsymbol{q}=0, \qquad (\mathrm{G\cdot 7})$$

$$\frac{1}{c^2}\frac{1}{a^5}\frac{\partial}{\partial t}[a^5(\mathcal{E}+P)\boldsymbol{u}]+\frac{1}{a^2}\left(\nabla P_1+\frac{\mathcal{E}+P}{c^2}\nabla\phi\right)$$
$$-\frac{\eta}{a^2}\left(\nabla^2\boldsymbol{u}+\frac{1}{3}\nabla\cdot\nabla\cdot\boldsymbol{u}\right)-\frac{1}{a^2}\frac{\zeta}{3}\nabla\cdot\nabla\cdot\boldsymbol{u}-\frac{1}{a^4}\frac{\partial a^4\boldsymbol{q}}{\partial t}=0, \qquad (\mathrm{G\cdot 8})$$

$$\boldsymbol{q}=-K\left(\frac{1}{a^2}\nabla T_1+T\frac{1}{c^2}\frac{\partial\boldsymbol{u}}{\partial t}+2\frac{\dot{a}}{a}T\frac{\boldsymbol{u}}{c}+\frac{T}{a^2}\frac{\nabla\phi}{c^2}\right), \qquad (\mathrm{G\cdot 9})$$

where the subscript 1 denotes the perturbed quantities, ϕ is gravitational potential and $\boldsymbol{u}$ relates to the proper velocity $\boldsymbol{V}$ as $\boldsymbol{V}=a\boldsymbol{u}$.

Coefficients of viscosity and thermal conductivity are obtained from the kinetic theory of the radiative gas.[112),135),194)] About it, Masaki[194)] has given the most complete treatment, which is given in the followings. Radiation field in the moving matter is generally anisotropic and inhomogeneous. Now, we expand the radiation intensity $B(k, x)$ in multipole components as follows:

$$B(k,x)=\widetilde{S}(\omega,x)+\widetilde{V}_a(\omega,x)n^a+\widetilde{T}_{ab}(\omega,x)n^{ab}+\cdots, \qquad (\mathrm{G\cdot 10})$$

with

$$\widetilde{S}(\omega,x)=\frac{1}{4\pi}\oint_{(k\cdot U)=\omega}B(k,x)d\Omega, \qquad (\mathrm{G\cdot 11a})$$

$$\widetilde{V}_a(\omega,x)=-\frac{3}{4\pi}\oint_{(k\cdot U)=\omega}n_aB(k,x)d\Omega, \qquad (\mathrm{G\cdot 11b})$$

$$\widetilde{T}_{ab}(\omega,x)=\frac{15}{8\pi}\oint_{(k\cdot U)=\omega}n_{ab}B(k,x)d\Omega \qquad (\mathrm{G\cdot 11c})$$

and so on, where

$$n^a=\frac{k^a}{(k\cdot U)}-U^a, \qquad (\mathrm{G\cdot 12a})$$

$$n^{ab}=n^an^b+\frac{1}{3}h^{ab}, \qquad (\mathrm{G\cdot 12b})$$

and so on, ω being the scalar product of the four vectors k and U, i.e., $\omega=(k\cdot U)$. In the above expression, the integration is taken over all the direction of the three vector $\boldsymbol{k}$ under the condition of $(k\cdot U)=\omega$.

If the interaction between matter and radiation is independent on energy, the transport equation of radiation is written as

$$k^a \frac{\partial}{\partial x^a} B(k,x) = -(l_{sc}^{-1} + l_{abs}^{-1})\omega B(k,x)$$
$$+\int \omega' n_e \frac{d\sigma_s(k' \to k)}{d\Omega} B(k',x)\, d\Omega' + \epsilon(k,x), \qquad (G\cdot 13)$$

where l_{sc} and l_{abs} are the mean-free paths of photons by scattering and absorption respectively, $d\sigma_s(k' \to k)/d\Omega$ is the angular differential cross section of scattering and $\epsilon_c(k,x)$ is the emission rate. For the Thomson scattering the differential cross section is given as

$$d\sigma_s(k' \to k) = \frac{\sigma_{Th}}{4\pi}\left(1 + \frac{3}{4} n_{ab} n'^{ab}\right) d\Omega. \qquad (G\cdot 14)$$

Substituting Eq. (G·10) in the right-hand of Eq. (G·13), we have

$$k^a \frac{\partial B(k,x)}{\partial x^a} = -\omega(l_{abs}^{-1}\widetilde{S} + l^{-1}\widetilde{V}_a n^a + l^{*-1}\widetilde{T}_{ab} n^{ab} + \cdots) + \epsilon, \qquad (G\cdot 15)$$

where

$$l = (l_{sc}^{-1} + l_{abs}^{-1})^{-1} \qquad (G\cdot 16)$$

and

$$l^* = \left(\frac{9}{10} n_e \sigma_{Th} + l_{abs}^{-1}\right)^{-1}. \qquad (G\cdot 17)$$

Taking the moments of Eq. (G·15) with respect to 1, n_a, n_{ab} and so on, we have the following set of relations:

$$\frac{1}{4\pi}\oint k^a \frac{\partial B}{\partial x^a} d\Omega = -\frac{1}{l_{abs}}\omega\widetilde{S} + \epsilon, \qquad (G\cdot 18)$$

$$-\frac{3}{4\pi}\oint n_a k^b \frac{\partial B}{\partial x^b} d\Omega = -\frac{1}{l}\omega\widetilde{V}_a, \qquad (G\cdot 19)$$

$$\frac{15}{8\pi}\oint n_{ab} k^c \frac{\partial B}{\partial x^c} d\Omega = -\frac{1}{l^*}\omega\widetilde{T}_{ab} \qquad (G\cdot 20)$$

and so on, where ϵ is assumed to be isotropic function.

Now, we consider the case where the assumption of the local thermodynamic equilibrium holds. Then, we may put as

$$\widetilde{S}^{(0)} = F(\omega/T), \quad \widetilde{V}_a^{(0)} = 0 \quad \text{and} \quad \widetilde{T}_{ab}^{(0)} = 0 \qquad (G\cdot 21)$$

as the zeroth order approximation, where T is temperature. If a characteristic length of radiation of T is much smaller than the mean-free path, we can obtain the first order correction from Eqs. (G·18)～(G·20) as follows:

$$\widetilde{S}^{(1)} = l_{abs}\left(\frac{DT}{T} + \frac{1}{3} U^a{}_{,a}\right) y \frac{dF}{dy}, \qquad (G\cdot 22)$$

$$\widetilde{V}_a^{(1)} = -\frac{l}{T}(h_a^b T_{,b} + TDU_a) y \frac{dF}{dy}, \tag{G·23}$$

$$\widetilde{T}_{ab}^{(1)} = -\frac{l^*}{2}\left(U_{a,c}h_b^c + U_{b,c}h_a^c - \frac{2}{3}h_{ab}U^c{}_{,c}\right) y \frac{dF}{dy}, \tag{G·24}$$

and so on, where $y = \omega/T$. The energy-momentum tensor of radiation is defined as

$$(T^{ab})_r = \int k^a k^b B(k, x) d\Gamma, \tag{G·25}$$

where $d\Gamma$ is the invariant volume of momentum space. Substituting Eq. (G·10) into Eq. (G·25), we have the energy-momentum tensor up to the first order approximation as shown in Eq. (G·1) with $\mathcal{E} = \mathcal{E}_r$ and $P = \mathcal{E}_r/3$, and the coefficients of conductivity and viscosity are obtained as

$$K = \frac{4}{3}\frac{\mathcal{E}_r}{cT} l \tag{G·26}$$

and

$$\eta = \frac{4}{15}\frac{\mathcal{E}_r}{c} l^* \tag{G·27}$$

respectively. For the Thomson scattering, η reduces to

$$\eta = \frac{8}{27}\frac{\mathcal{E}_r}{n_e \sigma_{Th} c} \tag{G·28}$$

which is different by the factor 10/9 from the expression obtained by Thomas.[135)]

Appendix H

——A size spectrum of turbulence——

In order to obtain an evolutionary feature of a size spectrum, we solve Eq. (5·32) under such simple assumption on the energy-transfer term $T(k, t)$ as

$$T(k, t) \simeq v(>k) E(k, t)/\lambda, \tag{H·1}$$

where $v^2(>k) = \int_k^\infty E(k', t) dk'$. This form is assumed from an idea of eddy-viscosity and a dimensional analysis of $T(k, t)$.

Transforming k and $E(k, t)$ into M_λ and $f(M_\lambda, t)$, Eq. (5·32) is re-written as, using Eq. (H·1) and neglecting the viscosity term,

$$-\frac{\partial f}{\partial t} = \left(\frac{\rho_m}{M_\lambda}\right)^{1/2} \frac{\{(\mathcal{E}+P)a^4\}_1}{(\mathcal{E}+P)a^4} \left(\int_0^{M_\lambda} f(M'_\lambda, t) \frac{dM'_\lambda}{M'_\lambda}\right)^{1/2} f(M_\lambda, t), \tag{H·2}$$

where

$$f(M_\lambda, t)=\left[\frac{(\mathcal{E}+P)a^4}{\{(\mathcal{E}+P)a^4\}_{\rm i}}\right]^2 E(k,t)\left(-\frac{dk}{dM_\lambda}\right)M_\lambda .$$

Approximating as $\int_0^{M_\lambda} f dM'_\lambda/M'_\lambda \simeq f(M_\lambda, t)$, Eq. (H·2) is solved as

$$f(M_\lambda, t)=\frac{f(M_\lambda, t_{\rm i})}{(1+\beta z)^2},$$

$$Z=\frac{1}{2t_{\rm i}}\int_{t_{\rm i}}^{t}\frac{a_i}{a}\frac{\{(\mathcal{E}+P)a^4\}_{\rm i}}{(\mathcal{E}+P)a^4}dt' \tag{H·3}$$

and

$$\beta=[F(M_\lambda, t_{\rm i})]^{1/2} t_{\rm i}/(M_\lambda/\rho_{\rm mi})^{1/3}.$$

If we assume

$$f(M_\lambda, t_{\rm i})=v_0^2(M_\lambda/M_0)^m, \tag{H·4}$$

Eq. (H·3) gives

$$f(M_\lambda, t)=\frac{v_0^2 x^m}{(1+bx^{m/2-1/3}Z)^2}, \tag{H·5}$$

where $x=M_\lambda/M_0$ and $b=v_0 t_{\rm i}/(M_0/\rho_{\rm mi})^{1/3}$. The factor Z increases as $a(t)/a_{\rm i}$ during the stage of $t>t_*$ but it remains constant in the stage of $t<t_*$. In the stage of $t<t_*$, the second term in the denominator in Eq. (H·5) can be rewritten as

$$bx^{m/2-2/3}Z=(M_I(t)/M_\lambda)^{1/3}, \tag{H·6}$$

where $M_I=\rho_{\rm m}\{v_0(M_I/M_0)^{m/2}t\}^3$ and the turning of the spectral index occurs at $M_I(t)$. For $m=0$, the M_I is the frozen mass defined by (5·16). Thus, the size spectrum is obtained as

$$F(M_\lambda, t)=\left[\frac{\{(\mathcal{E}+P)a^4\}_{\rm i}}{(\mathcal{E}+P)a^4}\right]f(M_\lambda, t)\frac{1}{c_s^2}. \tag{H·7}$$

In the dissipative region of the spectrum, i.e., $M_\lambda<M_{\rm dis.v}$, the effect of the expansion can be neglected and we can adopt a spectrum given by the theory in the non-expanding medium such as $E(k)\propto k^{-7}$ or

$$F(M_\lambda, t)\propto M_\lambda^2 \tag{H·8}$$

for $M_\lambda<M_{\rm dis.v}$.[197] Using Eqs. (H·7) and (H·8), a schematic evolution of $F(M_\lambda, t)$ is given in Fig. 19.

The heating rate is given as

$$\epsilon_d=-\frac{\mathcal{E}c_s^2}{c^2}\int_0^\infty\frac{\partial F}{\partial t}\frac{dM'_\lambda}{M'_\lambda}, \tag{H·9}$$

which reduces to Eq. (6·5) in $t'\ll t_*$.

References

1) R. C. Tolman, *Relativity, Thermodynamics and Cosmology* (University Press, Oxford, 1934).
E. A. Milne, *Relativity, Gravitation and World Structure* (University Press, Oxford, 1935).
G. C. Mcvittie, *General Relativity and Cosmology* (Chapman & Hall Ltd., London, 1956, revised 1964).
H. Bondi, *Cosmology* (University Press, Cambridge, 1960).
2) C. G. Lemaitre, *The Primeval Atom* (D. Van Nostrand Company, 1950); *La Structure et Evolution de L'Univers*, ed. R. Stoops (Inst. International de Phys. Solvay, Brussel, 1958), p. 53.
3) G. Gamow, Phys. Rev. **70** (1946), 572.
4) R. A. Alpher, H. A. Bethe and G. Gamow, Phys. Rev. **73** (1948), 803.
5) G. Gamow, Phys. Rev. **74** (1948), 505; Nature **162** (1948), 608; Rev. Mod. Phys. **21** (1949), 367; Kgl. Danske Videnskab Selskab Mat.-fys. Medd. **27** (1953), No. 10; Vistas in Astronomy **2** (1956), 1726; *Perspective in Modern Physics* (John Wiley & Sons, New York, 1966), p. 448.
R. A. Alpher, G. Gamow and R. Herman, Phys. Rev. **74** (1948), 1198; **75** (1949), 701; Proc. Natl. Acad. Sci. **58** (1967), 153.
R. A. Alpher, Phys. Rev. **74** (1948), 1577.
R. A. Alpher and R. Herman, Phys. Rev. **74** (1948), 1737; **75** (1949), 1089; Nature **162** (1948), 776.
6) H. Bondi and T. Gold, Month. Notices Roy. Astron. Soc. **108** (1948), 252.
7) F. Hoyle, Month. Notices Roy. Astron. Soc. **108** (1948), 372.
8) F. Hoyle and J. V. Narlikar, Proc. Roy. Soc. **A273** (1963), 1; **A290** (1966), 177.
9) R. A. Alpher and R. Herman, Rev. Mod. Phys. **22** (1950), 153.
10) C. Hayashi, Prog. Theor. Phys. **5** (1950) 224.
11) C. Hayashi and M. Nishida, Prog. Theor. Phys. **16** (1956), 613.
12) M. G. Mayer and E. Teller, Phys. Rev. **76** (1949), 1226.
13) R. E. Peierls, K. S. Singni and D. Wroe, Phys. Rev. **87** (1952), 46.
14) E. M. Burbidge, G. R. Burbidge, W. A. Fowler and F. Hoyle, Rev. Mod. Phys. **29** (1957), 547.
15) M. Taketani, T. Hatanaka and S. Obi, Prog. Theor. Phys. **15** (1956), 89.
16) A. R. Sandage, Astrophys. J. **133** (1961), 355; **134** (1961), 916.
17) K. Tomita and C. Hayashi, Prog. Theor. Phys. **30** (1963), 691.
18) M. Ryle and R. W. Clarke, Month. Notices Roy. Astron. Soc. **122** (1961), 349.
19) A. R. Sandage, Astrophys. J. **141** (1965), 1560.
19a) J. V. Peach, Astrophys. J. **159** (1970), 753.
20) G. G. Pooley and M. Ryle, Month. Notices Roy. Astron. Soc. **139** (1968), 515.
M. S. Longair, Soviet Phys.-Uspekhi **12** (1970), 673.
21) A. A. Penzias and R. W. Wilson, Astrophys. J. **142** (1965), 419.
22) R. H. Dicke, P. J. E. Peebles, P. G. Roll and D. T. Wilkinson, Astrophys. J. **142** (1965), 414.
23) P. J. E. Peebles, Phys. Rev. Letters **16** (1966), 410; Astrophys. J. **146** (1966), 542.
24) R. V. Wagoner, W. A. Fowler and F. Hoyle, Astrophys. J. **148** (1967), 3.
25) H. Sato, Prog. Theor. Phys. **38** (1967), 1083.
26) F. Hoyle and R. J. Tayler, Nature **203** (1964), 1108.
27) K. Greisen, Phys. Rev. Letters **16** (1966), 748.
G. T. Zatsepin and V. A. Kuzmin, JETP Letters **4** (1966), 78.
F. W. Stecker, Phys. Rev. Letters **21** (1968), 1016; Phys. Rev. **180** (1969), 1264.
28) R. J. Gould and G. Schreder, Phys. Rev. Letters **16** (1966), 252.
J. V. Jelley, Phys. Rev. Letters **16** (1966), 469.
P. Encrenaz and R. B. Partridge, Astrophys. Letters **3** (1967), 161.

28a) S. Hayakawa and D. Sugimoto, Prog. Theor. Phys. Suppl. No. 49 (1971), p. 148.
29) C. F. von Weizsäcker, Astrophys. J. **114** (1951), 165.
30) G. Gamow, Phys. Rev. **86** (1952), 251.
31) H. Nariai, Sci. Rep. Tohoku Univ. **39** (1956), 213; **40** (1956), 40.
32) P. J. E. Peebles, Astrophys. J. **142** (1965), 1317.
33) A. G. Doroshkevich, Ya. B. Zeldovich and I. D. Novikov, Soviet Astron.-AJ **11** (1967), 233.
34) E. M. Lifshitz, J. of Phys. (USSR) **10** (1946), 110.
E. M. Lifshitz and I. M. Khalatonikov, Advances in Phys. **12** (1963), 185.
35) H. Nariai and K. Tomita, Prog. Theor. Phys. Suppl. No. 49 (1971), p. 83.
36) S. Kato, H. Nariai and K. Tomita, Publ. Astron. Soc. Japan **19** (1967), 130.
37) Y. Sofue, Publ. Astron. Soc. Japan **19** (1969), 211.
38) M. Kondo, Y. Sofue and W. Unno, Prog. Theor. Phys. Suppl. No. 49 (1971), p. 120.
39) L. M. Ozernoi and A. D. Chernin, Soviet Astron.-AJ **11** (1967), 233; **12** (1968), 901.
40) H. Sato, T. Matsuda and H. Takeda, Prog. Theor. Phys. **43** (1970), 115.
41) H. Sato, Prog. Theor. Phys. **45** (1971), 370.
42) K. Tomita, H. Nariai, H. Sato, T. Matsuda and H. Takeda, Prog. Theor. Phys. **43** (1970), 1511.
43) T. Matsuda, H. Sato and H. Takeda, Prog. Theor. Phys. **46** (1971), 416.
44) Ya. B. Zeldovich, Advances in Astron. and Astrophys. Vol. 3 (1965), 241.
45) Ya. B. Zeldovich, Soviet Phys.-Uspekhi **9** (1967), 602.
46) C. Hayashi and H. Sato, Kagaku **36** (1966), 402 (in Japanese).
47) Ya. B. Zeldovich and I. D. Novikov, Ann. Rev. Astron. and Astrophys. **5** (1967), 627.
48) W. Davidson and J. V. Narlikar, Report on Prog. in Phys. **29** (1967), 539.
49) H. Y. Chiu, Ann. of Phys. **43** (1967), 1.
50) G. Dautcourt and G. Wallis, Forts. Phys. **16** (1968), 545.
51) S. W. Hawking and G. E. R. Ellis, Astrophys. J. **152** (1968), 25.
C. W. Misner, Phys. Rev. **186** (1969), 1328.
52) J. A. Wheeler, *Relativity, Gravitation and Topology*, edited by C. Dewitt and B. Dewitt (Gordon and Breach, New York, 1964), p. 315; *Battelle Rencoutre*, ed. by C. Dewitt and J. A. Wheeler (Benjamin, Inc., New York, 1968), p. 242; *Einsteins Vision* (Springer V, 1968).
53) M. Markov, Soviet Phys.-JETP **24** (1967), 584; Prog. Theor. Phys. Suppl. Extra Number (1965), 85.
54) N. Hokkyo, Prog. Theor. Phys. **39** (1968), 1078; **44** (1970), 801.
55) T. Tati, Prog. Theor. Phys. **37** (1967), 754.
56) R. Hagedron, Astron. and Astrophys. **5** (1970). 184.
57) V. B. Jakubov, Soviet Astron.-AJ **8** (1965), 708.
58) M. Kaufman, Astrophys. J. **160** (1970), 459.
59) Ya. B. Zeldovich, L. B. Okun and S. B. Pikelner, Soviet Phys.-Uspekhi **8** (1966), 702.
60) H. Y. Chiu, Phys. Rev. Letters **17** (1966), 712.
61) V. I. Man'ko, Soviet Phys.-Uspekhi **10** (1967), 262.
62) M. Goldharber, Science **124** (1956), 218.
63) H. Alfven and O. Klein, Ark. Fysik **23** (1962), 187.
H. Alfven, Rev. Mod. Phys. **37** (1965), 652; Phys. Today **24** (1971), 28.
H. Alfven and A. Eluvius, Science **164** (1969), 918.
64) G. Steigman, Nature **224** (1969), 477.
65) E. R. Harrison, Phys. Rev. **167** (1968), 1070.
66) R. Omnes, Phys. Rev. Letters **23** (1969), 38.
67) R. Omnes, Nature **223** (1969), 1349; Astron. and Astrophys. **10** (1971), 228.
68) R. A. Alpher, J. W. Follin and R. C. Herman, Phys. Rev. **92** (1953), 1347.
69) S. S. Gershtein and Ya. B. Zeldovich, JETP Letters **4** (1966), 120.
70) A. G. Doroshkevich, Ya. B. Zeldovich and I. D. Novikov, JETP Letters **5**(1967), 96.
71) B. Pontecorvo and Ya. Smorodinsky, Soviet Phys.-JETP **41** (1961), 239.
72) S. Weinberg, Phys. Rev. **128** (1962), 1457.
73) M. A. Markov, *The Neutrino* (D-1269, Dubuna, 1963).

74) S. Hayakawa, Prog. Theor. Phys. Suppl. Extra Number (1965), 532.
75) V. L. Ginzburg and G. F. Zhakov, JETP Letters **5** (1967), 223.
76) G. Marx, Nuovo Cim. **30** (1963), 1555.
77) J. Bernstein, M. Ruderman and G. Feinberg, Phys. Rev. **132** (1963), 1227.
78) P. Csonka and G. Marx, Nuovo Cim. **43A** (1966), 591.
79) T. de Graaf, Astron. and Astrophys. **5** (1970), 335.
80) S. Kitamura, private communication (1970).
81) E. Fermi and A. Turkevich, 1948, quoted in Ref. 9).
82) R. J. Tayler, Nature **217** (1968), 433.
83) Y. N. Smirnov, Soviet Astron.-AJ **8** (1965), 433.
84) F. Hoyle and R. J. Tayler, Nature **203** (1964), 1108.
85) R. J. Tayler, Quart. J. Roy. Astron. Soc. **8** (1967), 313.
86) A. O. J. Unsöld, Science **163** (1969), 1015.
87) I. J. Danziger, Ann. Rev. Astron. and Astrophys. **8** (1970), 161.
88) I. Iben, Ann. of Phys. **54** (1969), 164.
89) R. V. Wagoner, Astrophys. J. **151** (1967), 1369; Suppl. **18** (1969), No. 162.
90) S. W. Hawking and R. J. Tayler, Nature **209** (1966), 1278.
91) K. S. Thorne, Astrophys. J. **148** (1967), 51.
92) G. Greenstein, Nature **223** (1969), 938.
93) J. J. Mates and R. F. O'Connell, Astrophys. J. **160** (1970), 451.
94) R. H. Dicke, Astrophys. J. **152** (1968), 1.
95) R. Weymann, Astrophys. J. **145** (1966), 560.
96) Ya. B. Zeldovich and R. A. Sunyaev, Astrophys. Space Sci. **4** (1969), 301.
97) Ya. B. Zeldovich and E. V. Levich, Soviet Phys.-JETP **28** (1969), 1287.
98) R. A. Sunyaev and Ya. B. Zeldovich, Astrophys. Space Sci. **7** (1970), 20.
98a) R. A. Sunyaev and Ya. B. Zeldovich, Comments on Astrophys. Space Sci. **11** (1970), 66.
99) P. J. E. Peebles, Astrophys. J. **153** (1968), 1.
100) Ya. B. Zeldovich, V. G. Kurt and R. A. Sunyaev, Soviet Phys.-JETP **28** (1969), 146.
101) H. Takeda, H. Sato and T. Matsuda, Prog. Theor. Phys. **41** (1969), 840.
102) T. Matsuda, H. Sato and H. Takeda, Prog. Theor. Phys. **42** (1969), 219.
103) W. C. Saslaw and D. Zipoy, Nature **216** (1967), 976.
104) P. J. E. Peebles and R. H. Dicke, Astrophys. J. **154** (1968), 891.
104a) P. J. E. Peebles, Astrophys. J. **157** (1969), 1075.
105) T. Hirasawa, K. Aizu and M. Taketani, Prog. Theor. Phys. **41** (1969), 835.
106) T. Hirasawa, Prog. Theor. Phys. **42** (1969), 523.
107) H. Sato, Prog. Theor. Phys. **40** (1968), 781.
108) H. Sato, Prog. Theor. Phys. **37** (1967), 1032.
109) J. Silk, Nature **215** (1967), 1155.
110) G. Dautcourt, Month. Notices Roy. Astron. Soc. **114** (1969), 255.
111) J. Silk, Nature **218** (1968), 453.
112) P. J. E. Peebles and J. T. Yu, Astrophys. J. **162** (1970), 815.
113) R. A. Sunyaev and Ya. B. Zeldovich, Astrophys. Space Sci. **7** (1970), 3.
113a) R. A. Sunyaev and Ya. B. Zeldovich, Astrophys. Space Sci. **9** (1970), 368.
114) M. S. Longair and R. A. Sunyaev, Nature **223** (1969), 719.
115) R. K. Sacks and A. M. Wolfe, Astrophys. J. **147** (1967), 73.
116) A. M. Wolfe, Astrophys. J. **156** (1969), 803.
117) J. E. Gunn, Astrophys. J. **147** (1967), 61.
118) M. J. Rees and D. W. Sciama, Nature **217** (1968), 511.
119) S. W. Hawking, Month. Notices Roy. Astron. Soc. **142** (1969), 129.
119a) P. T. Saunders, Month. Notices Roy. Astron. Soc. **141** (1968), 427.
120) D. W. Sciama, Phys. Rev. Letters **18** (1967), 1065.
121) J. M. Stewart and D. W. Sciama, Nature **216** (1967), 748.
122) C. V. Heer and R. H. Kohl, Phys. Rev. **174** (1968), 1611.

123) J. J. Condon and M. O. Harwit, Phys. Rev. Letters **20** (1968), 1309; **21** (1968), 58.
124) J. Kristian and R. K. Sacks, Astrophys. J. **143** (1966), 380.
J. Kristian, Astrophys. J. **147** (1967), 864.
125) H. Nariai and Y. Ueno, Prog. Theor. Phys. **23** (1960), 305.
126) W. M. Irvine, Ann. of Phys. **32** (1965), 322.
127) S. W. Hawking, Astrophys. J. **145** (1965), 544.
T. Kihara, Publ. Astron. Soc. Japan **19** (1967), 121.
H. Nariai, K. Tomita and S. Kato, Prog. Theor. Phys. **37** (1967), 60.
E. R. Harrison, Rev. Mod. Phys. **39** (1967), 121.
G. B. Field and L. C. Shapley, Astrophys. Space Sci. **1** (1968), 309.
128) C. W. Misner, Nature **214** (1967), 40.
129) J. Silk, Nature **215** (1967), 1155.
130) C. W. Misner, Phys. Rev. Letters **19** (1967), 533; Astrophys. J. **151** (1968), 431.
130a) J. M. Stewart, Month. Notices Roy. Astron. Soc. **145** (1969), 347.
131) J. Silk, Astrophys. J. **151** (1968), 459.
132) E. R. Harrison, Month. Notices Roy. Astron. Soc. **141** (1968), 397.
133) H. Nariai, Prog. Theor. Phys. **44** (1970), 110; **45** (1971), 61.
134) Ya. B. Zeldovich and I. D. Novikov, Soviet Astron.-AJ **13** (1970), 754.
E. R. Harrison, Phys. Rev. **D1** (1970), 2726.
135) L. H. Thomas, Quart. J. Math. **1** (1930), 239.
136) E. R. Harrison, Nature **224** (1969), 1089; Astrophys. Letters **3** (1969), 133; Month. Notices Roy. Astron. Soc. **147** (1970), 279.
137) T. Kihara and K. Miyoshi, Publ. Astron. Soc. Japan **22** (1970), 245.
138) T. Matsuda, H. Sato and H. Takeda, Publ. Astron. Soc. Japan **23** (1971), 1.
139) A. D. Chernin, Nature **220** (1968), 250; **226** (1970), 440; JETP Letters **11** (1970), 210.
140) V. L. Ginzburg and L. M. Ozernoi, Soviet Astron.-AJ **9** (1964), 726.
141) A. S. Kompaneets, Soviet Phys.-JETP **4** (1957), 730.
R. Weymann, Phys. Fluids **8** (1965), 2112.
142) J. E. Gunn and B. A. Peterson, Astrophys. J. **142** (1965), 1633.
J. N. Bahcall and R. D. Ekers, Astrophys. J. **157** (1969), 1055.
P. D. Noerdlinger, Astrophys. J. **156** (1969), 841.
143) J. A. Koehler, Astrophys. J. **146** (1966), 504.
J. A. Koehler and B. J. Robinson, Astrophys. J. **146** (1966), 488.
144) A. A. Penzias and E. H. Scott, Astrophys. J. **153** (1968), L7.
A. A. Penzias and R. W. Wilson, Astrophys. J. **157** (1969), 799.
145) P. J. E. Peebles, Astrophys. J. **157** (1969), 45.
R. A. Sunyaev, Astrophys. Letters **3** (1969), 33.
146) R. J. Gould and W. Ramsay, Astrophys. J. **144** (1966), 587.
147) R. Weymann, Astrophys. J. **147** (1967), 887.
148) J. Bergeron, Astron. and Astrophys. **3** (1969), 42.
149) A. G. Doroshkevich and R. A. Sunyaev, Soviet Astron.-AJ **13** (1969), 15.
150) O. J. Eggen, D. Lyndenbell and A. R. Sandage, Astrophys. J. **136** (1962), 748.
151) E. E. Salpeter, Astrophys. J. **129** (1959), 608.
M. Schmidt, Astrophys. J. **129** (1959), 234; **137** (1963), 758.
J. W. Truran, C. J. Hansen and A. G. W. Cameron, Can. J. Phys. **43** (1965), 1616.
R. B. Partridge and P. J. E. Peebles, Astrophys. J. **147** (1967), 868; **148** (1969), 377.
B. M. Tinsley, Astrophys. J. **151** (1968), 547.
T. Matsuda, Prog. Theor. Phys. **43** (1970), 1491.
152) T. Hatanaka, S. Hayakawa, K. Ishida and M. Taketani, Prog. Theor. Phys. Suppl. No. 31 (1964), 2.
R. B. Larson, Month. Notices Roy. Astron. Soc. **145** (1969), 405.
J. H. Oort, Astron. and Astrophys. **7** (1970), 381.
153) B. E. J. Pagel, Quart. J. Roy. Astr. Soc. **11** (1970), 172.

154) J. L. Greenstein, Comments on Astrophys. Space Sci. **11** (1970), 85.
155) J. H. Oort, Nature **224** (1969), 1158.
156) L. M. Ozernoi, JETP Letters **10** (1969), 251.
L. M. Ozernoi and G. V. Chibisov, Astron. Zh. **47** (1970), 769.
157) E. R. Harrison, Month. Notices Roy. Astron. Soc. **148** (1970), 119.
158) T. F. Howell and J. R. Shakeshaft, Nature **216** (1967), 753.
159) A. A. Penzias and R. W. Wilson, Astron. J. **72** (1967), 315.
160) T. F. Howell and J. R. Shakeshaft, Nature **210** (1966), 1318.
161) P. G. Roll and D. T. Wilkinson, Phys. Rev. Letters **16** (1966), 405.
162) R. A. Stokes, R. B. Partridge and D. T. Wilkinson, Phys. Rev. Letters **19** (1967), 1199.
163) W. J. Welch, S. Keachie, D. D. Thornton and G. Wrixon, Phys. Rev. Letters **18** (1967), 1068.
164) M. S. Ewing, B. F. Burke and D. H. Staelin, Phys. Rev. Letters **19** (1967), 1251.
165) D. T. Wilkinson, Phys. Rev. Letters **19** (1967), 1195.
166) V. Puzhanov, A. E. Salomonovich and K. S. Stankevich, Soviet Astron.-AJ **11** (1968), 905.
A. E. Salomonovich, Soviet Phys.-Uspekhi **12** (1969), 1271.
167) P. E. Boynton, R. A. Stokes and D. T. Wilkinson, Phys. Rev. Letters **21** (1968), 462.
167a) M. F. Millea, M. McColl, R. J. Pedersen and F. L. Vernon, Phys. Rev. Letters **26** (1971), 919.
168) G. B. Field and J. L. Hitchcock, Phys. Rev. Letters **16** (1966), 817.
169) P. Thaddeus and J. F. Clauser, Phys. Rev. Letters **16** (1966), 819.
170) V. Bortolet, J. F. Clauser and D. Thaddeus, Phys. Rev. Letters **22** (1969), 307.
171) K. Shivanandan, J. R. Houck and M. O. Harwit, Phys. Rev Letters **21** (1968), 1460.
172) J. R. Houck and M. O. Harwit, Astrophys. J. **157** (1969), L45; Science **164** (1969), 1271.
173) D. Muehlenen and R. Weiss, Phys. Rev. Letters **24** (1970), 742.
174) R. B. Partridge and D. T. Wilkinson, Phys. Rev. Letters **18** (1967), 557.
175) D. T. Wilkinson and R. B. Partridge, Nature **215** (1967), 719.
176) E. K. Conklin and R. N. Bracewell, Nature **216** (1967), 777; Phys. Rev. Letters **18** (1967), 614.
177) A. A. Penzias and R. W. Wilson, Astrophys. J. **146** (1967), 345; Science **156** (1967), 1100.
178) E. E. Epstein, Astrophys. J. **148** (1967), L157.
179) R. N. Bracewell and E. K. Conklin, Nature **219** (1968), 1343.
180) E. K. Conklin, Nature **222** (1969), 971.
180a) S. P. Boughn, D. M. Fram and R. B. Partridge, Astrophys. J. **165** (1971), 439.
181) Ya. B. Zeldovich and I. D. Novikov, Soviet Astron.-AJ **11** (1967), 526.
182) J. R. Shakeshaft and A. S. Webster, Nature **210** (1968), 339.
183) Yu. N. Pariiskii, Soviet Astron.-AJ **12** (1968), 219.
184) A. M. Wolf and G. B. Burbridge, Astrophys. J. **150** (1969), 345.
185) V. Petrosian, J. N. Bahcall and E. E. Salpeter, Astrophys. J. **155** (1969), L57.
186) F. Hoyle, N. C, Wickramasinghe and V. C. Reddish, Nature **218** (1968), 1124.
187) R. V. Wagoner, Nature **224** (1969), 401.
M. O. Harwit, J. R. Houch and R. V. Wagoner, Nature **228** (1970), 451.
P. J. E. Peebles, Comments Astrophys. Space Sci. **3** (1971), 20.
188) M. Alexanian, Astrophys. J. **159** (1970), 745.
189) A. A. Penzias, J. Schraml and R. W. Wilson, Astrophys. J. **157** (1969), L49.
190) C. Hazard and E. E. Salpeter, Astrophys. J. **157** (1969), L87.
191) M. G. Smith and R. B. Partridge, Astrophys. J. **159** (1970), 737.
192) D. E. Osterbrock, Quart. J. Roy. Astron. Soc. **11** (1970), 199.
193) A. R. Sandage, Phys. Today **23** (1970), 34.
194) I. Masaki, Publ. Astron. Soc. Japan **23** (1971), 425.
195) C. E. Eckart, Phys. Rev. **58** (1940), 919.
196) G. A. Kluitenberg, S. R. de Groot and P. Mazun, Physica **19** (1953), 686, 1075.
J. Ehlers, Akad. Wiss. Mainz. Abh. Math.-Nat. Kl. (1961), Nr. 11.
M. Kranys, Nuovo Cim. **42** (1966), 51; **50** (1967), 48.
197) G. K. Batchelor, *The Theory of Homogeneous Turbulence* (University Press, Cambridge, 1953), Chap. 6.